

**FUNDAMENTAL STUDY OF BINDING CHARACTERISTICS  
OF CATALYZED WASTE OILS IN THE GREEN  
PRODUCTION OF ROOFING TILES**

By

**TEOH WEI PING**

A dissertation submitted to the Department of Environmental Engineering,  
Faculty of Engineering and Green Technology,  
Universiti Tunku Abdul Rahman,  
in partial fulfillment of the requirements for the degree of  
Master of Engineering Science  
August 2018

## **ABSTRACT**

### **Fundamental Study of Binding Characteristic of Catalyzed Waste Oils in the Green Production of Roofing Tiles**

**Teoh Wei Ping**

Excessive waste disposal is one of the environmental issues to be addressed since a few decades ago. In addition, construction industry is responsible for great amount of energy consumption and high carbon dioxide emissions level during the manufacturing process of masonry units. In this study, an alternative approach for manufacturing of roofing tiles was proposed. This study involved utilization of waste materials, including waste engine oil (WEO), used cooking oil (UCO) and fly ash to produce a novel, environmental friendly roofing tile. It is believed that the specific chemical reactions of waste oils (autocatalytic oxy-polymerization reaction) upon an extended heat curing process will induce the chemical changes in the waste oils to make them to become binders from liquid form to rigid solid state. This binder is proved can produce roofing tile with a flexural strength which is comparable to that of the existing roofing tiles. The analytical studies on the chemical changes involved in the stiffening of binders, and their interaction with other raw materials were carried out by using Fourier Transform Infrared Spectroscopy (FTIR), Thermogravimetric analysis (TGA) and Scanning Electron Microscope (SEM). In this study, four different types of innovated

roofing tiles were produced using different types of ingredients. A series of manufacturing process, such as mixing, compacting, coating and heat curing processes were carried out to determine the optimized parameters for the production of innovated roofing tiles. Standard specification tests for those roofing tiles were conducted in terms of flexural strength, water absorption and permeability as per requirement of American Society for Testing and Materials (ASTM C 67 – 07a, C 1167 – 03, and C 1492 – 03). The flexural strength achieved by each roofing tile produced from different ingredients is 3.26 MPa for WEO-GRT; 6.91 MPa for UCO-GRT; 3.25 MPa for WEO-RT and 10.5 MPa for UCO-RT. All of the tiles also have a percentage of water absorption lower than 6% and impermeable to water. All of them fulfill the requirements as per ASTM. Moreover, the embodied carbon (EC) and embodied energy (EE) of the innovated roofing tiles were found in between 0.077 to 0.154 kgCO<sub>2</sub>/kg and 0.154 to 0.423 MJ/kg respectively, which is much lower with respect to the conventional roofing tiles. Conclusively, conversion of existing resources, recycled and reused waste materials, manufacture of environmental friendly roofing tiles are the prominent outcomes of this research study.

## **ACKNOWLEDGEMENTS**

I have taken efforts in this project. However, it would not have been possible without the kind support and help of many individuals and organisations. Hence, I would like to take this opportunity to extend my sincere thanks to all of them.

First of all, I am highly indebted to my project supervisors, Dr. Ng Choon Aun and Dr. Chee Swee Yong for their guidance and constant supervision as well as for providing useful knowledge regarding the project and also for their support in completing the project.

Secondly, I would like to express my special thanks of gratitude to my parent, Teoh Bon Sing and Euw Mooi Kiew, lab assistants from Faculty of Science and Faculty of Engineering and Green Technology, who always lend me their hand when I encountered some problems in the project. Without their kind assistances, suggestions and encouragement, I would not able to complete my project in such perfect way.

Last but not least, my thanks and appreciations go to Universiti Tunku Abdul Rahman who giving me this precious chance to do this project so that I can gain the experience of the research.

## DECLARATION

I hereby declare that the dissertation is based on my original work except for quotations and citations which have been duly acknowledged. I also declare that it has not been previously or concurrently submitted for any other degree at UTAR or other institutions.

Name \_\_\_\_\_

Date \_\_\_\_\_

## APPROVAL SHEET

This dissertation/thesis entitled “**FUNDAMENTAL STUDY OF BINDING CHARACTERISTICS OF CATALYZED WASTE OILS IN THE GREEN PRODUCTION OF ROOFING TILES**” was prepared by TEOH WEI PING and submitted as partial fulfillment of the requirements for the degree of Master of Engineering Science at Universiti Tunku Abdul Rahman.

Approved by:

---

(Dr. NG CHOON AUN)

Date:.....

Supervisor

Department of Environmental Engineering

Faculty of Engineering and Green Technology

Universiti Tunku Abdul Rahman

---

(Dr. CHEE SWEE YONG)

Date:.....

Co-supervisor

Department of Chemical Science

Faculty of Science

Universiti Tunku Abdul Rahman

**FACULTY OF ENGINEERING AND GREEN TECHNOLOGY**

**UNIVERSITI TUNKU ABDUL RAHMAN**

**Date:** \_\_\_\_\_

**PERMISSION SHEET**

It is hereby certified that **TEOH WEI PING (ID: 16AGM06231)** had completed this dissertation entitled “FUNDAMENTAL STUDY OF BINDING CHARACTERISTICS OF CATALYZED WASTE OILS IN THE GREEN PRODUCTION OF ROOFING TILES” under the supervision of Dr. Ng Choon Aun from the Department of Environmental Engineering, Faculty of Engineering and Green Technology; and Dr. Chee Swee Yong from the Department of Chemical Science, Faculty of Science.

I hereby give permission to the University to upload the softcopy of my Master project in pdf format into the UTAR Institutional Repository, which may be made accessible to the UTAR community and public.

Yours faithfully,

\_\_\_\_\_

(TEOH WEI PING)

## TABLE OF CONTENTS

	<b>Page</b>
<b>ABSTRACT</b>	<b>II</b>
<b>ACKNOWLEDGEMENTS</b>	<b>IV</b>
<b>DECLARATION</b>	<b>V</b>
<b>APPROVAL SHEET</b>	<b>VI</b>
<b>PERMISSION SHEET</b>	<b>VII</b>
<b>TABLE OF CONTENTS</b>	<b>VIII</b>
<b>LIST OF TABLES</b>	<b>XI</b>
<b>LIST OF FIGURES</b>	<b>XIV</b>
<b>LIST OF ABBREVIATIONS</b>	<b>XVI</b>
<b>CHAPTER</b>	
<b>1.0 INTRODUCTION</b>	<b>1</b>
1.1 Global Warming	1
1.2 Waste Management	3
1.3 Waste Engine Oil (WEO)	4
1.4 Used Cooking Oil (UCO)	6
1.5 Roofing Tiles	7
1.6 Problem Statement	8
1.7 Novel Solution: Waste Oils-made Roofing Tiles	10
1.8 Objectives	11
1.9 Organization of Thesis	12
<b>2.0 LITERATURE REVIEW</b>	<b>13</b>
2.1 Current Breakthrough of Roofing Tiles	13
2.2 Environmental Impact of Conventional Building Materials	16
2.3 Review on Utilization of Waste Materials in the Production of Building Materials	21
2.4 Waste Oils	25
2.4.1 Waste Engine Oil	25
2.4.2 Used Cooking Oil	28
2.5 Fly Ash	32
2.6 Basic Requirements of Roofing Tiles	34
2.6.1 Transverse and Flexural Strength	34
2.6.2 Water Absorption	35
2.6.3 Permeable Characteristic	36
2.7 Summary of Literature Review	37
<b>3.0 METHODOLOGY</b>	<b>38</b>
3.1 Selection of Materials	38
3.1.1 Waste Engine Oil (WEO)	38
3.1.2 Used Cooking Oil (UCO)	39

3.1.3	Catalyst	40
3.1.4	Coal-fired Ash	41
3.1.5	Sand Aggregate	43
3.2	Methodology	44
3.2.1	Preliminary Analysis of Selected Materials	46
3.2.1.1	Fourier-Transform Infrared Spectroscopy (FTIR)	46
3.2.1.2	Thermal Gravimetric Analysis (TGA)	48
3.2.1.3	Viscometer	49
3.2.1.4	Particle Sizes Analysis	50
3.2.1.5	Sieve Analysis	50
3.2.2	Production of Roofing Tile Prototypes	51
3.2.2.1	Manufacturing Process of Trials Roofing Tiles	51
3.2.2.2	Optimization of Parameters	54
3.2.3	Physical and Chemical Analysis of Roofing Tile Prototypes	55
3.2.3.1	Transverse Strength / Flexural Strength Test	55
3.2.3.2	Water Absorption Test	56
3.2.3.3	Permeability Test	57
3.2.3.4	Stability of Roofing Tiles Toward Different Weather	58
3.2.3.5	Surface Morphology	60
3.2.4	Life Cycle Assessment of Novel Roofing Tiles	60
<b>4.0</b>	<b>RESULTS AND DISCUSSIONS</b>	<b>62</b>
4.1	Raw Materials Analysis Using Fourier Transform Infrared Spectroscopy (FTIR)	62
4.1.1	Used Cooking Oil (UCO) and Waste Engine Oil (WEO) Analysis Using Fourier Transform Infrared Spectroscopy (FTIR)	62
4.1.2	Fly Ash Analysis Using Fourier Transform Infrared Spectroscopy	66
4.2	Attenuated Total Reflectance Fourier Transform Infrared Spectrometry (ATR-FTIR)	68
4.2.1	ATR-FTIR Analysis of UCO	68
4.2.2	ATR-FTIR Analysis of WEO	74
4.3	Thermogravimetric Analysis (TGA)	79
4.3.1	Thermogravimetric Analysis (TGA) of UCO and UCO Film	79
4.3.2	Thermogravimetric Analysis (TGA) of WEO and WEO Film	81
4.4	Scanning Electron Microscope (SEM)	83
4.5	Optimization Process of Innovated Roofing Tiles & Their Mechanical Properties	85
4.5.1	Parameters Optimization of WEO-made Green Roofing Tiles	85
4.5.1.1	Optimization of WEO and Fly Ash Compositions	86

4.5.1.2	Optimization of Number of Marshall Compactions Applied	91
4.5.1.3	Optimization of Heat Curing Duration	93
4.5.1.4	Optimization of Types and Amount of Catalysts Added	95
4.5.1.5	Effect of Coating Layer on Trial Roofing Tiles	97
4.5.1.6	Optimized Waste Engine Oil-made Green Roofing Tiles (WEO-GRT)	99
4.5.2	Optimization Parameters of UCO-made Green Roofing Tiles (UCO-GRT)	104
4.5.2.1	Optimization of Curing Duration	106
4.5.2.2	Optimization of UCO and Filler Content	107
4.5.2.3	Optimization of Amount of Catalyze Incorporated	109
4.5.2.4	Optimized Used Cooking Oil-made Green Roofing Tile (UCO-GRT)	111
4.5.3	Comparison Study of UCO-RT and WEO-RT	115
4.5.3.1	Optimization of Fine Sand to Fly Ash Ratio	115
4.5.3.2	Optimization of Waste Oils Compositions	117
4.5.3.3	Water Absorption and Permeability	120
4.5.3.4	Specific Heat Capacity	121
4.5.3.5	Ultra-violate (UV) Acceleration Test	123
4.5.3.6	Freeze-thaw Analysis	126
4.6	Life Cycle Assessment	127
4.6.1	LCA of Catalyzed WEO-GRT	127
4.6.2	LCA of Catalyzed UCO-GRT	132
4.6.3	LCA of UCO-RT & WEO-RT	135
<b>5.0</b>	<b>CONCLUSIONS AND RECOMMENDATIONS</b>	<b>140</b>
5.1	Conclusions	140
5.1.1	General Conclusion	140
5.1.2	Conclusion for Objective 1	142
5.1.3	Conclusion for Objective 2	143
5.1.4	Conclusion for Objective 3	144
5.1.5	Conclusion for Objective 4	145
5.2	Limitations	146
5.3	Future Recommendations	147
	<b>REFERENCES</b>	<b>149</b>

## LIST OF TABLES

<b>Table</b>		<b>Page</b>
2.1	Advantages and disadvantages associated to different types of roofing tile	14-15
2.2	Embodied energy and carbon associated with production of masonry units	18
2.3	General information of cement	19
2.4	Physical and chemical changes of clay associated with ventilated temperature	20-21
2.5	Quantity of metals presented in WEO and their limitations	26
2.6	Standard limitation of transverse strength of roofing tiles (ASTM C 1167 – 03)	35
2.7	Standard limitation of percentage of water absorption of roofing tiles (ASTM C 1167 – 03)	36
3.1	Chemical composition and loss of ignition of fly ash	42
3.2	Initial selected values of parameters for the optimization process	54
4.1	Assignment of absorption signals in FTIR spectra	65
4.2	Assignment of absorption signals in FTIR spectra of fly ash	67
4.3	Characteristic temperature and residue percentage of UCO related samples	80
4.4	Characteristic temperature and residue percentage of WEO related samples	82
4.5	Initial selected values of parameters for the optimization process	86
4.6	Physical condition of prototypes produced from different composition of WEO	89-90

4.7	Average transverse breaking strength and water absorption of WEO-GRT produced from different binder and filler contents	91
4.8	Average dry transverse strength and flexural strength of WEO-GRT applied with different number of Marshall compactions	93
4.9	Average dry transverse strength and flexural strength of WEO-GRT heat cured at different durations	95
4.10	Dry transverse strength achieved by WEO-GRT incorporated with different types and amount of strong acids	97
4.11	Density of optimized WEO-GRT	100
4.12	Percentage of cold/boiling water absorption and saturation coefficient achieved by optimized catalyzed WEO-GRT.	102
4.13	Dry transverse strength, wet transverse strength and flexural strength achieved by optimized catalyzed WEO-GRT	103
4.14	Selected parameters to be optimized in the manufacturing process of UCO-GRT	105
4.15	Average dry transverse strength and flexural strength of UCO-GRT heat cured for different durations	107
4.16	Average dry transverse strength and flexural strength achieved by WEO-GRT produced with different composition of binder and filler content	109
4.17	The dry transverse strength and flexural strength of UCO-GRT incorporated with different composition of H <sub>2</sub> SO <sub>4</sub>	111
4.18	Density of optimized UCO-GRT	112
4.19	Physical properties of standard catalyzed UCO-GRT produced with optimized parameters	114
4.20	Dry transverse strength and flexural strength of roofing tiles produced from different fly ash to fine sand ratio	116

4.21	Breaking strength, flexural strength achieved and observation on the samples made from different composition of waste oil	119
4.22	Percentage of water absorption, flexural strength (wet condition) and permeation characteristic of samples produced from different composition of waste oil	121
4.23	Thermal properties of optimized roofing tiles	122
4.24	Weight loss of roofing tiles over freeze-thaw cycles	126
4.25	Embodied carbon of catalyzed WEO-GRT	130-131
4.26	Embodied Energy of catalyzed WEO-GRT	132
4.27	Embodied carbon of UCO-GRT	134
4.28	Embodied energy of UCO-GRT	135
4.29	Embodied energy of UCO-RT and WEO-RT	136
4.30	Embodied carbon of UCO-RT and WEO-RT	137-138
5.1	Optimized composition and manufacturing parameters for different types of tile	143-144

## LIST OF FIGURES

<b>Figures</b>	<b>Page</b>
1.1 Global CO <sub>2</sub> concentration since 1980s	2
1.2 Percentage distribution of waste engine oil from different sectors	5
1.3 Conventional roofing tiles produced from different materials	8
2.1 Fat composition in different cooking oil	29
2.2 Molecular structure of triglyceride	29
3.1 Physical appearance of virgin and waste engine oil	39
3.2 Physical appearance of virgin and used cooking oil	40
3.3 Coal-fired ash	42
3.4 Size distribution of sand aggregate	43
3.5 Sand aggregate	43
3.6 Overall flowchart of present research work	45
3.7 FTIR instrument	47
3.8 TGA instrument	49
3.9 Viscometer	49
3.10 Particle sizes analyzer	50
3.11 Sketch of the production of oil-made roofing tiles	53
3.12 Demonstration of flexural strength test	56
3.13 Demonstration of water absorption test	57
3.14 Demonstration of permeability test	58
4.1 FTIR spectrum of used cooking oil (UCO)	64
4.2 FTIR spectrum of waste engine oil (WEO)	64
4.3 FTIR spectrum of fly ash	67

4.4	Observation of UCO samples heat cured for different durations	69
4.5	Magnified ATR-FTIR spectrum of UCO ranging from 3800 to 2800 $\text{cm}^{-1}$	71
4.6	Magnified ATR-FTIR spectrum of UCO ranging from 1800 to 1650 $\text{cm}^{-1}$	72
4.7	Magnified ATR-FTIR spectrum of UCO ranging from 1500 to 600 $\text{cm}^{-1}$	73
4.8	ATR-FTIR spectrum of WEO (3800–2700 $\text{cm}^{-1}$ ) thermally treated at 190°C over 12 hours	76
4.9	Carbonyl region of WEO (1800 – 1600 $\text{cm}^{-1}$ ) thermally treated at 190°C over 12 hours	77
4.10	ATR-FTIR spectrum of WEO (1550 – 500 $\text{cm}^{-1}$ ) thermally treated at 190°C over 12 hours	78
4.11	TGA curves of UCO related samples	80
4.12	DTG curves of UCO related samples	80
4.13	TGA curves of WEO related samples	82
4.14	DTG curves of WEO related samples	82
4.15	SEM images of fly ash (a) x5000 magnification; (b) x10000 magnification	84
4.16	SEM images of UCO-made sample (a) x5000 magnification; (b) x10000 magnification	84
4.17	SEM images of WEO-made sample (a) x5000 magnification; (b) x10000 magnification	84
4.18	Percentage of water absorption and wet transverse strength of WEO-GRT which is (I) Uncoated; (II) Coated with single layer of WEO; and (III) coated with multiple layer of WEO	98
4.19	Specific heat capacity of UCO <sub>4.0</sub> , WEO <sub>3.5</sub> and other commercial building materials	123
4.20	Flexural strength of innovated roofing tiles along with the exposure duration towards UV light	125
4.21	Comparison study of EE and EC of innovated and conventional roofing tile	139

## LIST OF ABBREVIATIONS

ASTM	American Society for Testing and Materials
ATR	Attenuated Total Reflectance
CFA	Coal-fired ash
C <sub>n</sub>	Carbon number
CO <sub>2</sub>	Carbon dioxide
cm	Centimeter
cm <sup>-1</sup>	Reciprocal centimeter (unit of wavelength)
cP	Centipoise (unit of viscosity)
DOE	Malaysian Department of Environment
DTG	Derivative of thermal gravimetric analysis
EC	Embodied Carbon
EE	Embodied Energy
EPA	Environmental Protection Agency
FESEM	field emission scanning electron microscope
FTIR	Fourier Transform Infrared (Instruments)
GHGs	Greenhouse gases
g / kg	Gram / kilogram
g/cm <sup>3</sup>	Gram per volume (unit of density)
H <sub>2</sub> O	Water molecular
ICE	Inventory of Carbon and Energy
IPCC	Intergovernmental Panel on Climate Changes
LCA	Life Cycle Assessment
kg CO <sub>2</sub> /kg	Kilogram of carbon dioxide per kilogram (units of

	carbon dioxide emission)
kWh	Kilowatt hour (unit of power)
MJ/kg	Mega-joule per kilogram (units of energy)
MPa	Mega-pascal
Mt	Metric tons (unit of liquid)
mm	Millimetre
N / kN	Newton / kilo newton
°C	Celsius (unit of temperature)
PAHs	Polycyclic aliphatic hydrocarbons
ppm	Parts per million
Sdn. Bhd.	Sendirian Berhad (Private)
SEM	Scanning electron microscope (Instruments)
TGA	Thermal gravimetric analysis (Instruments)
UCO	Used cooking oil
UCO-GRT	Used cooking oil-made green roofing tile (Name of innovative new roofing tiles)
UCO-RT	Used cooking oil-made roofing tile (Name of innovative new roofing tiles)
UV	ultra-violet
WEO	Waste engine oil
WEO-GRT	Waste engine oil-made green roofing tile (Name of innovative new roofing tiles)
WEO-RT	Waste engine oil-made roofing tile (Name of innovative new roofing tiles)
WVO	Waste vegetable oil

## CHAPTER 1

### INTRODUCTION

#### 1.1 Global Warming

Global warming is a phenomenon that leads to the rising of average temperature of the Earth's climate system. The greenhouse gases (GHGs) emissions are the main contributors of global warming. GHGs would absorb and release the infrared radiation within the atmosphere, consequently warm the lower atmosphere. This process is the fundamental cause of global warming. Practically, GHGs is an important component in controlling the Earth's surface temperature to a suitable extent. Without the presence of naturally existing GHGs, the average temperature of Earth's surface would be  $-18^{\circ}\text{C}$  (NASA GISS, 1998). However, the global temperature is rising with a significant rate after the onset of Industrial Revolution since around 1750s'. It was noticed that the global  $\text{CO}_2$  concentration is increased gradually from 340 ppm in 1980 to 406 ppm in early 2017 (Dlugokencky and Pieter, 2018). The concentrated  $\text{CO}_2$  tends to trap more thermal energy released globally, consequently resulted in global warming and a series of environmental issues. The anticipated effects caused by global warming include dissertation, rising in sea level, precipitation changes and so on (Ning and Jinho, 2009). Figure 1.1 shows the global  $\text{CO}_2$  concentration since 1980s (Dlugokencky and Pieter, 2018).

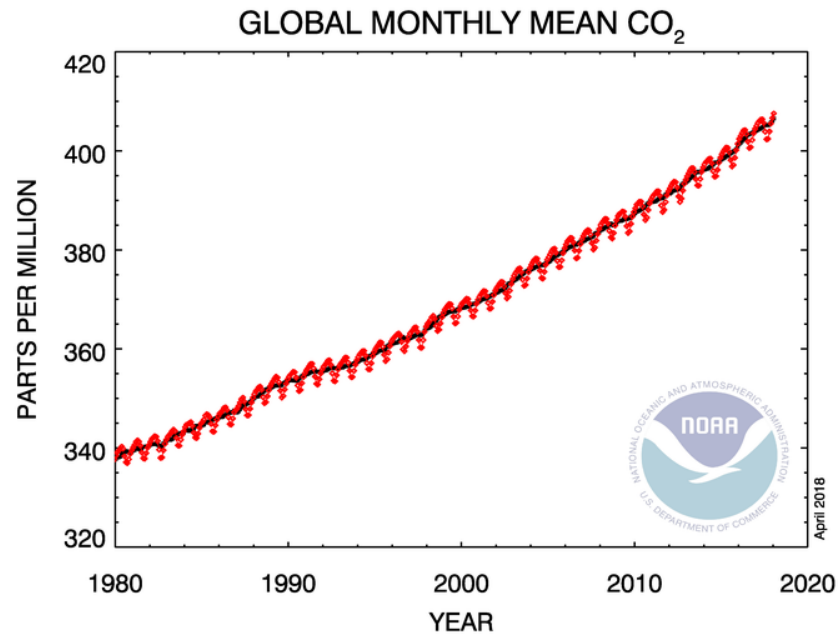


Figure 1.1: Global CO<sub>2</sub> concentration since 1980s (Dlugokencky and Pieter, 2018).

In Intergovernmental Panel on Climate Change (IPCC) Fifth Assessment Report (2013), the human influence has been concluded as the dominant factor that is for the observed warming since the mid-20<sup>th</sup> century. Although the extent of GHGs emissions varies among the nations, the most influential anthropogenic forcing to the global warming is the excessive emitted carbon dioxide (Hegerl et al., 2007). Illegally open burning, combustion of fossil fuel, agriculture activities, and deforestation are responsible to the mentioned problem. In addition, construction sector is also one of the greatest contributors to carbon dioxide emissions. As recorded in IPCC research (2007), 76.7% of global GHGs emitted is contributed by carbon dioxide (Li et al., 2015), while the urbanization area in developing countries solely accounted for 65.54% of the total carbon dioxide emitted (Wu et al., 2014). If GHGs emissions continues with its existing rate, it is

estimated that the global temperature would go beyond the historical value by 2047, or earlier if the problem is not addressed properly. This condition is potentially harmful to the ecosystems, biodiversity, and the livelihoods of human worldwide (Mora et al., 2013). Hence, the new policies on mitigating the GHGs emissions should be attempted as an effort to reduce the carbon dioxide emitted from the construction sector, as well as from other fields. Thus, preserve a greener and cleaner environment for the next generation is our priority.

## **1.2 Waste Management**

The beginning of industrialization, followed by the sustained population growth around the world, lead to the drastically increase of the resource consumption. This situation consequently releases greater amount of waste to the environment. The rapid generation of waste shows significant influences in deteriorating the level of sanitation in the cities, and adversely affecting the quality of urban life. In yearly basis, billions tonnes of waste is generated in Malaysia. Lack of holistic management system and weak environmental awareness are the major factors that lead to the deterioration of waste disposal issue. The current waste disposal approaches such as incineration and landfill are considered not environmental friendly.

Incineration is referred to subjection of waste materials into the combusting chamber to convert them into residues and gaseous products. The treatment system can effectively reduce the mass of waste products to 20 –

30% of their original volume. Hence, it is widely applied among the nations. Incineration approach is effective but controversial. Great amount of gaseous pollutants will be released, as well as great amount of energy is being consumed during the treatment process. Landfill is the oldest, most cost-effective approach in managing the waste material, by simply bury the waste generated in a specific site. Different from incineration or other resource recovery methods, landfill not requires the huge investment in infrastructure, as well as extensive manpower in maintaining the system. Hence it is widely applied in countries with large open spaces. However, several environmental issues are potentially caused by the waste management method. The decomposition gases, including methane and carbon dioxide will be released from the decaying organic waste (rotting foods); both of the gases are members of GHGs. Hence, it would contribute to global warming as discussed previously. Leachate is another adverse environmental issue to be concerned, in which the pollutant may contaminate the groundwater, aquifers or soils.

### **1.3 Waste Engine Oil (WEO)**

Engine oil serves as the lubricating agent for various types of automotive and vehicles' engine. In developed countries with lot of vehicles, waste engine oil (WEO) was generated in large quantities. On a global basis, it was estimated that about 24 million metric tons (Mt) of waste oil was generated per year (Maceiras et al, 2016), while highly industrialized nation such as the United States solely responsible for 7.6 metric tons of WEO generated. WEO was originated from various sectors, including automotive,

industrial, marine and so on (Maceiras et al, 2016). Figure 1.2 shows the percentage distribution of waste engine oil in different sectors (IETC, 2013).

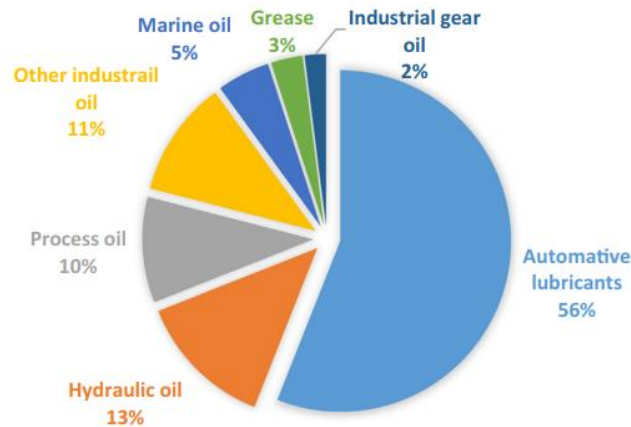


Figure 1.2: Percentage distribution of waste engine oil in different sectors

Unfortunately, up to 60% of generated waste engine oil is discharged into the landfill without proper treatments. Only 8% of them was recycled and refined for further applications (Nerin et al. 2000). As WEO contains significant amount of heavy metals and soot, it was classified as hazardous waste in certain nations (Grzegorz et al., 2015). Soil contamination by WEO is a common occurrence encountered in most of the developing countries, which is caused by the illegally disposal of WEO (Efsun et al., 2015). When WEO leaked into the drainage system, it will contaminate the fresh water resources, harm the marine ecosystem and indirectly threaten human health after being consumed (Alongi, 2012).

#### **1.4 Used Cooking Oil (UCO)**

Used cooking oil refers to vegetable oil that is physically and chemically degraded after long term of cooking and frying process, thus no longer suitable for cooking purpose. Used cooking oils were considered as waste materials and would lead to a series of disposal problems (Forth and Zoorob, 2006). Generally, it was reported that more than 30% of the used oils generated globally was being discarded (Negishia et al., 2003). In the UK and US, it was found that 90 million litre and 300 million gallons of UCO were generated every year from the field of commercial frying (Humayun et al., 2017a). Especially in nations with high population density such as China and India, million liters of UCO can be generated every day. It was noticed that European Union solely accounts for around 700,000 to 1,000,000 tons of UCO generation per year (Mangesh and Ajay, 2006).

In older era, the UCO generated from local restaurants was utilized as animal feed. However, government of European Union banned the practice since 2002, as waste cooking oil may contain harmful components. When the animals were being fed with the UCO, the harmful materials might indirectly transfer into human body, and consequently affect human health (Cvengros and Cvengrosova, 2004). Simply disposal of the UCO to the landfill would also create environmental problems. Thus, an alternative approach of recycling UCO in the production of Biodiesel (Mohammed and Bhargavi, 2015) paves a way to minimize the UCO disposal issue. Despite the advantages, the presence of free fatty acid, water and other impurities

subsequently limit the yield of Biodiesel. Refining of UCO seems to be necessary to enhance the yield. In addition, extra cost is required for the collection, purification, production stages and managing their by-products (Johnny et al., 2013). These conditions consequently increase the operating cost of Biodiesel production to an enormous extent, thus become the main obstacle that restrict the practice (Johnny et al., 2013).

### **1.5 Roofing Tiles**

Roofing tiles is one of the longest standing traditional construction materials besides bricks. It is the necessary part of all buildings, specifically designed to resist weathering, such as heavy rain and strong sunlight. In older era, terracotta and slate were widely used in the production of traditional roofing tiles. In current society, concrete and clay tiles are the most commonly found roofing tiles available in the market. Normally, concrete roofing tile is manufactured from cement, water and sand. Additional materials such as fly ash or plasticizer can be incorporated to enhance the mechanical properties of the tiles. The raw materials utilized in the manufacturing process can be varied accordingly, but usually involved Portland cement, blended hydraulic cement or other natural aggregates. In addition, the production of clay roofing tiles required high temperature, where the mixture of sand aggregate, water, additives and clay extracted from quarry was kiln fired over 1000°C. Furthermore, the modern roof tiles can be produced by using metal, ceramic or shingles, where different types of roofing tiles possess of their pro and cons. Figure 1.3 shows roofing tiles produced with various types of materials.

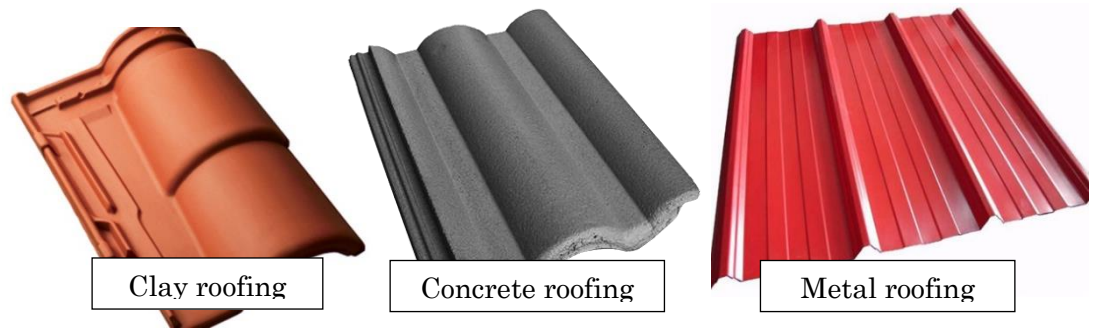


Figure 1.3: Conventional roofing tiles produced from different materials

## 1.6 Problem Statement

Excessive greenhouse gases emissions is one of the dilemmas issue in this modern era. Carbon dioxide, the major component of GHGs that has warming effect will subsequently contribute to the rising of global temperature. The cement manufacturing industry is the main source of carbon dioxide production. Materials used to produce clay-made roofing tile may be from nature, however, kiln firing process is necessary in rigidifying the clay-made products. The process is highly energy intensive and releases significant amount of CO<sub>2</sub> into the atmosphere. To reduce CO<sub>2</sub> emissions from construction industry, many attempts were carried out by using waste materials as ingredients for manufacturing of building materials. For example, replacement of aggregate in the cement pastes with fly ash generated from thermal power plants (Wang and Park, 2016); additional of rice husk ash generated from rice milling process in the concrete (Rawaid et al., 2011); and the incorporation of municipal solid waste incineration ash in the ceramic bricks (Haiying et al., 2011). The focus of this research is about replacing the traditional binders, such as cement and clay rather than aggregate in the

manufacturing process of building materials. The reason is because using waste oil to act as binder can significantly reduce embodied energy (EE) and embodied carbon (EC) of building materials.

In this modern era, cooking oil and engine oil are the most commonly used products, which are related with human life. Cooking oil served as an ingredient in cooking industry, while engine oil functioned as lubricator in vehicles and heavy machine. However, the service lifetime of cooking oil and engine oil are relatively low. After specific service duration, the waste oil will be disposed. Without the proper treatment, the waste oils will lead to extensive damage to the environment. They will create risks of contaminating water and soil with substances that contain substantial hazardous to animal, plant, and marine life, as much harmful to human life. The waste oil disposed in landfill will seep through the bottom of such landfill and subsequently contaminate groundwater supplies. In addition, the incineration of waste oils may result in significant levels of hazardous emissions to the environment, which may expose humans, wildlife, and vegetation to harmful substances. The waste oils can be recycled by re-refined into lubricants, processed into fuel oils, and used as raw materials for the refining and petrochemical industries. However, the cost performance of the recycled products is relatively low with respect to the yield of products. Several recycle treatments such as filtration, centrifugal separation and refining processes consequently increase the cost of the operating system. In addition, the requirement for the recycled products to meet the similar performance standards as the virgin oil subsequently decreases the trend of recycle of the waste oils.

### **1.7 Novel Solution: Waste Oils-made Roofing Tiles**

In this research study, an alternative approach was attempted by utilizing waste engine oil (WEO) and used cooking oil (UCO) as the alternative binders in the production of roofing tiles. Compared to conventional binder such as cement and clay, WEO and UCO possess of much lower embodied carbon (EC) and embodied energy (EE). Hence, utilization of waste oils as sole binder in the production of roofing tiles potentially reduce the negative impacts caused by conventional binder towards the environment. This practice is in line with the policy of Malaysia government to reduce the intensity of GHGs emissions by 40% before 2020. In addition, lower curing temperature is proposed for the thermal treatment of innovated roofing tiles. This attempt would minimize the energy requirement of the operating system, whilst reduce the EE and EC to 8 times lower with respect to the conventional products.

Furthermore, the manufacturing approach of utilizing 100% of waste materials was realized in the research study. Waste engine oil, used cooking oil and fly ash, which are the waste materials generated from automotive industry, cooking industry and thermal power plants respectively, were directly incorporated into the production of environmental-friendly roofing tiles in terms of EE and EC reduction. However, the leachate from the roofing tiles made from waste oil particularly engine oil is still a concern about its leachate effect on the environment. More researches are still needed to look into this issue to verify its effect on the environment. In spite of this unverified leachate

problem, the direct incorporation of waste materials in the production of roofing tile is able to avoid the additional cost required for refining and recycling system, whilst reduce the problem of excessive waste disposal issue.

### **1.8 Objectives**

1. To investigate the chemical reactions involved in the rigidification of roofing tiles during the heat curing process.
2. To optimize the composition of the materials used to produce innovated roofing tiles and its manufacturing processes.
3. To determine the mechanical properties and durability of optimized products.
4. To study the environmental impact in terms of embodied energy and embodied carbon of the roofing tiles made from waste oils.

## **1.9 Organization of Thesis**

The write-up of the thesis follows the same sequence as the research schedule of the postgraduate study. Chapter 1 involves the introduction of the conventional roofing tiles, as well as the crisis of global warming and waste management system in Malaysia. Along with Malaysia's initiatives to reduce the greenhouse gases emission, an alternative approach was attempted in the manufacturing of environmental friendly roofing tiles, as an effort to replace the conventional roofing tiles, which are considered as less environmental friendly. Chapter 2 provides a detailed literature review on the state-of-the-art about various types of roofing tiles, and the performance and durability of roofing tiles produced from various materials. Moreover, it discusses on the environmental impacts caused by the conventional roofing tiles. The review on the incorporation of waste in the existing building materials is also being studied. Chapter 3 reveals the analytical tests in determining the physical and chemical properties of waste materials involved in this study. In addition, it involves the manufacturing process of the waste oil-made roofing tiles, and the mechanical tests to investigate the properties of roofing tiles produced. The details of the analytical results of waste materials, optimization results and the discussions are elaborated in Chapter 4. Lastly, Chapter 5 concludes the findings of this study. In addition, limitation of this study and recommendations for future study can also be found in this chapter.

## CHAPTER 2

### LITERATURE REVIEW

#### 2.1 Current Breakthrough of Roofing Tiles

Roofing tiles are the most common construction materials. They are used as the topping of the buildings. It can be produced from various materials, from natural materials such as slate, wood, and clay to artificial products such as cement, asphalt, metal, and plastic polymers (Ableroof, 2017). Different roofing tiles have their respective pros and cons, which provide wide options for the buyers based on the following properties.

- a) Longevity
- b) Durability
- c) Weight
- d) Slope
- e) Aesthetics
- f) Environmental friendliness
- g) Local code

The advantages and disadvantages of various types of roofing tiles are listed in Table 2.1 (Lorecentral, 2017).

Table 2.1: Advantages and disadvantages of different types of roofing tiles  
(Ableroof, 2017; Lorecentral, 2017).

Types of roofing tiles	Advantages	Disadvantages
Asphalt	<ul style="list-style-type: none"> <li>- Good fire and wind resistance.</li> <li>- Moderate in weight.</li> <li>- Appropriate to variety of slope.</li> </ul>	<ul style="list-style-type: none"> <li>- Not very eco-friendly, due to relatively lower longevity and lower durability.</li> </ul>
Metal	<ul style="list-style-type: none"> <li>- Lightweight.</li> <li>- Recyclable.</li> <li>- High durability.</li> </ul>	<ul style="list-style-type: none"> <li>- Bad aesthetics, less attractive.</li> <li>- Moderate/High in price, according to the types of metal utilized.</li> </ul>
Plastic polymer	<ul style="list-style-type: none"> <li>- High durability.</li> <li>- Light/Moderate in weight.</li> <li>- Good wind resistance.</li> </ul>	<ul style="list-style-type: none"> <li>- May not work for all types of buildings.</li> <li>- More expensive than asphalt.</li> </ul>
Slate	<ul style="list-style-type: none"> <li>- Natural and recyclable.</li> <li>- High durability.</li> <li>- Good fire and wind resistance.</li> </ul>	<ul style="list-style-type: none"> <li>- Heavier.</li> <li>- Expensive.</li> </ul>
Wooden	<ul style="list-style-type: none"> <li>- Natural.</li> <li>- Good aesthetics provide natural look.</li> </ul>	<ul style="list-style-type: none"> <li>- Weak fire resistance.</li> <li>- Low longevity.</li> </ul>

Clay	<ul style="list-style-type: none"> <li>- High durability and longevity.</li> <li>- High fire resistance.</li> </ul>	<ul style="list-style-type: none"> <li>- Heavier, may require roof reinforcement.</li> <li>- Expensive.</li> <li>- Low wind resistance.</li> </ul>
Concrete	<ul style="list-style-type: none"> <li>- High durability and longevity.</li> <li>- High fire resistance.</li> <li>- Cheaper than clay and asphalt.</li> </ul>	<ul style="list-style-type: none"> <li>- Heavier, may require roof reinforcement.</li> <li>- May crack under heavy wind.</li> </ul>

In Malaysia, the conventional roofing tiles that are most commonly used are concrete and clay roofing tiles. Due to the hot but humid atmosphere in Malaysia, the durability of roofing tile plays an important role in prolonging their service duration. Hence, concrete and clay roofing tiles with high durability and sustainability are commonly used.

Along with the enhancement in the technology, the first solar shingles, or being known as photovoltaic roof tile was invented in 2005 (Roddy S. and Doug M., 2013). The implementation of Copper Indium Gallium Selenide solar cells (thin-film solar) in the invented roofing tile tends to convert the sunlight into electricity, and able to generate 12 watt per square feet of roof tile applied. Hence, it can be installed to structures connected with power grid, while the excessive electricity generated will be stored into the grid (Roddy S. and Doug M., 2013). However, the invented roofing tiles are relatively costly

compared with traditional products, but it is still commercially available in specific industries.

The introduction of smart concrete is a great achievement, which possessed a significant enhancement to the service lifetime of the cementitious materials. Smart concrete is different compared to normal concrete. It was implemented with an intelligent system that possessed of self-sensing properties, whilst able to react upon the external stimulus (Baoguo et al., 2015). The mechanism of self-healing in cementitious materials can be categorized into various groups, which are (i) autogenous self-healing (Edvardsen, 1999); (ii) self-healing by mineral admixtures (Roig-Flores et al., 2015); (iii) self-healing by bacteria (Luo et al., 2015); and (iv) self-healing by adhesive agents (Thao et al., 2009). Even though the physico-chemical healing process, influencing factors and service condition of these self-healing mechanisms are different from each other, they are effective in sealing the cracks to certain extent, and restore the mechanical properties of the cracked concrete (Haoliang et al., 2016). Hence, the leakage problems caused by cracks can be avoided, at the same time prolonged the service lifetime of concrete building materials.

## **2.2 Environmental Impact of Conventional Building Materials**

According to IPCC research 2007, 76.7% of emitted global greenhouse gases are contributed by carbon dioxide emission. Over 33% of them are released from the construction sector and continue to increase rapidly,

especially in both the developed and developing countries. After the Copenhagen Conference held in 2009, most of the countries have undertaken specific action to mitigate greenhouse gases emission. However, most of the effort are worthless due to rapid development of urbanization and industrialization (Li and Chen, 2016). Various pollutants and greenhouse gases will be released into the atmosphere during the manufacturing process of traditional building materials, which are responsible for deterioration to the situation. The main factor that leads to high pollutants' emissions during the production of masonry units is due to high amount of energy is needed to produce cement clinker and harden clay (Humayun et al., 2017a). To overcome this issue, a lot of effort was done by utilizing waste materials in replacement of commercially available materials (Beddu et al., 2016), for example: replacing the aggregate by fly ash in the production of concrete block (Pardon et al., 2015). However, an investigation study reported by Hammond & Jones (2011) stated that, as compared to clay, cement and ceramic which are contributing for binding effect in the building materials, aggregate possess of relatively low embodied carbon and embodied energy. Hence, more attention should be focused on evaluating the energy requirement for binder, and replacing it with an alternative, environmental friendly material. Table 2.2 shows the embodied energy and carbon associated with the production of masonry units (Hammond and Jones, 2011).

Table 2.2: Embodied energy and carbon associated with production of masonry units (Hammond and Jones, 2011)

Materials	Embodied Energy, EE (MJ/kg)	Embodied Carbon, EC (KgCO <sub>2</sub> /kg)
Clay brick	3.0	0.32
Aggregate	0.083	0.0048
Cement	5.50	0.93
Concrete (8/10MPa)	0.70	0.65
Clay tiles	6.5	0.45
Ceramic tile	12.0	0.74

Concrete is the most widely used building materials in the world. However, it is well known as building materials with high embodied CO<sub>2</sub> value. The concrete building materials are normally produced using cement, water, sand aggregate and other additives. Cement, as it is commonly known, is a mixture of compounds produced by burning of limestone and clay together under extremely high temperature ranging from 1400 to 1600°C (Kosmatka and Panarese, 1988). The composition of cement with their corresponding chemical formula and weight percentage is shown in Table 2.3 (Hewlett and Young, 1987).

Table 2.3: General information of cement (Hewlett and Young, 1987)

Cement Composition	Weight Percent (%)	Chemical Formula
Tricalcium silicate	50	$\text{Ca}_3\text{SiO}_5$ or $3\text{CaO}.\text{SiO}_2$
Dicalcium silicate	25	$\text{Ca}_2\text{SiO}_4$ or $2\text{CaO}.\text{SiO}_2$
Tricalcium aluminate	10	$\text{Ca}_3\text{Al}_2\text{O}_6$ or $3\text{CaO} .\text{Al}_2\text{O}_3$
Tetracalcium aluminoferrite	10	$\text{Ca}_4\text{Al}_2\text{Fe}_2\text{O}_{10}$ or $4\text{CaO}.\text{Al}_2\text{O}_3.\text{Fe}_2\text{O}_3$
Gypsum	5	$\text{CaSO}_4.2\text{H}_2\text{O}$

When water is added to cement, each of the cement particle will undergo hydration reaction to bind and hold other raw materials together to form a synthetic conglomerate. However, cement was the key contributor to the embodied CO<sub>2</sub> impact in the concrete. It was noticed that the average embodied CO<sub>2</sub> in United States is around 100 kg CO<sub>2</sub> per ton of cementitious products (The Concrete Centre, Mineral Product Association, 2017). However, the embodied carbon of concrete can be varied according to the materials incorporated. In previous study, it was noticed that the addition of fly ash could significantly reduce the overall greenhouse gases emission associated with the production of concrete, while the overall reduction value can be as high as 40% depending on the mix compositions and the application (Strine Environments, 2018).

Clay is a finely-grained natural rock or soil material that combines one or more clay minerals with possible traces of quartz (SiO<sub>4</sub>), metal oxides (Al<sub>2</sub>O<sub>3</sub> , MgO etc.) and organic matter (Guggenheim and Martin, 1995). In the

production of clay-made building materials, it usually involves kiln-firing process to promote the maturity, or commonly known as hardening process of clay. The variation in temperature during fired-up and cooled down the clay resulted in several physical and chemical changes in clay body. This process consequently turned the clay from a soft, fragile substance to a hard, rigid body which is impervious to water and wind (Beth, 2017). Table 2.4 shows the physical and chemical changes within the clay along with the temperature (Beth, 2017).

Table 2.4: Physical and chemical changes of clay associated with ventilated temperature (Beth, 2017).

Approximate Temperature (°C)	Physical and Chemical Changes
100	<ul style="list-style-type: none"> <li>- At the boiling temperature of water, any remaining atmosphere water will be converted into the steam, and evaporate out from clay.</li> <li>- Compaction of clay and minor shrinkage occur.</li> </ul>
300 – 800	<ul style="list-style-type: none"> <li>- The carbon, sulfur and other organic materials in clay body will be burnt off.</li> </ul>
350 – 800	<ul style="list-style-type: none"> <li>- The atmosphere water was evaporated under 100°C. However, chemically bonded H<sub>2</sub>O was remained, which occupied up to 14% by weight of clay body.</li> <li>- Under elevated temperature, the hydrogen bonds will break and release the chemically bonded H<sub>2</sub>O from clay body.</li> </ul>

	- The weight of clay will decrease, but no physical shrinkage occurs.
573	- Quartz inversion occurs – The crystallization of silica oxide under specific temperature.
900	- Sintering begins to occur. The clay particles will stick together and begin to fuse to each other.
1005 – 1390	<ul style="list-style-type: none"> <li>- Vitrification and maturation of clay body occur.</li> <li>- Vitrification is a gradual process in which the most easily melt materials will dissolve and filling the spaces between the more refractory particles. The melt particles will promote further melting, subsequently compacting and strengthening the clay body.</li> <li>- Mullite (aluminium silicate), which are long, needle-like crystal will form in this stage. It acts as binder by strengthening the clay body even further.</li> </ul>

### **2.3 Review on Utilization of Waste Materials in the Production of Building Materials**

Roofing tiles are widely used building materials applied around the world. Conventional roofing tiles are manufactured from ordinary Portland cement (OPC) concrete, or kiln firing of clay under high temperature. Hence, roofing tiles have relatively high embodied carbon and embodied energy. Recently, the interest on the energy efficiency of building materials was grown among the society. This trend is rising due to the increase of environmental

awareness of the citizens towards the importance of sustainable constructions. In addition, the shortages of natural resources for manufacturing of conventional building materials are encountered around the world. Hence, this led to a challenge for the researchers to replace the existing resources with alternative, more environmental friendly materials. As an effort for environmental protection and sustainable development, bundles of researches were carried out by incorporating the waste in the production of building materials. The embodied carbon building materials may decrease significantly according to the types of the waste materials incorporated. Literature highlighted that the CO<sub>2</sub> emission in the case for building showing decrease by 30% when materials with lower embodied carbon were utilized instead of conventional materials. This shows the importance of materials selection in controlling the carbon footprint of building materials (González and Navarro, 2006).

Coal-fired ash (CFA) is one of the most common waste products incorporated in the building materials since decades as reported. It was found that the physical properties of building bricks were being enhanced when ashes (Class C and F fly ashes, bottom ash, rich husk ash and so on) were incorporated in the fabrication of building bricks (Zhang, 2013). In addition, the incorporation of 20% of municipal solid waste incineration ash in the building brick significantly enhanced its compressive strength, whilst decreased the probability of shrinkage and leakage, which is the mostly encountered issue for ceramic bricks (Haiying et al., 2011). Besides, using of fly ash up to 50% concentration able to develop clay bricks with greater fired

compressive strength and heat insulation capability (Mei-In et al., 2001). Moreover, the utilization of pulverized coal ash can increase the durability of the binding materials, reduce energy consumption and conserve other nature and raw materials (Adams, 2015). However, excessive addition of fly ash (>50%) showed adverse effect toward the bricks, which might reduce the compressive strength of masonry units (Kumar, 2001) and workability of the materials (Garbacz and Sokolowska, 2013).

In 2009, the feasibility of utilizing polluted river sediments in the production of building bricks was conducted (Samara et al., 2009). In the manufacturing process, pre-treated sediments was used to replace 15% of quartz sand in the normal bricks. It was later undergone different qualification tests. As a result, the bricks showed significant increase in terms of compressive strength and firing shrinkage, whilst lowering of the porosity and water absorption (Samara et al., 2009). Similar properties enhancement was indicated in the production of lightweight clay bricks together with mixture of waste materials, which composed of sawdust, compost, marble and spent earth from oil filtration. The optimized result was obtained by incorporating 5% of sawdust, 10% of compost, 15% of marble and 15% of spent earth from oil filtration in the clay mixture, followed by heat cured under 1050°C (Eliche-Quesada et al., 2012). Yet importantly, the production of masonry units without the addition of Portland cement was studied by replacing it with limestone powder waste and fly ash (Turgut, 2010). The mixture of limestone waste and fly ash was wetted, compacted, and cured in water tank for 7, 28 and 90 days, followed by oven dried at 105°C. Even though the mechanical

properties of building blocks produced were not as good as cementitious products, the possibility of utilizing limestone powder waste, fly ash and water only in the production of masonry unit was proved.

Instead of clay and cementitious products, the investigation studies on waste replacement were also being conducted on geo-polymerized building materials. By using sodium hydroxide as alkaline activator, geo-polymer bricks were manufactured by utilizing copper mine tailings (Ahmari and Zhang, 2012). The physical and mechanical properties of geo-polymer brick produced were optimized by controlling the water contents, concentration of activator, forming pressure, and curing temperature. As a result, the brick products successfully met the ASTM standards in terms of compressive strength, water absorption and abrasion resistance. In their further study, cement kiln dust was incorporated in the production of copper mine tailing-made geo-polymer bricks (Ahmari and Zhang, 2013). The results showed significant enhancement on the physical and mechanical properties and the durability of brick produced. However, it led to slightly increment in the water absorption, but it was still within the acceptable limit. It is noticed that investigation studies on many other types of waste materials are also being conducted for geo-polymer building materials, including blast furnace slag (Hu et al., 2008); mine tailing with fly ash (Zhang et al., 2011); red mud with rice husk ash (He et al., 2013) etc. All of the researches showed positive results toward the possibility of waste materials to be incorporated in the production of building materials.

## **2.4 Waste Oils**

Generally, waste oils can be classified into two main categories, which are:

- a) waste engine oil;
- b) used cooking oil.

### **2.4.1 Waste Engine Oil**

Engine oil, also known as lubricating or motor oil, are usually used for the lubrication of internal combustion engine. Engine oil is comprised of base oil, which are manufactured from petroleum-based hydrocarbon derived from crude oil. Typically engine oil consist of hydrocarbon with carbon number ( $C_n$ ) of  $C_{18}$  to  $C_{34}$  in each molecule (Chris, 2007), polyalphaolefins and up to 20% of ester for better dissolution of additives (Schlosberg et al., 2001). Additives may be incorporated to enhance the properties of engine oil, particularly anti-wear additive to reduce the friction and wear on moving parts; detergents and dispersants to clean the engine from varnish and sludge; and oxidation inhibitor to prevent the oxidation at elevated operating temperature, and hence reduce the possibility of rust and corrosion within the engine.

However, engine oil will be contaminated by both physical and chemical impurities after long term of operation. When the level of contamination reached a significant extent, engine oil will lost its original properties, and no longer suitable for lubrication purpose. The discharged

engine oil will be known as waste engine oil (WEO). During the operation, the high temperature and pressure atmosphere within the engine would partially oxidize the components of engine oil, thus chemically affected its original properties (Shiva et al, 2014). The impurities generated from the wearing parts of engine components is responsible for the physical contamination in WEO. In addition, the heavy metal especially high quantities of lead (Pb) infiltration during the wearing process would further contribute to the hazardous characteristic of WEO (El-Fadel and Khoury, 2001). Hence, proper treatment is necessary before disposal of WEO to the landfill. Table 2.5 shows the quantity of metals present in the WEO and the maximum level permitted by the United State Environmental Protection Agency (EPA) and the Malaysian Department of Environment (DOE).

Table 2.5: Quantity of metals presented in WEO and their limitations (You et al., 2011).

Constituents	Symbol	United State Maximum Allowable Level	Malaysia Maximum Allowable Level
Arsenic	As	5 ppm	5 ppm
Ash	-	NA	NA
Cadmium	Cd	2 ppm	2 ppm
Chromium	Cr	10 ppm	10 ppm
Lead	Pb	100 ppm	100 ppm
Sulfur	S	NA	NA
Total Halogen	-	4000 ppm	1000 ppm

As an effort to minimize the environmental issue caused by the improper disposal of waste, the WEO generated from various industries were collected and reproduced for further application. At present, WEO can be regenerated through stripping, hydrogenation and distillation process. It was noticed that by utilizing Iranian nano-porous Ca-bentonite as indicator, WEO can be recovered and reuse as lube oil through distillation and adsorption techniques (Salem et al., 2015). However, the regenerated WEO showed lower quality due to the chemical changes in the oil composition, thus failed to meet the commercial standards. Another recovery approach was attempted by non-isothermal pyrolysis of WEO together with polystyrene, and successfully converted the WEO into diesel fuel (Kim et al., 2013). Nevertheless, the high energy consumed during the treatment process was another issue to be considered. Therefore, a more feasible and environmental tactic should be proposed to utilize the WEO, purposely to enhance the global recycle rate of WEO.

Direct incorporation of WEO in the production of building materials seem as an effective way to recycle the WEO for further application. No filtration is needed to get rid of the solid particles from WEO prior to the manufacturing process, hence it will not increase the operating cost. On the contrary, it might reduce the cost for the original raw materials that was being replaced. In 1918, the first attempt of incorporating WEO in building materials was carried out. By substituting the air entraining chemical admixture in concrete with WEO, it was noticed that freeze-thaw resistance and durability of the product were being enhanced (Mindess and Young, 1981). In addition,

incorporation of WEO as a mediator can also improve the fluidity (Bilal et al., 2003) and compressive strength (Kamal et al., 2014) of construction materials. Under specific condition, the integration of WEO in the pavement materials offered the stiffness reduction. Therefore, the cracking resistance of the pavement produced was significantly increased (Nurul et al., 2015). The research findings on utilization of WEO as sole binder of building materials is limited. However, some researchers used WEO as additive for concrete production to (i) reduce total porosity of concrete (Nasir et al., 2011) (ii) enhance concrete's durability and (iii) lower concrete's water permeation (Beddu et al., 2016).

#### **2.4.2 Used Cooking Oil**

Cooking oils are the purified consumable oil, which can be originated from either plant or animals. Saturated fats, mono- and polyunsaturated fats are the abundant components present in cooking oil. The compositions of cooking oil might vary according to the sources. Cooking oil was classified as most important renewable resources globally, as it can be directly extracted from vegetable and herbs (Karak, 2012), as well as obtained from animals. Figure 2.1 shows the fat composition presence in different types of cooking oils (ChartsBin statistics collector team, 2011). It was noticed that saturated fats are solid under room temperature, while most of them are extracted from animal products. However, it can be found in certain plant sources, such as palm oil, palm kernel oil, and coconut oil. While most of the unsaturated (both monounsaturated and polyunsaturated) are extracted from plants and fishes.

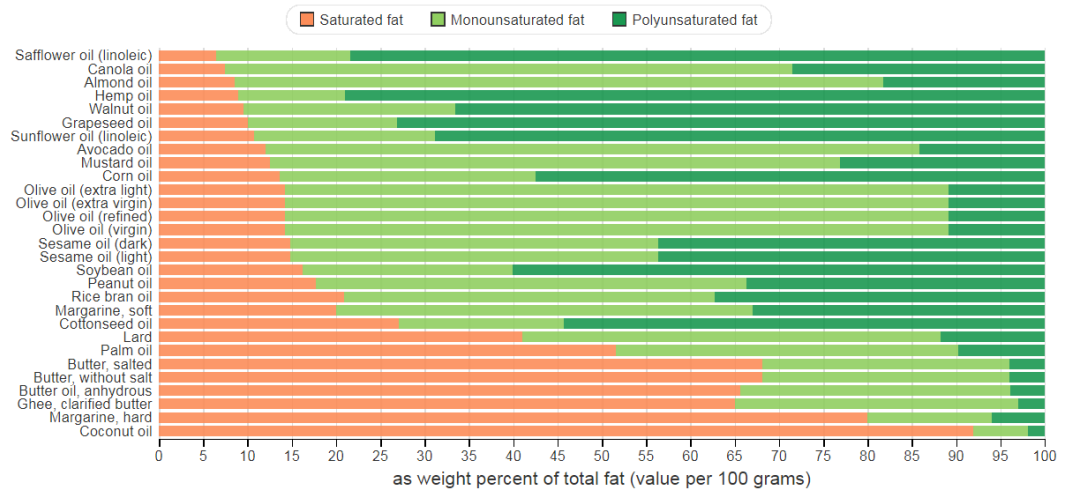


Figure 2.1: Fat compositions in different cooking oils

Due to Malaysia is second largest palm oil producer, the oil used by Malaysian mostly is palm oil. Vegetable oil including palm oil is composed of triglycerides, which are built up with one glycerol with three fatty acids. Each fatty acid possess of different carbon numbers ranging from C<sub>8</sub> to C<sub>18</sub>, and different extent of unsaturation, depending on the types and sources of the oils.

Figure 2.2 shows the typical molecular structure of a triglyceride.

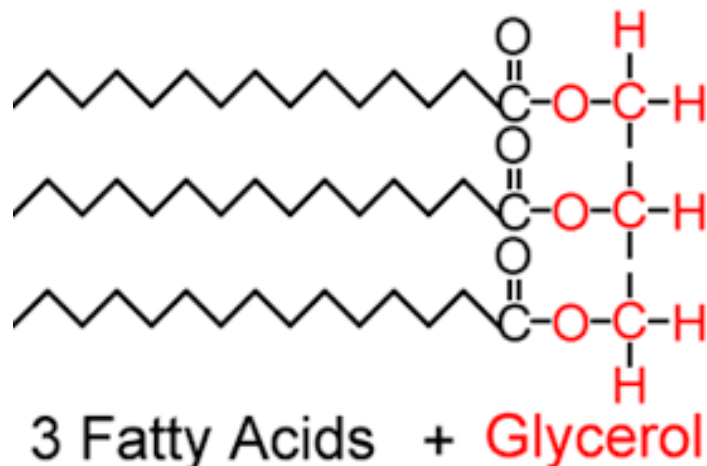


Figure 2.2: Molecular structure of triglyceride

During the frying process, the cooking oil is continuously exposed to high temperature, while the presence of oxygen (from air) and moisture (from air and foods) consequently subjected to the degradation of cooking oil (Huseyin et al., 2011). The degradation reactions occur under the phenomenon including:

- a) Hydrolysis reaction. Triglyceride is hydrolysed when it reacts with water molecule under high temperature. This reaction produces glycerol and free fatty acids (Gertz C., 2000).
- b) Oxidation reaction. The molecule of oil is oxidized when exposed to high temperature in the presence of oxygen. The oxidation products including oxidized monomeric, dimeric, and oligomeric triglycerides, and some volatile compounds (Stevenson et al., 1984).
- c) Polymerization involves reactions (a) and (b), under high temperature. Dimeric and polymeric triglycerides with aliphatic structure are the products generated from this reaction (Choe and Min, 2007).

The occurrence of aforementioned degradation reactions subsequently lead to the changes in the physical and chemical properties of cooking oils, including increase of viscosity, free fatty acid (FFA) content, number of polymerized triglycerides, and decrease in smoke points and the number of unsaturated compounds. When the level of degradation reaches a significant extent, the cooking oil will no longer appropriate to be used for consumption

again. Thus, in this study, the used cooking oil (UCO) is referred as waste vegetable oil (WVO).

In recent years, the recycle and reuse of UCO was focused on the biodiesel productions. However, production of biodiesel requires complex physical and chemical treatments. The high operating and management costs make them less competitive to be considered as substantial replacements of traditional fossil fuel (Enweremadu and Mbarawa, 2009). Thus, direct incorporation of WVO in other applications seems as an alternative approach which might significantly decrease the impacts in terms of environmental, energetic and economic aspects, with respect to the biodiesel production (Capuano et al., 2017).

In practice, WVO can be utilized as an additive to rejuvenate the aged asphalt binder. The results indicated that WVO could effectively softening the aged asphalt binders. Meanwhile, the physical and rheological properties of the WVO-modified asphalt binders can be improved to that of their corresponding virgin asphalts (Meizhu et al., 2014). Moreover, several positive effects can be drawn by the additional of WVO into the original asphalt cement. The results showed that incorporation of an appropriate amounts of WVO could significantly enhance the ductility and workability of the binder, whilst increase the flash and fire points and made the modified asphalt binder safer to be work with (Aslam et al., 2018). In addition, the concept of utilizing WVO as a sole binder during manufacturing of building materials was proved possible (Forth and Zoorob, 2006). This approach was

further investigated and it was revealed that the chemical reaction occurs on double bonds and secondary oxidation products within the waste vegetable oil after going through thermal treatments. The reaction increases the viscosity and hardness of waste vegetable oil which is suitable to be used as binders of building materials (Heaton et al., 2014). Furthermore, replacement of traditional binders such as cement and clay with WVO might reduce the use of virgin resources. Furthermore, replacing of the traditional binders with waste oils were indirectly decrease the embodied carbon and embodied energy of building materials (Humayun et al., 2017a).

## **2.5 Fly Ash**

Recently, the deteriorated global issues have drawn the public's attention toward the importance of sustainable building construction. More attentions are focused on evaluating the energy efficiency of building materials, by investigating the alternative approach to control and minimize the energy consumption and carbon dioxides emissions of the building materials. Thus, plenty of researches were carried out, which involved the replacement of existing resources with waste, recycled materials which was considered as more environmental friendly in terms of embodied carbon and embodied energy.

Fly ash is one of the commonly used waste materials utilized in controlling the energy efficiency of building materials. The popularity of fly ash to serve as fillers in construction materials is increased as it can be

obtained in abundant amount with a lower price. Normally, fly ash is incorporated in the cementitious products to fill up the interior voids. It is functioned to minimize the porosity whilst enhance the mechanical properties of the masonry units. In addition, the embodied energy for fly ash is considered as negligible and its embodied carbon is approximately 0.14 kg CO<sub>2</sub>/equivalent (Chani et al., 2003). Hence, incorporation of fly ash tends to reduce the energy requirements, whilst increase the durability of binding materials and conserve the existing resources from being exhausted.

Fly ash can be classified into two categories, Class C and Class F in accordance with their chemical compositions. Fly ash is a heterogeneous materials, which mainly composed of SiO<sub>2</sub>, Al<sub>2</sub>O<sub>3</sub>, Fe<sub>2</sub>O<sub>3</sub> and CaO. As defined in ASTM C 618, the main difference between both classes of fly ash is the amount of pozzolanic content. The pozzolanic compounds (silica oxide, alumina oxide, and iron oxide) occupied more than 70% of the composition of Class F fly ash, while Class C fly ash only possessed 50% to 70% of these compounds. Hence, the pozzolanic effect of Class F ashes is higher than Class C ashes. Due to the presence high extent of pozzolanic compounds, fly ashes are able to mitigate against chemical and sulfate attack, alkali silica reaction as well as corrosion of reinforcement (Nurcan et al., 2012). In addition, Class C ashes contain at least 20% of calcium oxide in terms of its total volume. Normally Class F fly ash contains minute amount of calcium oxide; but some of the sources may possess 8% to 16% of calcium oxide. Furthermore, both classes of fly ash show excellent performance in reducing the permeability of concrete, while Class F fly ash tends to give better permeability resistance.

## **2.6 Basic Requirements of Roofing Tiles**

### **2.6.1 Transverse and Flexural Strength**

Transverse strength, which is also being referred as compressive strength, is the ability of materials to withstand a load in the axial direction while the whole area under compression. Transverse strength can be differentiated and conducted in two different conditions, which are dry and wet, respectively. The minimum transverse strength requirement of each condition is different, while roofing tiles can be categorized into high profile, medium profile or low profile according to the transverse strength achieved (see Table 2.6). Flexural strength is the ability of the material to a bear load without bending. It was derived from compressive strength and being expressed in MPa. The flexural strength is highly related to the porosity or density of construction materials. It was noticed that high-density concretes possessed hard concrete matrices, which amplified its transverse strength. In addition, increase of 1% of porosity in the concrete materials would reduce its strength by 6%.

Table 2.6: Standard limitation of transverse strength of roofing tiles (ASTM C 1167 – 03)

	Transverse Strength Requirements (N)	
	Dry	Wet
High Profile	1779	1334
Medium Profile	1334	1001
Low Profile	1334	1001

### 2.6.2 Water Absorption

The real time weight of construction materials is highly dependent on the water absorption capability. Construction materials with high water absorption capability would absorb water and become heavier. This phenomenon has a great possibility to cause structural damage in the construction framework. The risk will increase especially for roofing tiles materials, which were directly exposed to rainwater and water vapour from atmosphere. Therefore, it is important to use non-hygroscopic ingredient to produce roofing tiles. If it is unavoidable that the hygroscopic ingredient must be used in producing roofing tiles, the surface of the roofing tiles can be coated with a layer of water resistance materials.

In the construction industry, various allowable limits for percentage of water absorption of roofing tiles were set for the classification of roofing tiles. According to the ASTM C 1167 – 03, roofing tiles could be categorized into three different grades, where each grade having different limitations for water

absorption (see Table 2.7). In addition, limitation for lightweight concrete roofing tiles is higher, which reaches up to 20%. Saturation coefficient is an indication of the probable resistance of building materials to freezing and thawing. The water absorption achieved by the roofing tile must not exceed 6% as per ASTM C 1167-03 requirement.

Table 2.7: Standard limitation of percentage of water absorption of roofing tiles (ASTM C 1167 – 03)

Grades	Absorption Requirements	
	Maximum Water Absorption (%)	Maximum Saturation Coefficient
1	6	0.74
2	11	0.80
3	13	0.84

### 2.6.3 Permeable Characteristic

Malaysia is a country with immense amount of rainfall. Considering the situation, the permeable characteristic is the most important criteria to be concerned during the manufacturing of roofing tiles. Permeable characteristic of concrete roofing tiles was influenced by certain factors, including the size, shape, porosity, as well as the density of the concrete matrix. According to the ASTM C 67 – 07a, permeability test was conducted by observing the bottom part of the roofing tiles. No water droplets should be able to penetrate through the roofing tiles. If water droplets are found at the bottom part of roofing tiles, the tiles are considered failed the permeability test.

## **2.7 Summary of Literature Review**

Roofing tile is one of the most important building materials in construction industry. However, the manufacturing processes of the conventional roofing tiles is responsible for high carbon emissions and huge energy consumption. In addition, waste engine oil, used cooking oil, and fly ash are the waste products generated from different sectors, which lost their initial properties during their service lifetime. The waste materials have their specific properties, which would lead to several enhancement when incorporated in the manufacturing of building materials. However, the advantages that can be obtained from the waste materials are limited, as excessive waste incorporation would adversely affect the original properties of the final products. Hence, the idea of combining all waste materials in a single manufacturing process was attempted, which involved all the selected waste materials in the manufacturing process of roofing tiles. The waste materials were used to replace the traditional binder and aggregate used in the manufacturing process. A novel product which is considered as more eco-friendly is obtained at the end of the manufacturing process. A series of fundamental studies had been carried out to determine the characteristic of the novel product, and the waste materials, which is suitable to be used in the innovated manufacturing process. Lastly, the ASTM standards are used as the guidelines of the manufacturing process of the innovated roofing tiles.

## CHAPTER 3

### METHODOLOGY

#### 3.1 Selection of Materials

##### 3.1.1 Waste Engine Oil (WEO)

Waste engine oil (WEO) used in this project served as an alternative binder in the production of roofing tiles. It was obtained from the local automotive centers. The oil was a collection of used lubricating oil residues from various vehicles. WEO is highly contaminated by both physical and chemical impurities during the operation of the engine. Generally, waste engine oil is constituted of a vast range of branched aliphatic and aromatic hydrocarbons, a great amount of gasoline, additives, and nitrogen and sulfur compounds with respect to the fresh engine oil (Elena and John, 2003). The qualitative analysis on the blended WEO showed the presence of diminutive amounts of heavy metals (Pb, Zn, As, Ag, Ge, Sb, Tl, V and Fe) which can commonly found in lubricating oil (Grzegorz et al., 2015). However, the contamination extent of WEO is depended on the combustion process, operation temperature and contaminant sources (Al-Ghouti and Al-Atoum, 2009). The viscosity and molecular structure of the WEO might vary according to the extent of contamination process in different vehicles (Jia et al., 2014). Hence, the collected WEO with similar physical (based on

rheological testing) and chemical properties (based on FTIR analysis) were blended and utilized in this study. Figure 3.1 shows the physical observation of a fresh and a waste engine oils. It was noticed that the fresh engine oil is gold in color and translucent, while after a series of heating and lubricating process in engine, the oil turned into black and opaque.

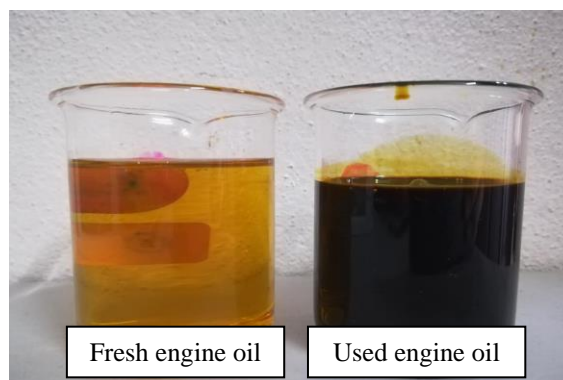


Figure 3.1: Physical appearance of a virgin and a waste engine oil

### 3.1.2 Used Cooking Oil (UCO)

Used cooking oil (UCO) which is the discarded vegetable oil was collected from local restaurants. It can serve as an alternative binder of the innovated roofing tiles proposed in this research study. Different from the virgin vegetable oil, UCO consists of significant amount of free fatty acids, which was released from the hydrolysis of triglycerides during cooking or frying process. The presence of free fatty acids would increase the acidity of the cooking oil, while polymerization of triglyceride would increase the viscosity of the used oil. It can also be observed that UCO are brownish yellow in color, which is darker compared to virgin cooking oil which is yellow in color. This phenomenon is due to the presence of a greater amount of impurities in the UCO. As the degree of contamination might vary based on

the service duration, the UCO collected was mixed thoroughly before being utilized for the binding purpose. Figure 3.2 shows the physical appearance of a virgin and a used cooking oil.

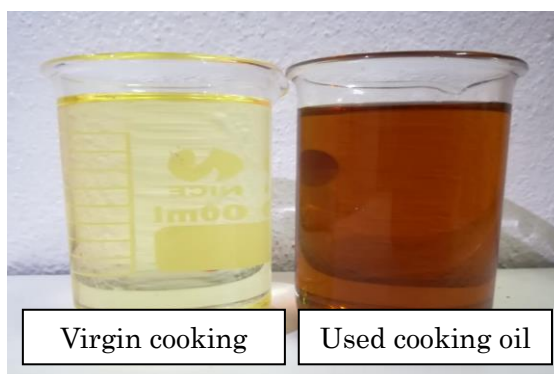


Figure 3.2: Physical appearance of a virgin and a used cooking oil

### 3.1.3 Catalyst

In order to develop the greater strength of roofing tiles, a high extent of polymerization reaction is necessary. Hence, catalyst including hydrochloric acid (HCl), nitric acid (HNO<sub>3</sub>) or sulfuric acid (H<sub>2</sub>SO<sub>4</sub>) is added into roofing tiles to enhance the rate of polymerization reaction. Catalyst is able to lower the activation energy required to trigger a polymerization reaction, thus increasing the energy efficiency of the manufacturing process (Marvin, 1974). However, catalyst will not be consumed at the end of the chemical reaction. The excessive catalyst will not further enhance the rate of polymerization reactions, contrarily, it may disrupt the interaction and development of polymer chains (Teoh et al., 2018). Hence, AR grade of strong acid with original concentration of 8.33M was diluted to 0.1M through simple dilution method before incorporated into the production.

### 3.1.4 Coal-fired Ash

Coal-fired ash (CFA) is in brownish color released from thermal power plant (see Figure 3.3). CFA is composed of both fly and bottom ash. The ashes can be classified into two different classes, which are Class C and F ashes depending on their chemical composition. Class F ash has greater amount of pozzolanic components which can develop the strength of roofing tiles via pozzolanic reaction (J. Paya et al., 2000). In addition, fly ash has higher fineness than bottom ash, and can contribute an extra compressive strength by packing effect (Jatuphon et al., 2005). However, fly ash can only react with water molecules from atmosphere to trigger the pozzolanic reaction. As no water was added as an ingredient in the manufacturing process, the pozzolanic reaction and packing effect is negligible.

In this study, fly ash was collected from TNB Janamanjung Sdn. Bhd. and it is served as filler in the production of roofing tiles. The chemical composition of fly ash was analyzed using Energy-dispersive X-ray spectroscopy (EDX). The data obtained is shown in Table 3.1. As the total amount of  $\text{SiO}_2$ ,  $\text{Al}_2\text{O}_3$  and  $\text{Fe}_2\text{O}_3$  is greater than 70% whilst the volume of CaO is less than 15%, the fly ash utilized in this study was categorized as class F as per ASTM C 618 – 12a (Pardon et al., 2015). The average particle size of the fly ash in terms of number and volume is 2.124  $\mu\text{m}$  and 14.415  $\mu\text{m}$  respectively and its specific gravity is 0.26 .

Table 3.1: Chemical composition and loss of ignition of fly ash

Oxide Components	Percentage Constitution (%)	ASTM C 618 – 12a
Silicon dioxide (SiO <sub>2</sub> )	58.73	SiO <sub>2</sub> + Al <sub>2</sub> O <sub>3</sub> + Fe <sub>2</sub> O <sub>3</sub> ≥ 70%
Aluminium oxide (Al <sub>2</sub> O <sub>3</sub> )	27.64	
Ferrous oxide (Fe <sub>2</sub> O <sub>3</sub> )	5.06	
Calcium oxide (CaO)	3.44	-
Magnesium oxide (MgO)	2.12	-
Sodium oxide (Na <sub>2</sub> O)	1.26	-
Sulfur trioxide (SO <sub>3</sub> )	0.89	≤ 5.0%
Loss of Ignition (LOI)	1.68	≤ 6.0%



Figure 3.3: Coal-fired ash

### 3.1.5 Sand Aggregate

The mixture of mining and river sand was utilized as aggregate in the production of roofing tiles (see Figure 3.5). Fine sand functioned to enhance the strength of the tiles produced. ASTM C 127-88 was referred to determine the specific gravity of sand aggregate, while the size distribution of fine aggregate used was investigated in accordance to ASTM C 136 as shown in Figure 3.4.

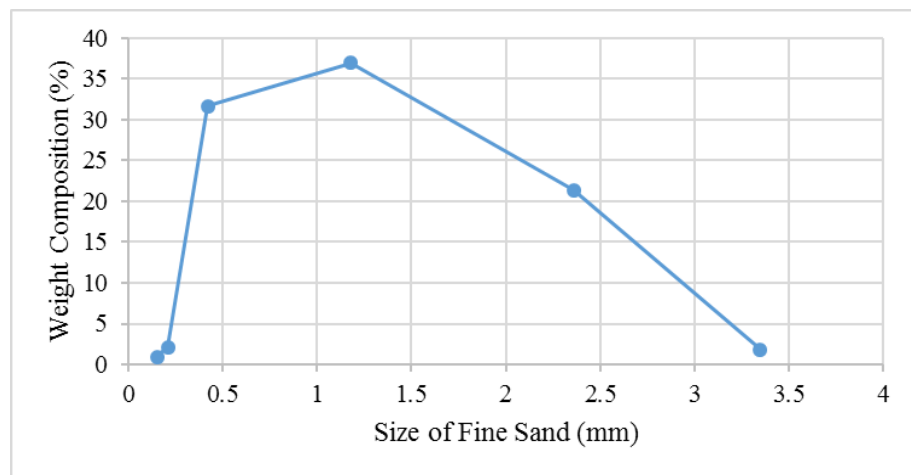


Figure 3.4: Size distribution of sand aggregate



Figure 3.5: Sand aggregate

## 3.2 Methodology

This research study consisted of several experimental procedures. Figure 3.6 showed the overall research flowchart, which summarized the present research work to provide an overview of the research activities that have been carried out throughout the study. The research activities are divided into three step:

- I. Determination of the waste materials which are most suitable for the production of innovated roofing tiles.
- II. Optimization of the composition of raw materials and the operating condition of the manufacturing process of innovated roofing tiles.
- III. Investigation of the physical and chemical properties of the innovated roofing tiles produced.
- IV. Result analysis and report writing.

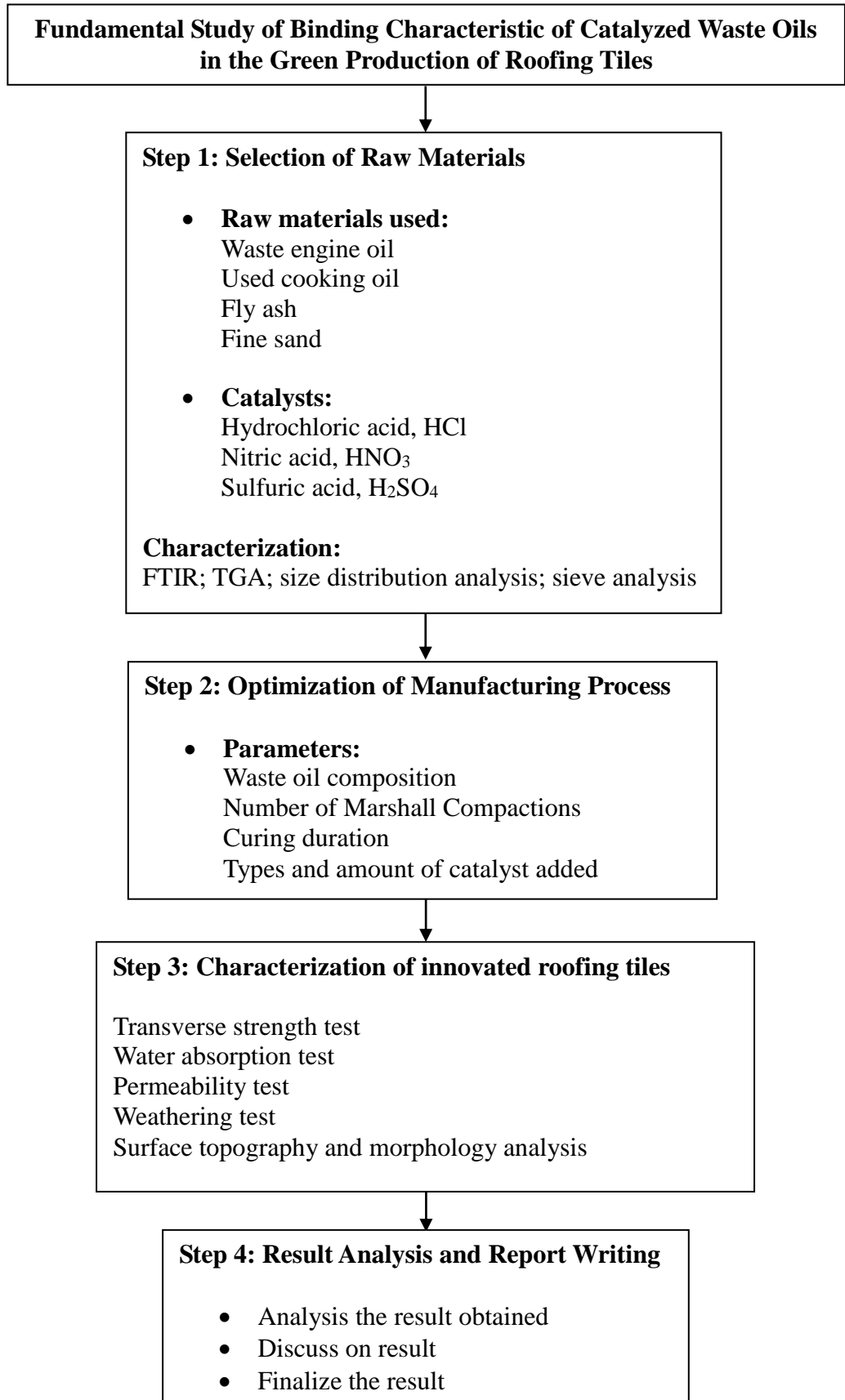


Figure 3.6: Overall flowchart of present research work

### 3.2.1 Preliminary Analysis of Selected Materials

#### 3.2.1.1 Fourier-Transform Infrared Spectroscopy (FTIR)

Fourier-transform Infrared spectrometry is a traditional analysis approach used to investigate the chemical structures and functional groups presented in the samples. In this study, the functional groups of WEO and UCO were determined by using FTIR analysis spectroscope, *Model PerkinElmer Spectrum RX 1* equipped with *Perkin Elmer Spectrum™ 10 software platform*. A drop of waste oil was placed on the face of a highly polished salt plate. A second plate was placed on the top of the first plate in order to spread the liquid sample in a thin layer between the plates. The plates were clamped together and mount onto the sample holder for FTIR analysis. The FTIR spectra of the samples were measured in a frequency range of 4000-400 $\text{cm}^{-1}$ . Every sample was scanned for 16 times with resolution of 4  $\text{cm}^{-1}$ . The spectroscopy results obtained were tabulated using MATLAB software.

In the liquid waste oils, the carbonyl groups (C=O) and double bonds (C=C) were responsible to the hardening properties of binder (Heaton et al., 2014). Hence, the preliminary binding potential of WEO and UCO as binder can be determined by analyzing the waste oils obtained. In addition, the oxidation extent of waste oils was investigated by determining the ratio of area of carbonyl vibration with respect to its area of saturated C-C band (Negulescu et al., 2006). Those absorption peaks are located at around 1710  $\text{cm}^{-1}$  (Elena and John, 2003) and 1450  $\text{cm}^{-1}$  (Mariana et al., 2012) respectively. It can be

used as the initial indicator to predict the strength that can be developed by using the corresponding binder. The equation below illustrates the calculating method for the relative degree of oxidation of samples.

$$\text{Relative degree of oxidation} = \text{Ratio } \text{C=O/C-C} = A_1/A_2$$

where  $A_1$  = Surface area of C=O bond (located around  $1710 \text{ cm}^{-1}$ )

$A_2$  = Surface area of C=C bond (located around  $1450 \text{ cm}^{-1}$ )

During the thermal treatment, the occurred chemical reaction would lead to the changes of the molecular structure of waste oils. Upon the analysis, the samples of waste oils were heat cured for different durations. According to Peterson (1984), the oxy-polymerization occurred during the thermal treatment will produce polar oxygen-containing functional groups, which contributed to the hardening of the binder. Hence, by identifying the variation of these functional groups and observe the growth or loss in the intensity of spectral bands along with the curing duration, the extent of oxidation reaction occurred can be quantified.



Figure 3.7: FTIR instrument

### 3.2.1.2 Thermal Gravimetric Analysis (TGA)

Thermogravimetric analysis is a thermal analysis approach in which the mass of samples were measured over time along with the elevating temperature. TGA spectrum provides useful information about the chemical phenomena, including the decomposition temperature and thermal stability of the waste oils. In the desired temperature range, the mass loss of the samples along with the temperature was recorded. Hence, the decomposition temperature and the thermal stability of waste oils can be evaluated. Furthermore, the first derivative of the TGA spectrum (DTG spectrum) can be used to indicate the inflection points useful for in-depth interpretation of the samples.

The thermogravimetric analysis of waste oil samples were carried out by using *Mettler Toledo SDT A851* thermogravimetric analyzer equipped with *STARe Eval Evaluation Software* for data analysis. About 3 – 5 mg of waste oil sample was first loaded into an alumina cup and later placed it in the thermogravimetric analyzer. The temperature of thermogravimetric analyzer was raised with ramping rate of 10 °C/min from 25 to 900 °C under the flow of nitrogen gas at 100 ml/min. The decomposition temperatures of waste oil samples can be determined based on the following temperatures: On-set temperature, inflection temperature and end temperature. These temperatures represent the temperatures at initial weight loss, the maximum weight loss and the final weight loss. These temperatures can be easily determined from the differential thermogravimetric (DTG) curve.



Figure 3.8: TGA instrument

### 3.2.1.3 Viscometer

Viscosity of the waste oils is an important property to be considered while being utilized in the production of roofing tiles. The viscosity of oil samples were analyzed using *Brookfield Viscometer*. It has four different spindles for conducting the viscosity test, which is ranging from 61 to 64 mm, where the thinner spindle is more suitable for more viscous liquids. As the viscosity of both the waste oils is not very viscous, the spindles with 63 and 64 mm were used in determining the viscosities of WEO and UCO.



Figure 3.9: Viscometer

#### 3.2.1.4 Particle Sizes Analysis

The size distribution of coal-fired ash was investigated by using a *Malvern Mastersizer 2000* particle sizes analyzer equipped with *Malvern Panalytical Software* for data evaluation. In order to obtain an accurate result, the coal-fired ash was oven-dried prior to the analysis. A small amount of coal-fired ash was dispersed in the deionized water and injected into the analyzer. The average particle size of coal-fired ash was determined in terms of volume and number.



Figure 3.8: Particle sizes analyzer

#### 3.2.1.5 Sieve Analysis

According to the ASTM C 136, the size distribution of the sand aggregate utilized in the research study was carried out by using a sieve shaker. Prior to the analysis, 1 kg of sand aggregate was washed with tap water to eliminate any dust particles or impurities that might affecting the binding matrix of the roofing tiles produced, followed by drying at  $110 \pm 5^{\circ}\text{C}$ . When conducting the sieve analysis, the sand aggregate was separated into different sizes by passing through a series of sieves, from the coarsest sieve at the top,

and the finest sieve at the bottom. The size graduations of the sieves used are 3.35, 2.36, 1.18, 0.425, 0.212 and 0.15 mm respectively. The fineness modulus of the sand aggregate was carried out according to the weight of aggregates retained in each size of sieves.

### **3.2.2 Production of Roofing Tile Prototypes**

#### **3.2.2.1 Manufacturing Process of Trials Roofing Tiles**

The alternative approach of manufacturing the environmental friendly roofing tiles involved three stages, which are mixing, compacting, and heat curing processes. Mixing process involved mechanical blending of the raw materials incorporated under ambient temperature; compacting involved molding of samples into specific shape; and heat curing process involved hardening of the samples under a specific temperature.

Materials preparation and storing process are two important steps to be concerned to produce a good roofing tile. Prior to the manufacturing process, the WEO and UCO collected were filtered through filter funnel with 0.5 cm thick cotton to eliminate any impurities leftover during the lubricating or cooking process. The oils were stored under ambient temperature and avoided from direct exposure to sunlight. In some cases, the selected strong acid would be added and mixed thoroughly with the waste oils before the manufacturing process. Pretreatment of coal-fired ash is also necessary by sieving through a 0.75 mm sieve in order to separate any coal particles that does not pulverized

completely during the burning process in the thermal power plant. Furthermore, the sand aggregate utilized in the manufacturing of roofing tiles was washed and oven dried at  $110 \pm 5^\circ\text{C}$ .

In order to produce a proper roofing tile with significant strength, thoroughly mixing of the raw materials is necessary. The alternative binder (WEO or UCO) was blended with coal-fired ash and sand aggregate by using a bench mounting mixer for 15 – 20 minutes, or until no clumps remained in the mixture. The resultant mixture would then be transferred into a round Marshall mold with the radius of 100 mm (production of prototypes for analysis purpose) or standard mold with the size of  $390 \times 240$  mm (manufacturing of standard tiles for final verification purpose), and compacted accordingly by using a Marshall compactor. As an effort to develop the strength of roofing tiles, the compacted samples were heat cured in a ventilated oven under  $190^\circ\text{C}$ . In addition, the selected tiles with high percentage of water absorption were coated with oil film as protective layer. Prior to the coating process, the tiles were heat cured for 4 hours in order to maintain the shape of tile. By referring to the standard coating method shown in ASTM D 825, the waste oil was coated on the selected tiles by using a spray gun. The coated tiles would then be heat cured for another 20 hours (or until the optimized heat cured duration). Figure 3.11 shows the manufacturing process of the alternative roofing tiles.

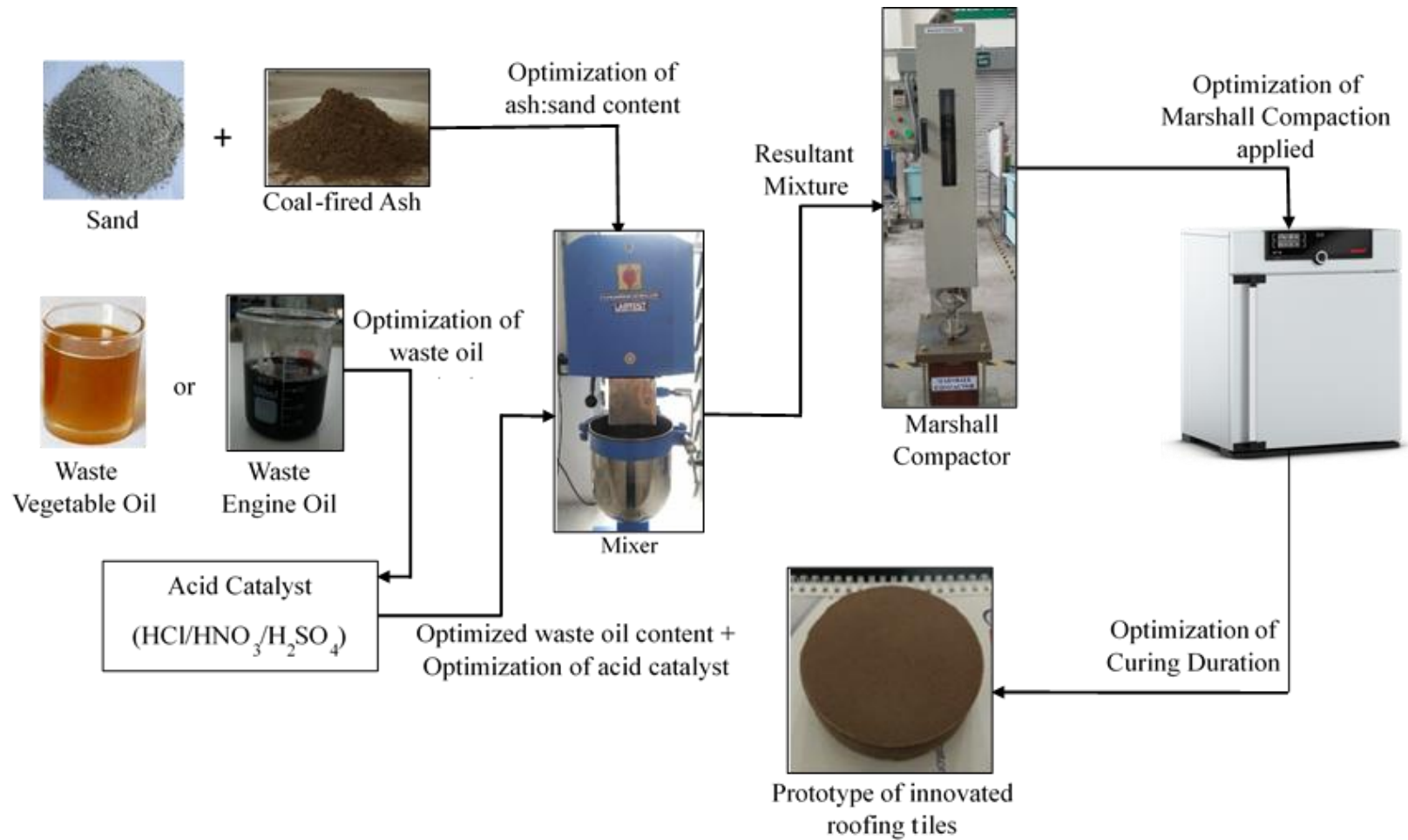


Figure 3.11: Sketch of the production of oil-made roofing tiles

### 3.2.2.2 Optimization of Parameters

In order to determine the greatest strength that can be achieved by using alternative binders in the production of roofing tiles, a series of parameters to be optimized were formulated as per manufacturing process, which include optimization of binder composition, aggregate and filler contents, number of compactions applied, curing duration, and types and amounts of catalysts incorporated. The optimization sequence and the initial optimizing values of each parameter are listed in Table 3.2:

Table 3.2: Initial selected values of parameters for the optimization process

Optimization sequence	Parameters	Optimizing range
1	Waste oil composition	1 – 10%
2	Aggregate: filler ratio	20:80 to 80:20
3	Number of compactions	10 – 28 bowls
4	Curing duration	6 – 72 hours
5	Types of catalysts	HCl; HNO <sub>3</sub> ; H <sub>2</sub> SO <sub>4</sub>
	Amounts of catalyst	0.0025 – 0.02% with respect to total weight of samples

### 3.2.3 Physical and Chemical Analysis of Roofing Tile Prototypes

#### 3.2.3.1 Transverse Strength / Flexural Strength Test

Transverse strength, synonymous with modules of rupture, is referred to the breaking load required to rupture the specimen. In this study, the transverse strength of trial roofing tiles were determined as described in ASTM C 1167 – 03 and ASTM C1492 – 03. Transverse strength can be classified into dry and wet, which referred to the condition of the testing specimens. For the dry transverse strength test, the specimens were dried under  $110 \pm 5^\circ\text{C}$  for 24 hours prior to the analysis; while for the wet transverse strength test, the specimens were tested in wet condition after a 24 hours immersion in water with  $24 \pm 6^\circ\text{C}$ . All of the tests were conducted under three-point bending mode by using a Materials Testing Machine (*T-machine, model LTSH-50KN*) equipped with *U.T.M Operation Program* for data evaluation. The specimens were rest horizontally on the two supporters with span of  $2/3$  with respect to the length of tiles, while loading force was applied in a direction perpendicular to the upper surface of the specimens. The flexural

$$\text{Flexural Strength (MPa)} = \frac{3 \times P \times L}{2 \times W \times d^2}$$

strength (MPa) of the trials roofing tiles can be calculated as follows:

where: P = loading force / dry transverse strength (N)

L = span length (mm)

W = width of the specimen (mm)

d = thickness of the specimen (mm)

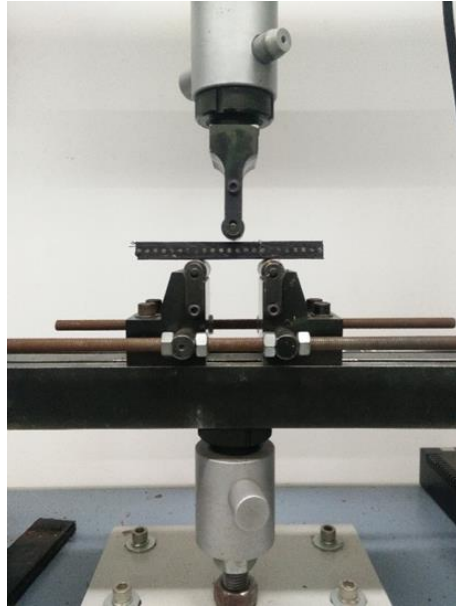


Figure 3.12: Demonstration of flexural strength test

### 3.2.3.2 Water Absorption Test

Percentage of water absorption is one of the most common physical tests for roofing tiles. This process determines the ability of specimens in absorbing water. The test was conducted by referring to the ASTM C 64 – 07a. Firstly, the dried weights of specimens were obtained after being oven dried at  $110 \pm 5^\circ\text{C}$ , and two successive measurements at 2 hours interval should indicate a variation of weight no more than 0.2% in comparison with the later one. Next, the specimens were immersed in a water tank at temperature of  $24 \pm 6^\circ\text{C}$  and being covered to avoid the external interruption. In addition, the saturation coefficients of the specimens were further investigated by using cold water and boiling water submersion method. The percentage of water absorption and saturation coefficient for a specimen can be calculated as follows:

$$\text{Water Absorption (\%)} = \frac{W_s - W_d}{W_d}$$

$$\text{Saturation Coefficient} = \frac{W_s - W_d}{W_b - W_d}$$

where:  $W_d$  = weight of dried specimen

$W_s$  = weight of saturated specimen after immersed in cold water for 24 hours

$W_b$  = weight of saturated specimen after being immersed in boiling water for 5 hours



Figure 3.13: Demonstration of water absorption test

### 3.2.3.3 Permeability Test

The permeability test is conducted in accordance with ASTM C 1167-03. An open-bottom trough, designed to surround at least 4/5 of the surface of the specimen, was fix horizontally above the tiles. The space between the specimen and trough was sealed with watertight sealant material to prevent the

occurrence of leakage. Water was added into the trough for at least 50 mm height from the upper surface of the specimen. It was then allowed to stand on a supporting frame for up to 24 hours. The underside of the specimen was observed periodically for sign of water droplets. No penetration of water on the underside of the specimen after 24 hours duration is indicative of impermeability of the tiles.



Figure 3.14: Demonstration of permeability test

#### **3.2.3.4 Stability of Roofing Tiles Toward Different Weather**

A roofing tile was designed mainly to resist towards different weather, regardless the extremely hot, dry or cold, humid condition. Hence, the service performance and period of a roofing tile are strongly related to its structure stability. In this research, ultra-violet (UV) accelerated weathering test and freeze-thaw cycles were carried out to determine the stability of roofing tiles produced toward UV and repeatedly freeze-thaw conditions.

In UV accelerated weathering tests, the optimized roofing tiles were produced and exposed to UV lamps for a specific duration. The tests were conducted by using two *Philips Ultraviolet light bulb*, with the peak wavelength at 370 nm. The UV intensity of one UV lamp is estimated by having UV intensity released by five suns. It is estimated that the total period the roofing tiles being exposed to the UV light released by the sun is 8 hours (from 9 am to 5 pm) a day. The exposure of a specimen to two UV lamps at the same time for the duration of 24 hours is equal to the exposure of the specimen to UV light from the sun for 30 days. Exposure period of the specimens to the UV light were varied with 5 years interval started from 15 years to 30 years. Effect of the roofing tiles exposed to UV light were discussed in Sector 3.2.3.1.

The freeze-thaw stability of roofing tiles was conducted in accordance with the ASTM C 67 – 07a. The optimized roofing tiles were also analyzed for their effects after being subjected to the freezing and thawing chambers repeatedly for 50 cycles. Firstly, the specimens were dried in a ventilated oven with a temperature of  $110 \pm 5^{\circ}\text{C}$ , and the dried weights were recorded. The specimens were examined carefully for any cracks or damages before being submerged in a thawing chamber containing distilled water (ambient temperature) for  $4 \pm 1/2$  hours. The specimens were then removed from the thawing chamber, after drying their surface, they were kept in the freezing chamber at the temperature of  $-15^{\circ}\text{C}$  for  $20 \pm 1/2$  hours. One complete process from thawing chamber to freezing chamber was considered as one cycle. To determine the freeze thaw stability of trial roofing tiles produced, the

specimens were tested for 50 cycles, and the weight losses of the specimens were recorded for every 10 cycles. Prior to determining the weight of the specimens, they were oven dried at  $110 \pm 5^{\circ}\text{C}$  for  $44 \pm 1$  hours, and the specimens were examined again for cracks or damages.

### **3.2.3.5 Surface Topography and Morphology**

In this study, waste engine oil and used cooking oil were served as the binder to hold the aggregate and filler together to form a binding matrix with significant strength. Relationship between the raw materials, the surface topography and morphology of the specimens were understood better from the images obtained from scanning electron microscope (SEM). The images were taken using *LEICA Cambridge S360* scanning electron microscope. A fine piece of roofing tile specimen was scratched from the interior part of the prepared roofing tile, and put on the top of a copper sample stub stacked with a double sided carbon tab. In addition, coal-fired ash sample was prepared in pellet form by using a manual hydraulic press. Those specimens were analyzed using secondary electron image (SEI), back-scattering electron imaging (BEI) and Inlens modes.

### **3.2.4 Life Cycle Assessment of the Innovated Roofing Tiles**

In line with the Malaysia government policy, the environmental impact of the novel roofing tiles produced was evaluated through the life cycle assessment (LCA). LCA involved quantitative analysis of the carbon dioxide

(CO<sub>2</sub>) emission and energy consumption rates during the manufacturing process of the building materials. Hence by calculating the embodied carbon (EC) and embodied energy (EE) of the novel roofing tiles produced from this study, the environmental suitability of the products can be estimated.

Embodied carbon assessment of the novel roofing tiles involves quantifying the total carbon emissions, which include carbon emitted during “cradle to gate”, “cradle to site” and “cradle to grave” processes. Cradle to gate carbon emission is referred to the emission of carbon compounds from the materials incorporated in the manufacturing process (Gartner, 2004), and carbon compounds released during the operation progress (Dixit et al., 2010). Cradle to site emission accounts for the carbon compounds emitted during transportation of raw materials to the factory, and the travelling of products to the construction sites. While cradle to grave emission is referred to carbon emissions involved in the end-of-life of the masonry units. The embodied carbon of the roofing tiles produced can be obtained by summing up the carbon emissions from each category.

Embodied energy accounts for the total energy consumption during the manufacturing process and that during the operation and processing. The embodied energy of the raw materials incorporated into the roofing tiles was obtained from literature review and based on the assumption. In addition, the transportation estimation and the assumption of energy consumed also involved in the calculation of EE and EC.

## CHAPTER 4

### RESULTS AND DISCUSSIONS

#### **4.1 Raw Materials Analysis Using Fourier Transform Infrared Spectroscopy (FTIR)**

In this research study, waste oils (both used cooking oil and waste engine oil) were served as the sole binder in the manufacturing process of building materials. Under an elevated temperature, the thermal energy applied would trigger chemical reactions between various components in the waste oils. The occurrence of oxy-polymerization reaction consequently turns the liquid waste oils into a gummy structure, and subsequently to a solid, rigid binder after an efficient duration. To have a better understanding on the chemical reaction occurred during the thermal treatment, FTIR analysis was utilized to determine the functional groups presented in the waste oils. The corresponding functional groups responsible to the occurrence of chemical reaction were justified in the following sections.

##### **4.1.1 Used Cooking Oil (UCO) and Waste Engine Oil (WEO) Analysis Using Fourier Transform Infrared Spectroscopy (FTIR)**

Figures 4.1 and 4.2 show the FTIR spectra of UCO and WEO, respectively. By comparing the spectra, it can be found that most of the

absorption peaks present in the spectra are located at similar wavenumbers. UCO possessed free fatty acid constituted of different carbon numbers, while WEO consisted of vast range of branched aliphatic or aromatic hydrocarbons. Hence, two strong absorption peaks that are contributed by asymmetrical and symmetrical C–H stretch bonds can be found in both the UCO and WEO spectra which are located at around  $2921\text{ cm}^{-1}$  and  $2851\text{ cm}^{-1}$  respectively. In addition, two absorption peaks located at around  $1464\text{ cm}^{-1}$  and  $1375\text{ cm}^{-1}$  represented by asymmetrical and symmetrical C–H bend bonding are the contributions of those hydrocarbon components. By comparing both the spectra, two notable differences were encountered, which are the absorption peaks located at  $1743\text{ cm}^{-1}$  and  $1161\text{ cm}^{-1}$ . Those absorption peaks are belonged to carbonyl (C=O) group and carbon-oxygen (C–O) bonds contributed by ester compounds. Carbonyl (C=O) groups presented in waste oils are corresponding to the chemical reaction in developing the strength of the roofing tiles produced. The absorption peaks shown on the spectra of both the binders were indicated and compared to determine the capability of waste oils in developing the strength of roofing tiles. To ensure the fair comparison study, the oxidation extents of waste oils was calculated. This method involved calculating the ratio of peaks area of carbonyl to asymmetrical C–H bend peak. Based on those spectra, the peak areas of C–H groups of UCO and WEO were found similar to each other. However, it is obvious that the intensity of the C=O absorption peak in the UCO spectrum is much stronger than that in WEO spectra. As a result, the oxidation extents of UCO and WEO were calculated to be 1.74 and 0.26 respectively. The degree of oxidation is served as an initial indicator to predict and estimate the strength of building materials

produced by utilizing waste oils as the sole binder. UCO with higher oxidation extent indicated more carbonyl containing species which are available in the UCO, and able to contribute in developing the strength of roofing tiles. Hence, it was expected that stronger and harder binding matrix could be produced by using UCO instead of WEO in the manufacturing process of roofing tiles. Table 4.1 shows the assignment summary of absorption signals in FTIR spectra of UCO and WEO.

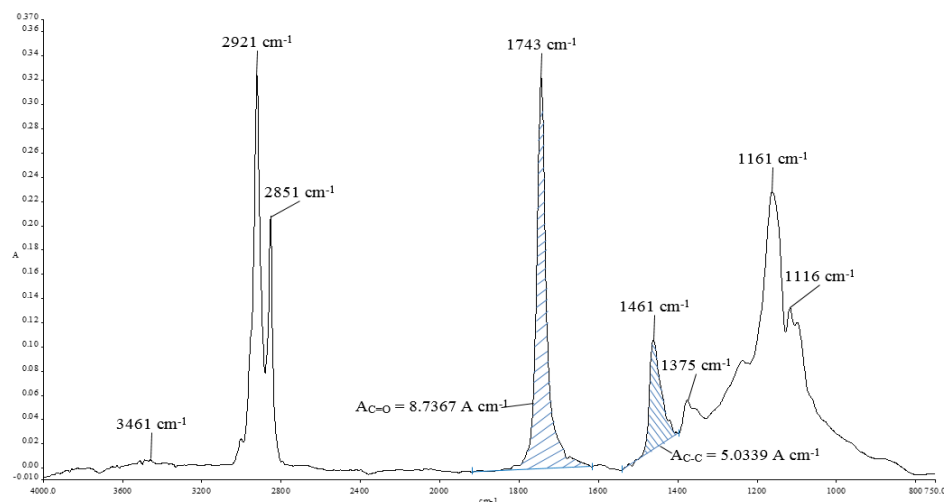


Figure 4.1: FTIR spectrum of used cooking oil (UCO). Shaded region represented the peak area of corresponded absorption peaks

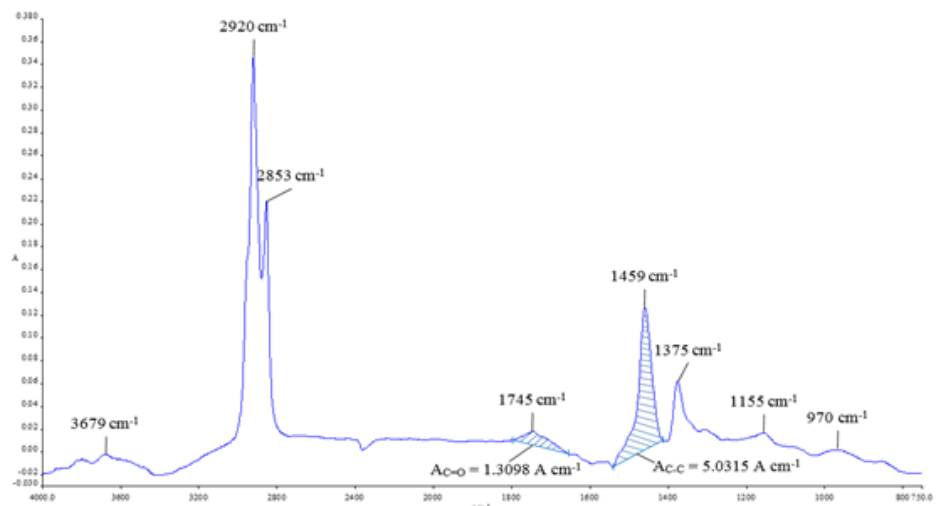


Figure 4.2: FTIR spectrum of waste engine oil (WEO). Shaded region represented the peak area of corresponded absorption peaks

Table 4.1: Assignment of absorption signals in FTIR spectra (Mohammad and Lina, 2009; Heaton et al., 2014; Humayun et al., 2017a)

Functional groups	Absorption peak (UCO spectrum)	Absorption peak (WEO spectrum)	Suspected components present
-OH stretch	3461	3679	Fatty acids, carboxylic acid
=C-H stretch		-	Unsaturated hydrocarbon chain
Antisymmetric C-H stretch	2921	2920	Aliphatic hydrocarbon chain.
Symmetric C-H stretch	2851	2853	- C <sub>8</sub> to C <sub>18</sub> for UCO; - C <sub>15</sub> to C <sub>50</sub> for WEO.
C=O stretch	1743	1745	Aldehyde, ketone, carboxylic acid, or other secondary oxidative products.
Antisymmetric C-H bend	1461	1459	Aliphatic hydrocarbon chain.
Symmetric C-H bend	1375	1375	- C <sub>8</sub> to C <sub>18</sub> for UCO; - C <sub>15</sub> to C <sub>50</sub> for WEO
Antisymmetric C-O stretch	1161	1155	Ester compounds
=C-H out-of-plane bend	1116	-	Unsaturated hydrocarbon chain
CH <sub>2</sub> (>C <sub>4</sub> )	-	970	Long hydrocarbon chain

#### 4.1.2 Fly Ash Analysis Using Fourier Transform Infrared Spectroscopy

Fly ash which is utilized in the manufacturing process of innovative roofing tiles was also subjected to FTIR analysis. Figure 4.3 shows the FTIR spectrum of the fly ash. The data obtained is tabulated in the form of wavenumber with corresponding minerals presented. By comparing the observed absorption peak with available literature, several types of mineral, which might be presented in the sample were identified. The big broadened band centered at  $1035\text{ cm}^{-1}$  shows the presence of Si–O stretching of clay mineral, which may be contributed by kaolinite in the fly ash (Ramasamy et al., 2006). In addition, the absorption peak located at  $755\text{ cm}^{-1}$  indicated the presence of quartz in the utilized fly ash, with Si–O symmetrical stretching vibrations (Clara and Sugirtha 2016). Furthermore, the Si–O–Si bending vibration is observed at the wavenumber of  $462\text{ cm}^{-1}$ , which is corresponded to the presence of feldspar (Sivakumar et al., 2012).  $\text{SiO}_2$  is the major component presented in fly ash. As  $\text{SiO}_2$  is a polar in nature, it would attract and form hydrogen bonds when in contact with water molecules from the atmosphere. Hence, the broad absorption peak in the region around 3600 to  $3300\text{ cm}^{-1}$  is assigned as the –OH stretching vibration, indicating the presence of water molecules. Table 4.2 shows the band assignments of fly ash with corresponding minerals.

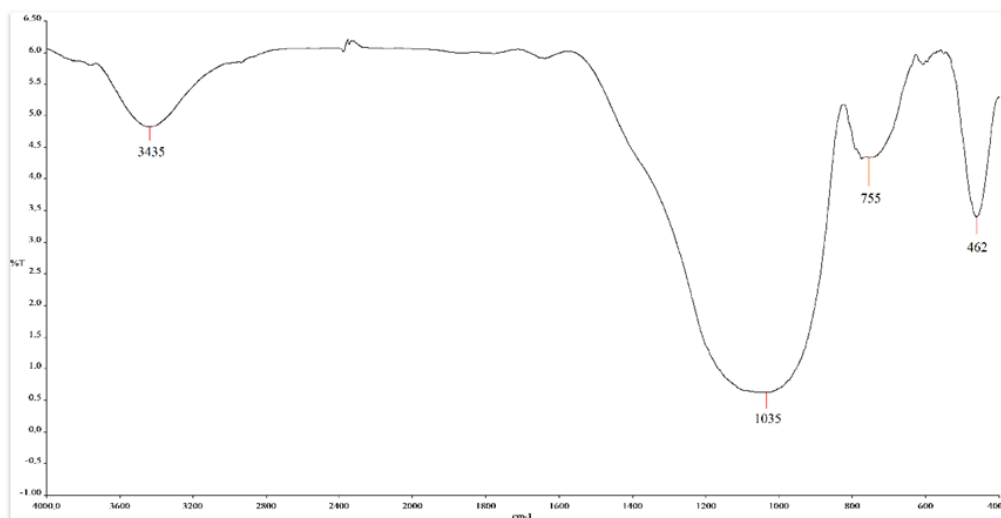


Figure 4.3: FTIR spectrum of fly ash.

Table 4.2 Assignment of absorption signals in FTIR spectra of fly ash

Absorption band (cm <sup>-1</sup> )	Functional groups	Minerals	References
3435	-OH stretch	Adsorbed water molecules	Clara and Sugirtha 2016
1035	Si-O stretch	Kaolinite	Ramasamy et al., 2006
755	Si-O symmetric	Quartz	Clara and Sugirtha 2016
462	Si-O-Si bend	Feldspar	Sivakumar et al., 2012

## **4.2 Attenuated Total Reflectance Fourier Transform Infrared Spectrometry (ATR-FTIR)**

The occurrence of chemical reactions within the waste oils, which leads to the hardening of roofing tiles was investigated and analyzed using ATR-FTIR facilitated with thermal treatments. The intensities of absorption peaks in an ATR-FTIR spectrum represents the amount of functional groups presented in the analyzed samples. Hence, the growth and drop of the peaks' intensity indicates the changes of the waste oils' components. These phenomena can be used in justification of the chemical reactions occurred upon the thermal treatment.

### **4.2.1 ATR-FTIR Analysis of UCO**

In order to investigate the chemical reaction of UCO at an elevated temperature, similar amount of UCO samples (without catalyst) were heat cured under 190°C in a ventilated oven for different curing durations. The curing duration was varied from 6 hours to 48 hours. Based on the observation, the UCO samples heat cured from 6 to 30 hours remained in the liquid state at the end of the heat curing process, with an increased viscosity along with the curing duration. After heat cured for 42 hours, the UCO samples turned into the solid state and formed a soft, flexible oil film. Figure 4.4 shows the observation of the UCO samples that were heat cured for different durations.

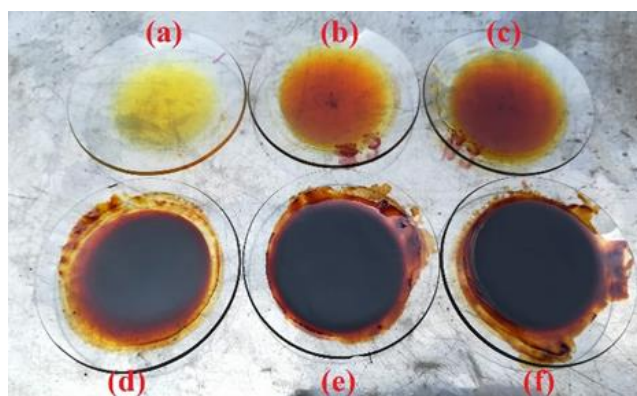


Figure 4.4: Observation of UCO samples heat cured for (a) 6 hours; (b) 12 hours; (c) 18 hours; (d) 30 hours; (e) 42 hours and (f) 48 hours.

Figures 4.5, 4.6, and 4.7 show the ATR-FTIR spectra of UCO magnified at different ranges of wavenumber. From the expanded spectra of UCO range from  $3800$  to  $2700\text{ cm}^{-1}$ , the broad and discrete peak located in between  $3600 - 3350\text{ cm}^{-1}$  indicated the present of isolated hydroxide ion ( $-\text{OH}$ ) and a broad range of hydroxyl containing species, which may be contributed by carboxylic acid ( $-\text{COOH}$ ) involved in hydrogen bonding in the UCO. Along with the heat curing process, the intensity of this absorption peak grows gradually. This phenomenon are caused by the formation of free fatty acids as a product of the hydrolysis reaction, in which triglycerides would react with  $\text{H}_2\text{O}$  at high temperatures to give one glycerol and three fatty acids at the end of the reaction.

From the expanded ATR-FTIR spectrum of UCO ranging from  $1800 - 1650\text{ cm}^{-1}$ , the absorption peak centered around  $1740\text{ cm}^{-1}$  belongs to the carbonyl ( $\text{C}=\text{O}$ ) functional groups, preferably contributed by ester linkage in triacylglycerol (Heaton et al., 2014). Along with the prolonged thermal treatment, the intensity of this peak was increased gradually. The growth in the

corresponding peak's intensity indicated the increase in the number of ester C=O groups in the samples. Since carbonyl group is the product of condensation polymerization reaction, this phenomenon indicated the occurrence of chemical reactions during the thermal treatment. However, it was observed that broadening of the C=O absorption peak occurred during the thermal treatment, and the center of the absorption peak were slightly shifted to the lower wavenumber. This condition is due to the increase in the concentration of carbonyl containing secondary oxidation products within the waste oil, such as ketones and aldehydes produced from the decomposition of hydrogen peroxides. However, the presence of these secondary oxidative products will also lead to the growth in the C=O absorption peak. Hence, the occurrence of condensation polymerization can be further investigated through two adjacent absorption peaks allocated at  $1161\text{ cm}^{-1}$  and  $1116\text{ cm}^{-1}$  respectively (as in Figures 4.7). Those absorption peaks represented the asymmetrical and symmetrical C-O stretching vibrations solely contributed by ester compounds. Hence, the growing of the intensity of these absorption peaks further proved the occurrence of condensation polymerization reactions during the heat curing process.

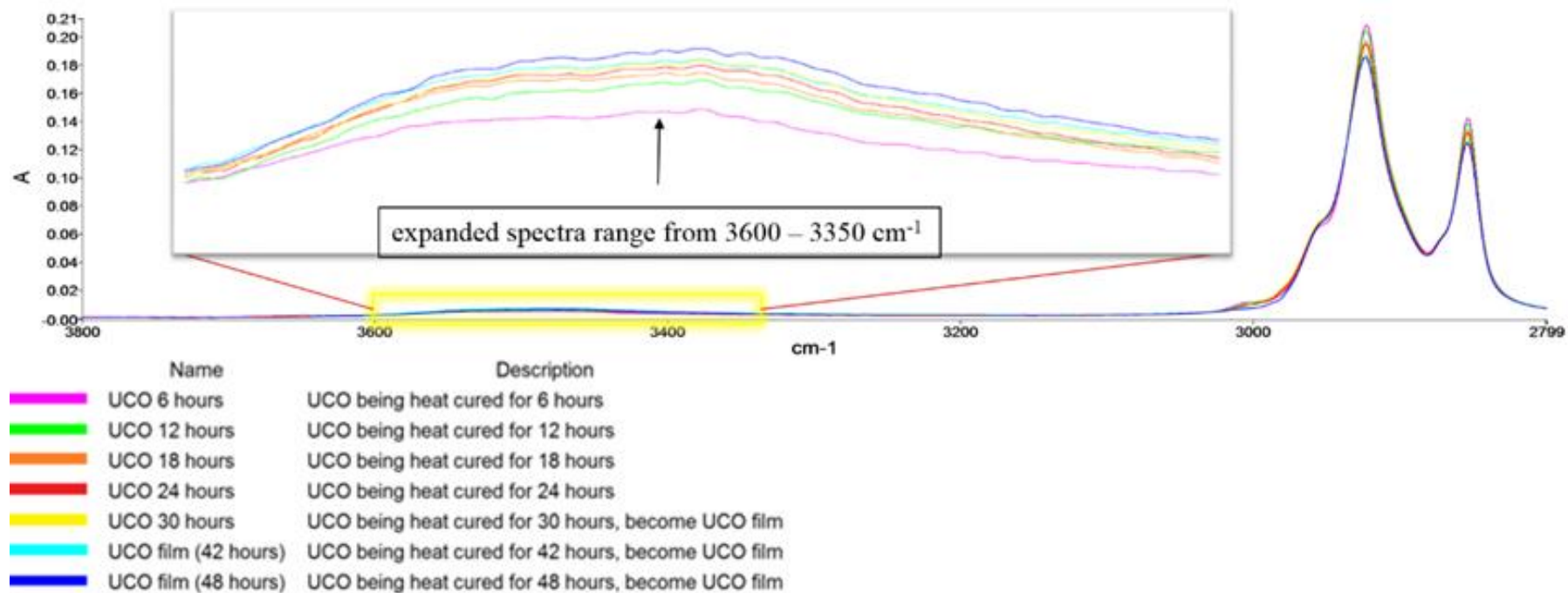


Figure 4.5: Magnified ATR-FTIR spectrum of UCO ranging from 3800 to 2800  $\text{cm}^{-1}$

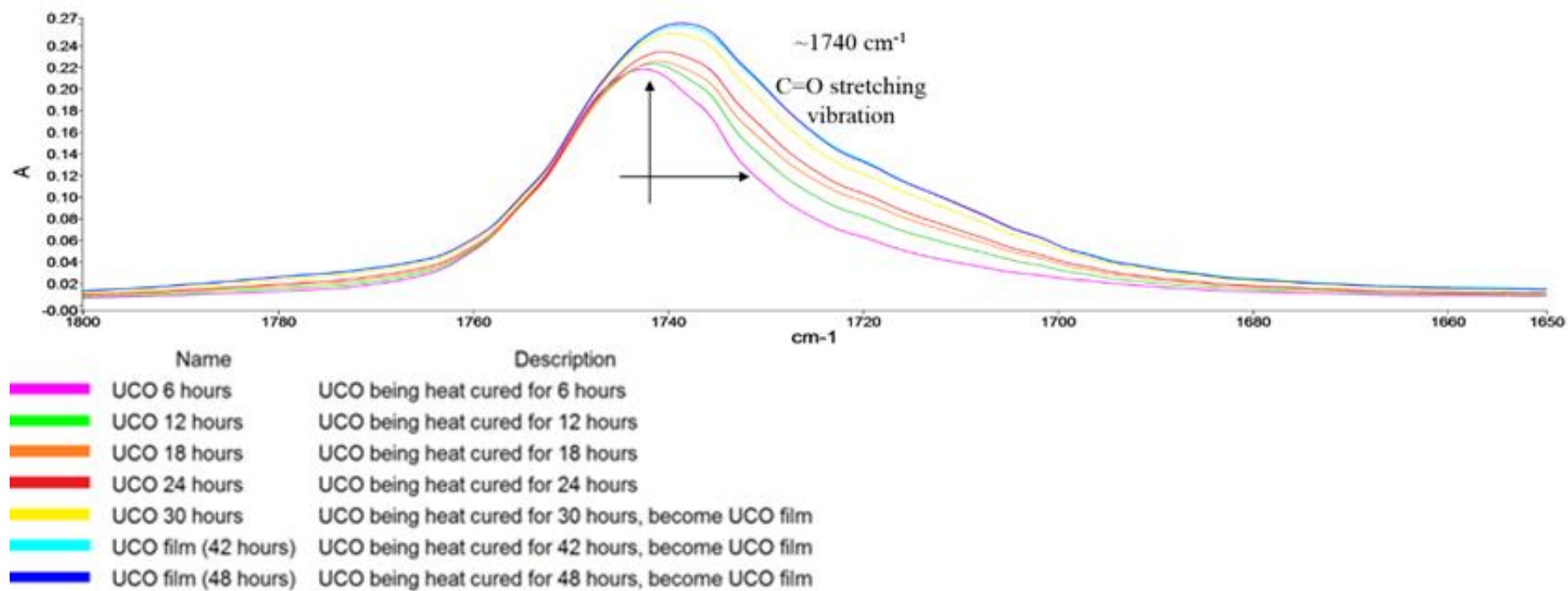


Figure 4.6: Magnified ATR-FTIR spectrum of UCO ranging from 1800 to 1650 cm<sup>-1</sup>

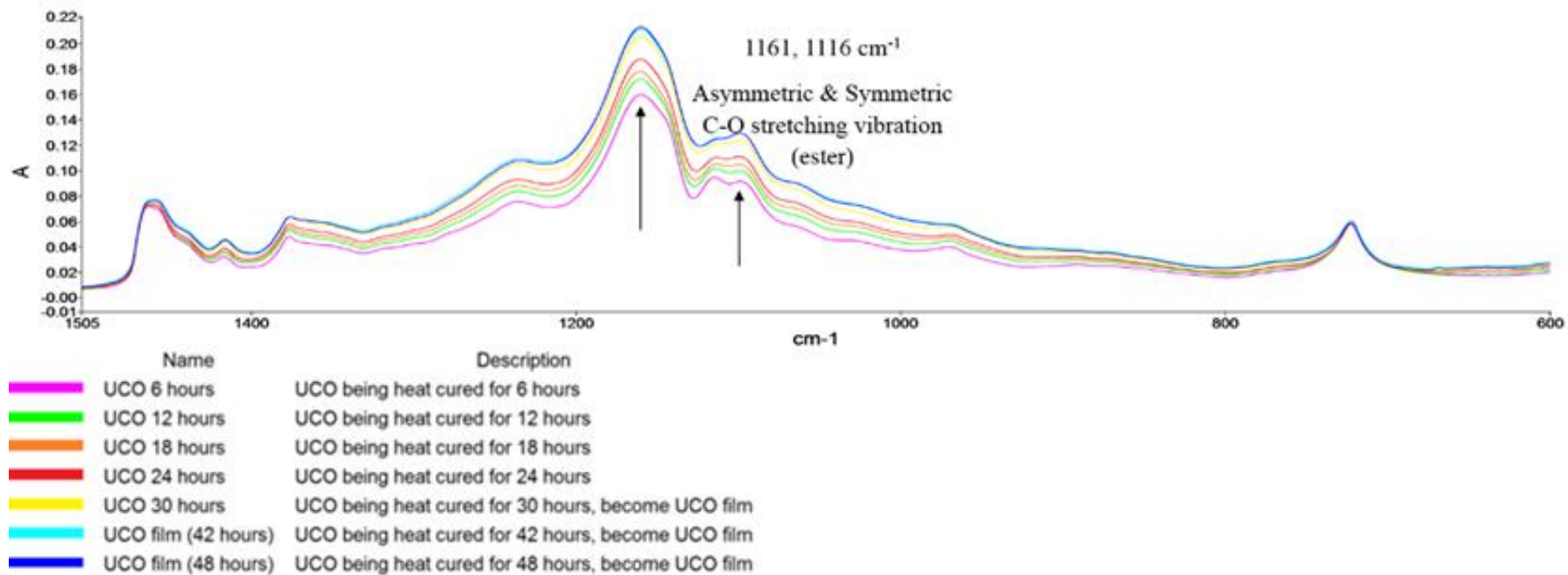


Figure 4.7 Magnified ATR-FTIR spectrum of UCO ranging from 1500 to 600  $\text{cm}^{-1}$

#### 4.2.2 ATR-FTIR Analysis of WEO

The chemical changes of WEO after thermal treated at 190°C over different heat curing periods were investigated and analyzed using ATR-FTIR. Different from the UCO samples that were investigated based on the uniform interval of curing duration, the investigation study on WEO samples focused on the chemical changes occurred during the early stages of thermal treatment. Hence, the heat curing duration for WEO samples were varied from 40, 120, 360 and 720 minutes. Figures 4.8, 4.9 and 4.10 indicated the growth and loss of the intensity of various functional groups presented in WEO. Generally, the intensity changes of the absorption peaks are similar to that seen in UCO. Figures 4.8 shows the changes of FTIR region over the range of 3800 – 2700  $\text{cm}^{-1}$ , associated with  $\nu(\text{O-H})$  and  $\nu(\text{C-H})$ . Along with the thermal treatment, the expansion of the O-H peak revealed the formation of carboxylic acid, which was resulted from the oxidation reaction between WEO components with oxygen molecules blended into the WEO. In addition, the development of broad absorption band was caused by the decomposition of hydro peroxides under elevated temperature and produced secondary oxidative compounds (Yazici and Deveci, 2010). The minute enhancement in intensity indicated that the rate of carboxylic acid formation is greater.

Complex oxy-polymerization reaction was happened progressively during the thermal treatment. The thermal energy will trigger the chemical reactions between carboxylic acid with glycol to produce larger molecular species (Humayun et al., 2017a). The chemical reaction occurred was

anticipated as the condensation polymerization reaction. The proposed polymerization reaction was verified through the growth in the intensity of the carbonyl band along with the increment of oxidation extent. As shown in Figure 9, the oxidation extent of WEO increased during the curing process. However, a series of secondary oxidative products produced along with the thermal treatment would contribute to the feature of carbonyl peaks at around  $1700\text{ cm}^{-1}$  (Michael and John, 2007). The decomposed products involved aldehydes and ketones, possessed of absorption peaks with weaker intensity. Hence, they were being overlapped by ester band with higher vibration frequency (Heaton et al., 2014). Since the absorption band of ester was subjected to interferences to the same extent as the other bands, the occurrence of condensation polymerization can be measured with another ester-related band, constituting of two conjugated bands located at  $1151$  and  $1098\text{ cm}^{-1}$  which are associated with C–O ester bond. As shown in Figure 4.10, both absorption peaks show an increment in intensity upon the thermal treatment, indicated the occurrence of polymerization reactions which produce ester compounds under applied heat energy. When two or more molecules were combined, the process leads to the formation of higher molecular weight species. As the size of the molecules is directly affecting the viscosity of the waste engine oil, the occurrence of polymerization reaction will lead to the increase of viscosity. When the molecular size growth continuously to such an extent, they are no longer able to remain in liquid state. Solid materials, such as varnish or sludge will present in the oil. At the end of the thermal treatment, all of the waste engine oil would be converted into solid form, resulted in the formation of a hard, rigid binder.

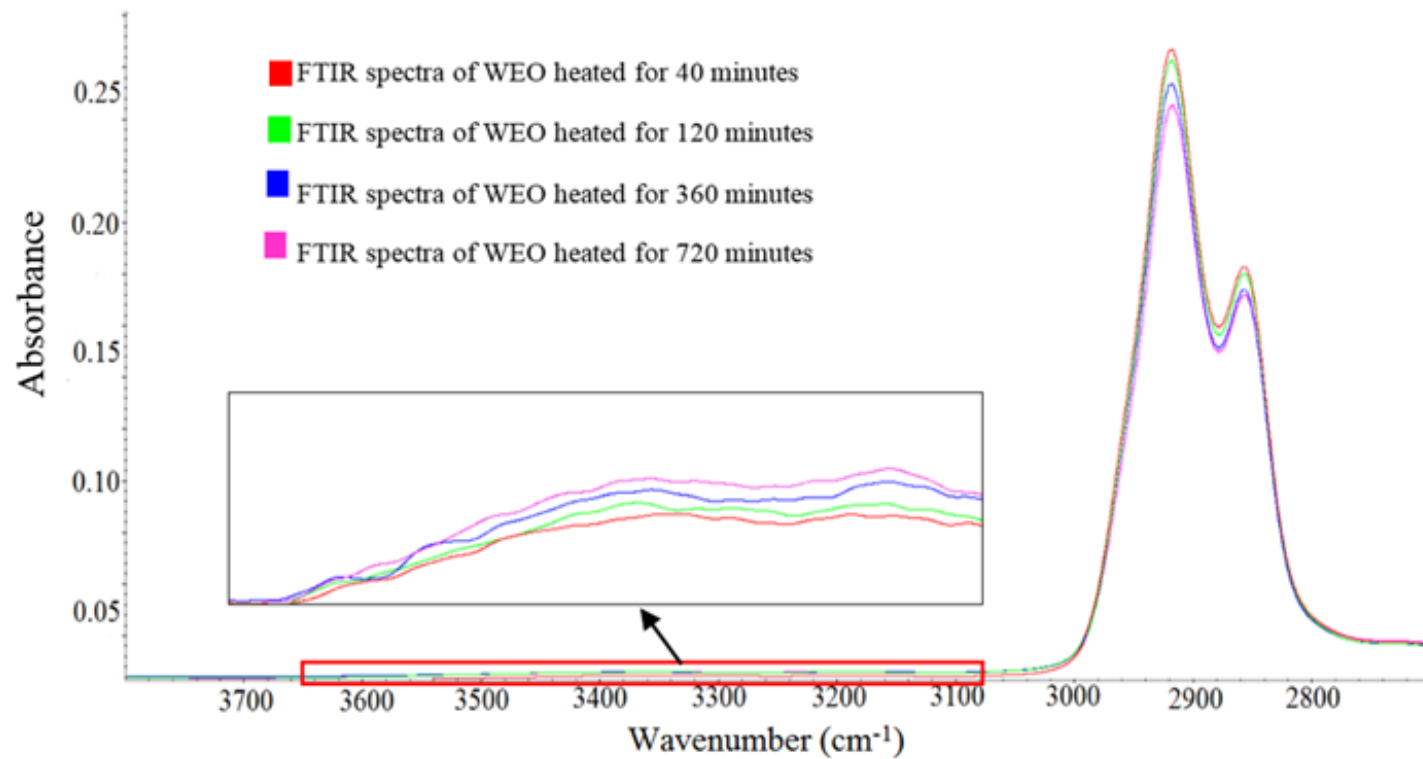


Figure 4.8: ATR-FTIR spectrum of WEO ( $3800\text{--}2700\text{cm}^{-1}$ ) thermally treated at  $190^\circ\text{C}$  over 12 hours. Inset shows the expanded region at  $3700\text{--}3100\text{cm}^{-1}$

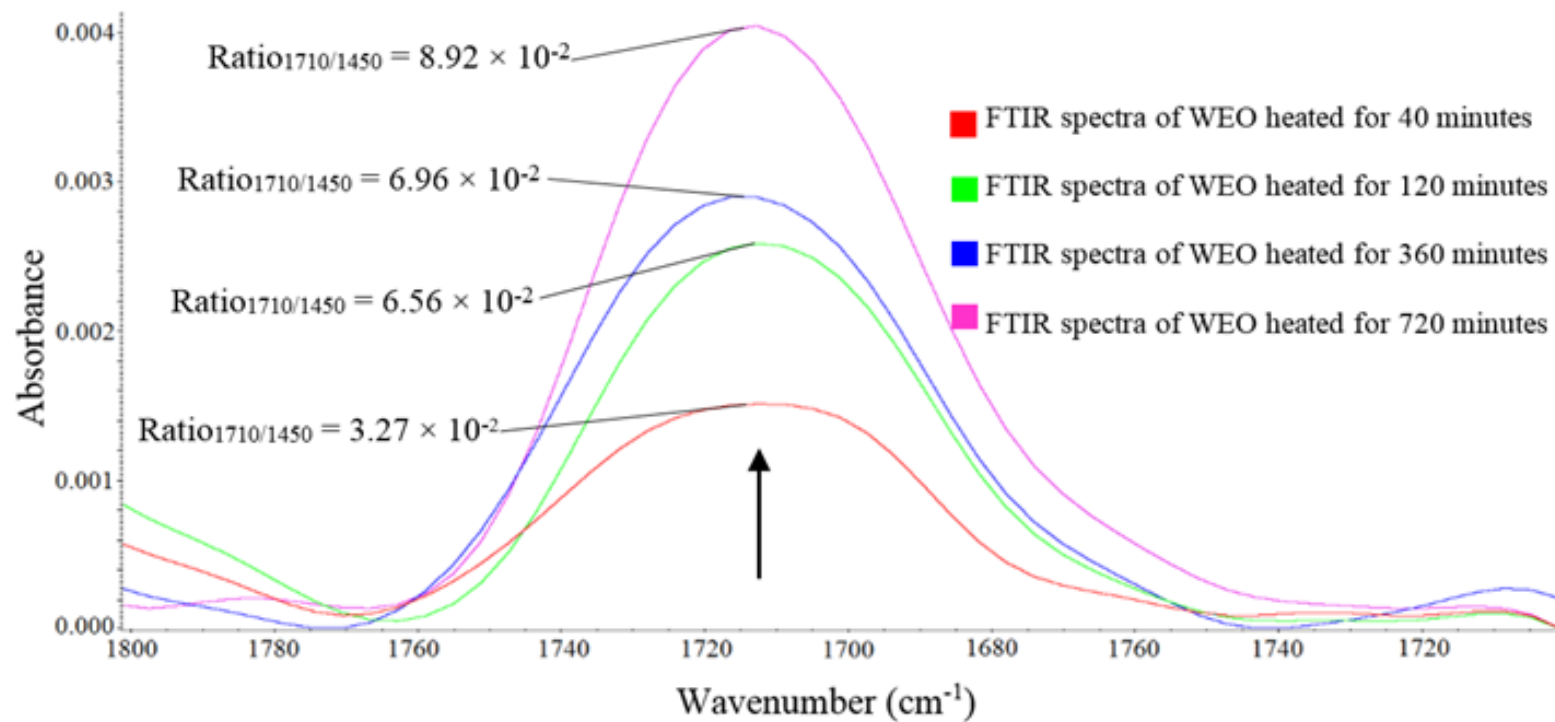


Figure 4.9: Carbonyl region of WEO (1800 – 1600 cm<sup>-1</sup>) thermally treated at 190°C over 12 hours. Arrow indicates the growth of absorption bands.

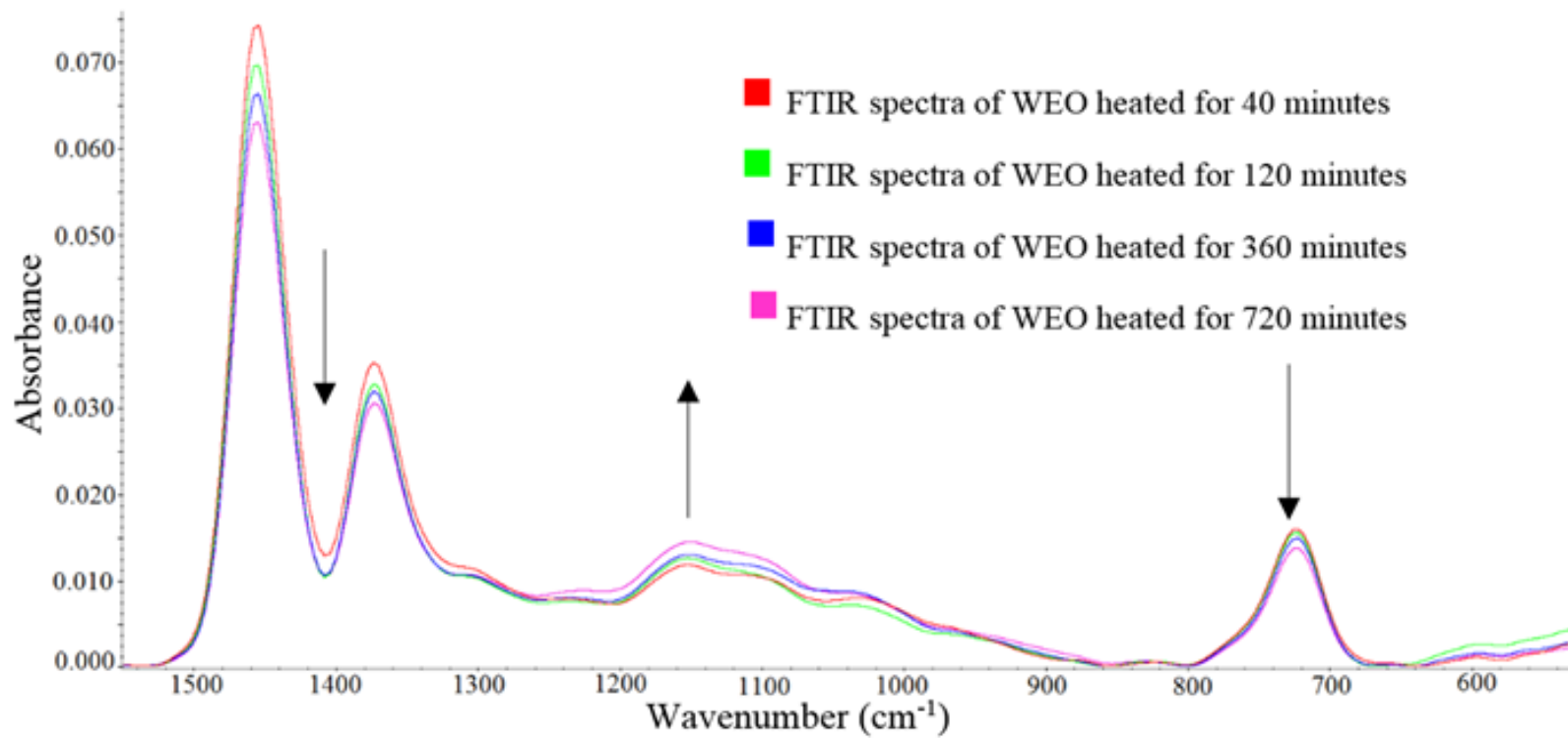


Figure 4.10: ATR-FTIR spectrum of WEO ( $1550 - 500 \text{ cm}^{-1}$ ) thermally treated at  $190^\circ\text{C}$  over 12 hours. Arrow indicates the changes of absorption band with time.

### **4.3 Thermogravimetric Analysis (TGA)**

The thermal characteristic of UCO and WEO samples were investigated by using thermogravimetric analysis. TGA thermogram shows the weight-loss pattern of waste oils along with the elevating temperature. In addition, the first derivative of the TGA spectrum indicates the maximum decomposition temperature of the samples, in which the samples were decomposed at the fastest rate. The oil film produced from WEO and UCO after being heat cured for more than 48 hours were also subjected to the analytical testing. The comparison study between waste oils and their films indicates the intermolecular changes caused by the thermal treatment.

#### **4.3.1 Thermogravimetric Analysis (TGA) of UCO and UCO Film**

The data of TGA of UCO and its corresponding film produced are shown in Figures 4.11, 4.12 and Table 4.3 that have indicated that the weight loss of the UCO and UCO film are 97.8% and 85.2% respectively. From the derivative thermogravimetric (DTG) spectrum, the maximum decomposition rate of UCO and UCO films are determined to occur at 416.7°C and 428.3°C respectively. The increment in the decomposition temperature was caused by the polymerization of waste oils components during the heat curing process. Hence, higher thermal energy was required to break down the covalent bonding within the UCO film. Furthermore, only one weight loss pattern was encountered for both UCO and UCO films.

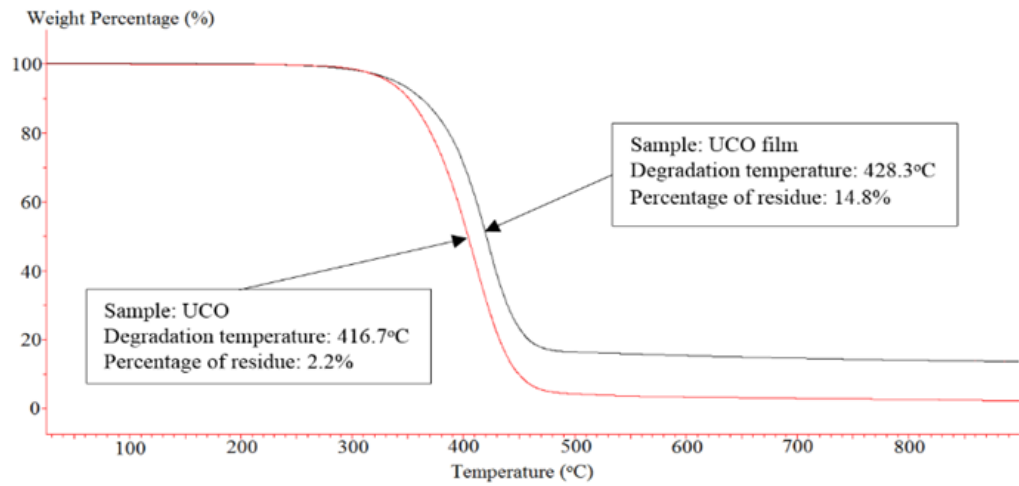


Figure 4.11: TGA curves of UCO related samples

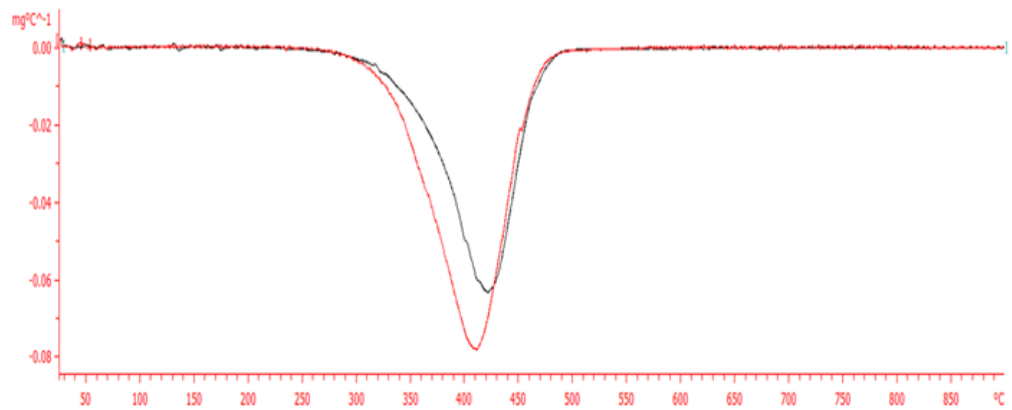


Figure 4.12 DTG curves of UCO related samples

Table 4.3: Characteristic temperature and residue percentage of UCO related samples

Sample	Maximum decomposition rate point (°C)	Percentage of residue (%)
UCO	416.7	2.2
UCO film	428.3	14.8

### **4.3.2 Thermogravimetric Analysis (TGA) of WEO and WEO Film**

The TGA and DTG thermogram of WEO related samples and the data obtained are showed in Figures 4.13, 4.14 and Table 4.4. As shown in the spectra, the percentage of residues of WEO and WEO films are 0.6% and 17.4% respectively. In addition, the maximum decomposition rates of WEO and WEO film occur at 324.7 and 382.8 °C respectively, which are relatively lower than UCO corresponding samples. As in UCO samples, the polymerization reaction occurred in WEO during the heat curing process leads to the formation of larger molecules, subsequently increase the decomposition temperature of the WEO film. In the TGA spectrum, only one weight loss pattern was found. However, the DTG curve of WEO shows that in addition to the major decomposed component, a minor decomposed component is encountered, with highest thermal decomposition rate at around 440°C.

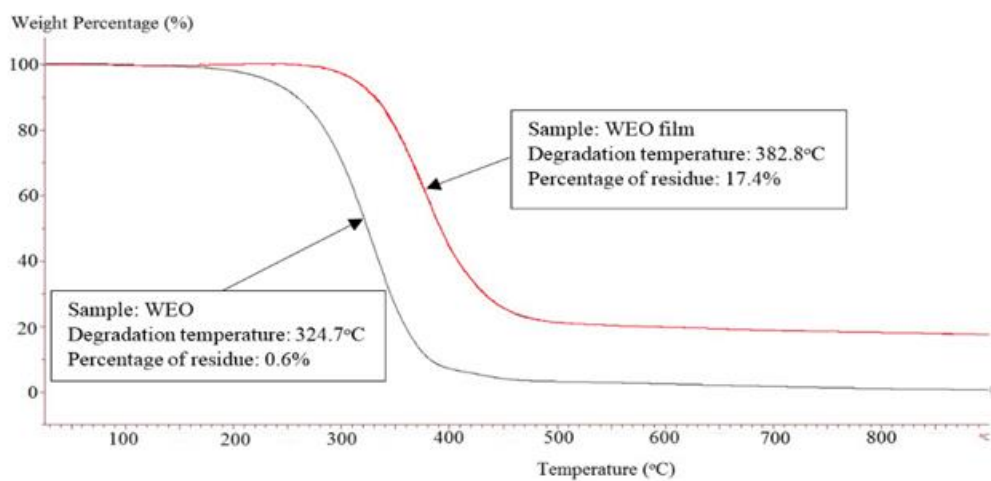


Figure 4.13: TGA curves of WEO related samples

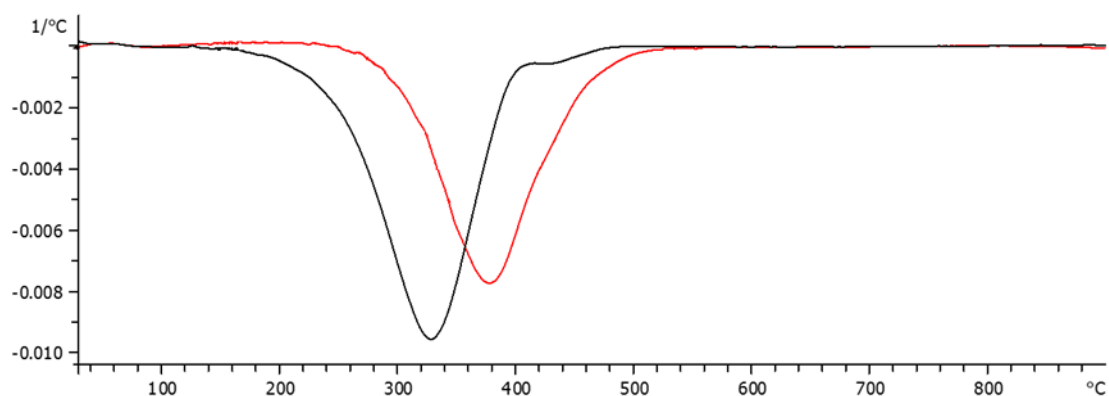


Figure 4.14: DTG curves of WEO related samples

Table 4.4: Characteristic temperature and residue percentage of WEO related samples

Sample	Maximum decomposition rate point (°C)	Percentage of residue (%)
WEO	324.7	0.6
WEO film	382.8	17.4

#### **4.4 Scanning Electron Microscope (SEM)**

SEM is one of the most widely used techniques to investigate the surface morphology of a sample. In this experiment, three different types of samples, which are fly ash, UCO-made and WEO-made roofing tiles were prepared in pellet form before subjected to the test. The SEM images of fly ash, UCO-made and WEO-made samples are shown in Figures 4.15, 4.16 and 4.17.

In the SEM image of fly ash, most of the particles observed are spherical in shape. However, some components with irregular shape are also can be found in the sample. In addition, those rounded particles were widely distributed in the sizes as shown in Figure 4.15 (a). The spherical particles represented the fly ash sample (Clara and Sugirtha, 2016).

Similar phenomenon was encountered in SEM images of oil-made prototypes, in which the samples were built of irregularly sized spherical particles. Apart from the smooth surface of fly ash particles as in Figure 4.15, the surface of oil-made samples are generally crinkled. The crinkled surface is caused by the waste oil layer covered on the fly ash surface, which served as the connection bond between particles. Those network-like components are functioning as linkages between fly ashes to form a proper binding matrix.

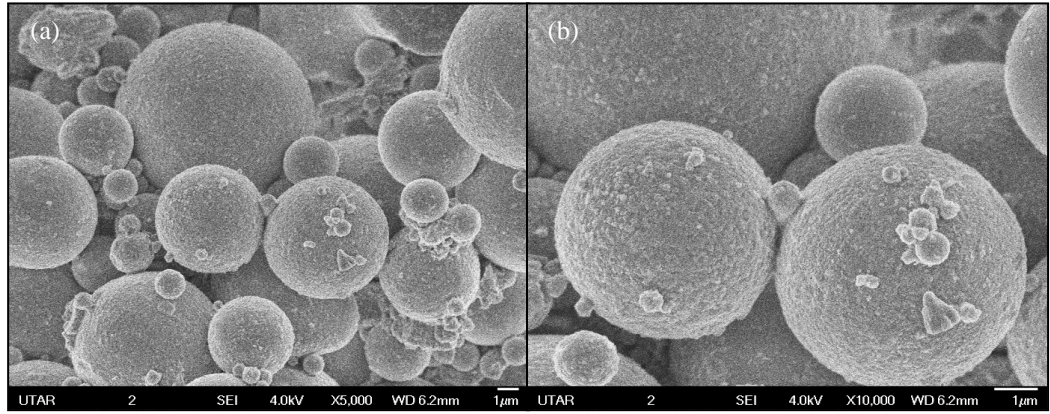


Figure 4.15: SEM images of fly ash (a) x5000 magnification; (b) x10000 magnification

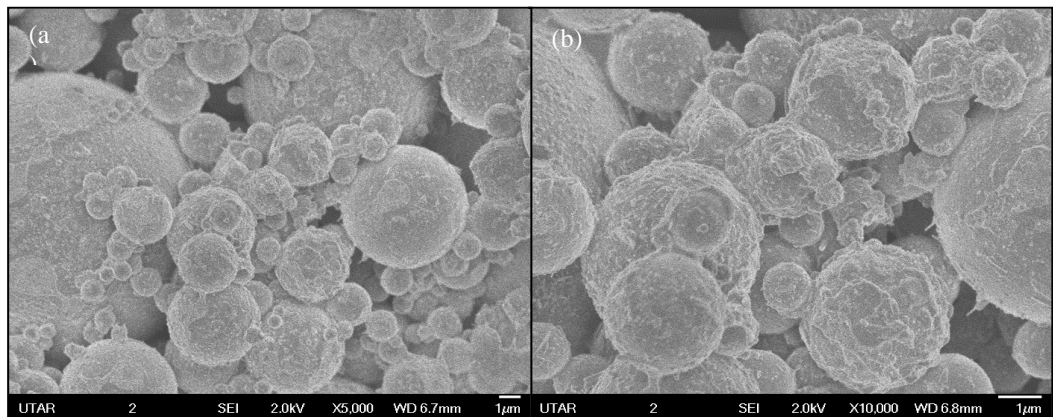


Figure 4.16: SEM images of UCO-made roofing tile (a) x5000 magnification; (b) x10000 magnification

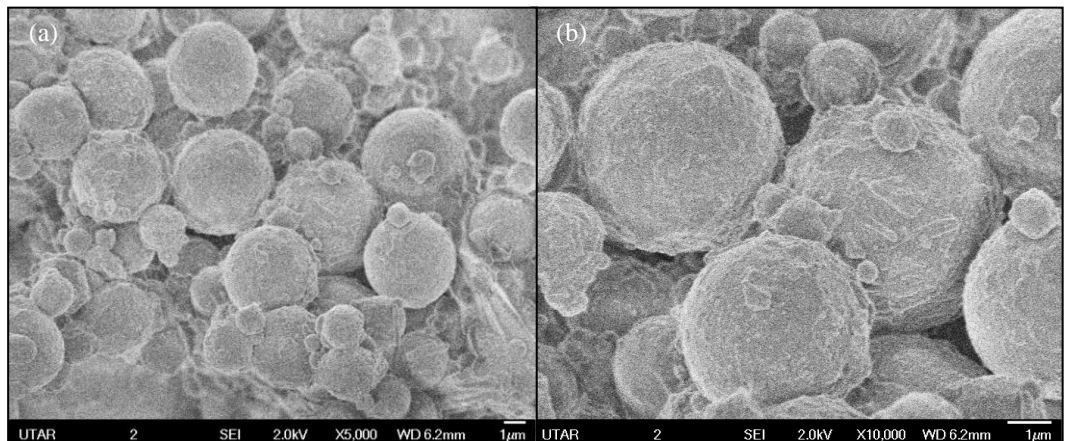


Figure 4.17: SEM images of WEO-made roofing tile (a) x5000 magnification; (b) x10000 magnification

## **4.5 Optimization Process of Innovated Roofing Tiles & Their Mechanical Properties**

This section involves the optimization of parameters in the manufacturing process of innovated roofing tiles. The roofing tiles produced were tested for their flexural strength, water absorption ability and permeation characteristics. The roofing tiles which had achieved the greatest strength, fulfilled the maximum water absorption requirement and impermeable to water were justified as the optimized roofing tiles. The corresponding parameters used in the manufacturing process of optimized roofing tiles are known as optimized parameters. This section is separated into three parts: namely, Part (I) manufacturing of waste engine oil-made green roofing tiles (WEO–GRT); Part (II) manufacturing of used cooking oil-made green roofing tiles (WEO–GRT); and Part (III) comparison study of WEO-made and UCO-made roofing tiles (WEO-RT and UCO-RT). Green roofing tiles are referred to the innovated roofing tiles, which were produced by using only waste oils and fly ash. While the roofing tiles produced in Part (III) were made of fly ash, sand aggregate and waste oils in the manufacturing process.

### **4.5.1 Parameters Optimization of WEO-made Green Roofing Tiles**

In the optimization process of WEO-made green roofing tiles, the initial selected parameters together with their optimizing ranges were deemed appropriate as per Table 4.5.

Table 4.5: Initial selected values of parameters for the optimization process

Optimization sequence	Parameters	Selected ranges
1	- Percentage of WEO incorporated	- 1.0 – 10.0 %
2	- Number of Marshall compactions applied	- 10 – 28 times
3	- Curing durations	- 6 – 72 hours
4	- Types of catalysts added - Amount of catalyst added	- HCl; HNO <sub>3</sub> ; H <sub>2</sub> SO <sub>4</sub> - 0.25 – 2.00% with respect to the total weight of prototypes.

#### 4.5.1.1 Optimization of WEO and Fly Ash Compositions

In the optimization process of binder and filler contents, a series of triplicate prototypes were produced with initial estimated appropriate proportion. The other manufacturing parameters were set at the estimated suitable extent, including (i) blending duration of 15 minutes; (ii) 15 times of Marshall Compactions; (iii) curing temperature of 190°C; (iv) 24 hours curing duration; and (v) without the addition of catalyst. Preliminary study was carried out by using different percentages of WEO in the production of trial roofing tiles, ranging from 1.0 to 10.0% with 0.5% intervals. The physical observations of the prototypes produced were recorded in Table 4.6. The results obtained indicated that the prototypes produced by using less than 4%

of WEO tended to break easily even after going through the heat curing process, which may be caused by the insufficient binder in developing the strength of the prototypes produced. In addition, the prototypes produced by using WEO more than 7.5% failed to maintain in proper shape during and after the heat curing process, hence it was justified as not a suitable percentage for the production of roofing tiles. Hence, only the prototypes produced with percentage of WEO ranging from 4.0 to 7.5% were subjected to further investigation to determine their transverse breaking strength and water absorption ability. From the results obtained, as shown in Table 4.7, it was found that the percentage of waste engine oil incorporated in the manufacturing of roofing tiles is not proportional to its strength. The highest strength was achieved with specimens having 5% WEO. Preliminary, it was deduced that an extra thermal treatment was required to complete the mentioned chemical reactions within the WEO. Insufficient thermal treatment has resulted in declination of strength when more than 5% of WEO was utilized in the manufacturing of trial roofing tiles. Furthermore, the percentage of WEO incorporated in the production process was found inversely proportional to the percentage of water absorbed by the prototypes. This condition may be due to the mutually exclusive behavior between nonpolar WEO and polar water, which retarded the infiltration of water molecules into the specimens. However, the presence of  $\text{SiO}_2$  as the main component of fly ash resulted in its hygroscopic behaviour. The strong adhesion energy of  $\text{SiO}_2$  towards water exposure led to the aggressive water absorption during immersion in water (Tsui et al., 2005). Therefore, the existence of water molecules would destruct the interaction between the dried WEO polymer

network and fly ash, significantly affected the wet transverse strength achieved by the prototypes. In order to overcome the issue of excessive water absorption, an alternative approach of applying a layer of uniform thickness WEO film on the exposed surface of specimens was attempted in accordance to ASTM D 824. This protective layer prevents the direct exposure of specimen to water or moisture from atmosphere. The ability and the effect of WEO protective layer is discussed in Sector 4.5.1.5.

Table 4.6: Physical condition of prototypes produced from different composition of WEO

No.	Percentage of waste engine oil (%)	Description	Observation	Conclusion
1.	1.0 – 3.5	<ul style="list-style-type: none"> <li>- The prototypes are able to support self-weight</li> <li>- Unstable</li> <li>- Broken easily while being handled</li> </ul>		No further investigation was carried out
2.	4.0 – 4.5	<ul style="list-style-type: none"> <li>- The prototypes are able to support self-weight</li> <li>- The edge of prototypes can be broken easily</li> </ul>		Proceed to further investigation study

3.	5.0 – 7.5	<ul style="list-style-type: none"> <li>- The prototypes are able to support self-weight</li> <li>- Stable</li> <li>- Show significant strength</li> </ul>		Proceed to further investigation study
4.	7.5 – 10.0	<ul style="list-style-type: none"> <li>- The prototypes are unable to support self-weight during the heat curing process</li> <li>- Too wet even after heat curing process</li> <li>- Ruptured</li> </ul>		No further investigation was carried out

Table 4.7: Average transverse breaking strength and water absorption of WEO-GRT produced from different binder and filler contents

Tiles No.	Percentage of waste engine oil (%)	Percentage of coal-fired ash (%)	Transverse Strength (N)		Water absorption (%)
			Dry	Wet	
1	4.0	96.0	346 ± 13.6	92 ± 7.8	18.11 ± 1.33
2	4.5	95.5	405 ± 14.2	98 ± 8.2	16.88 ± 1.01
3	5.0	95.0	1269 ± 34.7	232 ± 12.3	16.40 ± 0.58
4	5.5	94.5	1095 ± 80.1	263 ± 11.4	15.40 ± 0.44
5	6.0	94.0	975 ± 33.5	316 ± 8.2	14.74 ± 0.75
6	6.5	93.5	913 ± 40.2	285 ± 7.8	14.59 ± 0.45
7	7.0	93.0	982 ± 73.2	335 ± 9.6	13.80 ± 0.74
8	7.5	92.5	995 ± 80.9	356 ± 10.4	13.68 ± 0.29

\*Min. dry transverse strength = 1779 N (ASTM C 1167 – 03; C 1492 – 03)

\*Min. wet transverse strength = 1334 N (ASTM C 1167 – 03; C 1492 – 03)

\*Max. percentage of water absorption = 6% (ASTM C 1167 – 03)

#### 4.5.1.2 Optimization of Number of Marshall Compactions Applied

To minimize the energy requirement of the manufacturing of UCO-GRT, triplicated trial roofing tiles were manufactured under the estimated appropriate parameters as per Table 4.5 and optimized binder and filler contents (tiles no.3 in Table 4.7). In the optimization process, the number of Marshall compactions needed to produced single prototypes was varied from

10 to 28 times, with 2 times interval. The main purpose of compacting the specimens prior to the heat curing process is narrowing the pore sizes between the raw materials (WEO and fly ash) to promote the development of proper matrix during the curing process. The dry transverse strength and flexural strength achieved by the triplicate samples applied with different compaction bowls are shown in Table 4.8. From the results obtained, the strength achieved by samples no. 1, 2 and 3 were relatively low, which may be due to the low compactness of the tiles. At the end of thermal treatment, one of the specimens no. 1 was found to crack externally, probably due to the accidentally trapped of air molecules between WEO and fly ash. Hence, its expansion upon thermal treatment resulted in cracking from interior part of the specimens. Moreover, the strengths of the prototypes increased gradually for every two times compaction and achieved greater strengths started from compaction rate of 20. The dry transverse strength achieved by those specimens are approximately 1905 N, fulfilling the minimum standard requirements for a high profile roofing tiles as per ASTM C 1492-03. Additional compaction applied after 20 bowls would not lead to significant enhancement in the strength. Hence, the Marshall compaction of 20 times was selected as the optimized value of this parameter.

Table 4.8: Average dry transverse strength and flexural strength of WEO-GRT applied with different number of Marshall compactions

Tiles No.	No. of Marshall Compactions	Dry Transverse Strength (N)	Flexural Strength (MPa)
1	10	445 ± 23.8	0.71 ± 0.04
2	12	695 ± 13.5	1.11 ± 0.02
3	14	718 ± 21.4	1.15 ± 0.03
4	16	1495 ± 53.1	2.39 ± 0.08
5	18	1529 ± 47.7	2.44 ± 0.07
6	20	1905 ± 55.6	3.04 ± 0.09
7	22	1898 ± 44.4	3.03 ± 0.07
8	24	1941 ± 53.5	3.10 ± 0.08
9	26	1922 ± 31.1	3.07 ± 0.05
10	28	1899 ± 34.0	3.03 ± 0.05

\*Min. dry transverse strength = 1779 N (ASTM C 1167 – 03; C 1492 – 03)

#### 4.5.1.3 Optimization of Heat Curing Duration

In the manufacturing process of waste oil-made roofing tiles, thermal energy served as an important initiator in triggering the chemical reaction of the waste oils. Hence, the duration of thermal treatment was considered as one of the most important parameters as it is strongly related to the completeness of the chemical reactions of WEO leading to the rigidifying of the roofing tiles. Table 4.9 shows the mechanical properties of the specimens achieved, which were being heat cured from 6 to 42 hours, with 6 hours interval. The

data obtained reveals that the specimens, which were cured for less than 24 hours possessed relatively low transverse breaking strengths. This phenomenon is generally caused by incomplete polymerization of the WEO components was due to the insufficient curing duration. This situation resulted in the production of tiles with weak binding matrix and low flexural strength. The strength of the prototypes achieved the greatest extent after going through a 24 hours heat curing process. However, excessive thermal treatment applied beyond this period would adversely affect the binding strength of trial roofing tiles, resulted in the declination in strength. As claimed by Noor et al. (2015), to prolong the heat curing process after the optimized duration would induce internal cracks to decrease the strength of roofing tiles. Conclusively, the greatest strength can be achieved when the specimens were heat cured for 24 hours and it is fulfilling the minimum standard requirement of 1779N as per ASTM C 1492-03.

Table 4.9: Average dry transverse strength and flexural strength of WEO-GRT heat cured at different durations

Tiles No.	Curing duration (hours)	Dry Transverse Strength (N)	Flexural Strength (MPa)
1	6	474 ± 13.9	0.76 ± 0.02
2	12	554 ± 15.7	0.88 ± 0.02
3	18	1104 ± 48.2	1.76 ± 0.08
4	24	1905 ± 55.6	3.04 ± 0.09
5	30	1183 ± 35.9	1.89 ± 0.06
6	36	685 ± 21.2	1.09 ± 0.03
7	42	499 ± 20.7	0.80 ± 0.03

\*Min. dry transverse strength = 1779 N (ASTM C 1167 – 03; C 1492 – 03)

#### 4.5.1.4 Optimization of Types and Amount of Catalysts Added

Based on the results of previous optimization tests, triplicate trial roofing tiles were produced with 5% of WEO and 95% of fly ash, applying 20 bowls of Marshall Compactions, followed by curing for 24 hours. In order to further enhance the strength developed by the trial roofing tiles, three different types of strong acids were incorporated separately as a catalyst during the blending process of raw materials. The amount of catalysts were altered in the range of 0.25 – 22.5% with respect to the total weight of the specimens produced. Addition of catalysts was to enhance the rate of polymerization reaction in the WEO, which helps to increase the completeness of the binding

matrix of tiles produced. Table 4.10 reveals the transverse breaking strength achieved by three different types of catalyzed specimens with varying percentage added. Generally, incorporation of  $\text{HNO}_3$  and  $\text{H}_2\text{SO}_4$  in the manufacturing process successfully enhanced the strengths of trial roofing tiles produced. Addition of  $\text{HCl}$  showed negative effect to the strength of roofing tiles, in which the strength achieved by the specimens without the addition of  $\text{HCl}$  is higher than the specimens incorporated with  $\text{HCl}$ . Different acid-catalyzed specimens achieved their maximum strength with different percentage of catalyst added, which are 0.75% for  $\text{HCl}$ , 0.25% for  $\text{HNO}_3$  and 0.75% for  $\text{H}_2\text{SO}_4$ . The strength of specimens declined when extra acids were added beyond the optimized value, as they might obstruct the formation of WEO polymer. Oxy-polymerization reaction which responsible in increasing viscosity of the oil (Johnson et al., 2015). During thermal treatment, intra-chemical reactions between the long chain carboxylic acid in the WEO would lead to the formation of dimers or trimers which are consisting of one or more functional groups. These functional groups enable the occurrence of poly-esterification with the presence of diols in the WEO to form a high molecular weight polymer that would bind the filler effectively to form a proper binding matrix. The presence of strong acid, preferable  $\text{H}_2\text{SO}_4$  as  $\text{H}^+$  ion donor would catalyze the rate of reaction, ensure the fully polymerization of WEO. Hence, the greatest strength achieved by trial roofing tiles produced under acid catalyzed poly-esterification is 2298N, which is much higher than the strength of trial roofing tiles manufactured under self-catalyzed reaction (without any catalyst added), which is only 1905N.

Table 4.10: Dry transverse strength achieved by WEO-GRT incorporated with different types and amount of strong acids

Percentage of acid added (%)	Dry transverse strength achieved by different types of acid catalysed roofing tiles (N)		
	HCl	HNO <sub>3</sub>	H <sub>2</sub> SO <sub>4</sub>
0.0025	1351 ± 27.2	2004 ± 59.6	-
0.005	1484 ± 34.6	1616 ± 40.1	1106 ± 28.3
0.0075	1830 ± 41.9	1577 ± 45.1	2298 ± 61.1
0.01	1431 ± 39.0	1468 ± 34.6	1968 ± 36.5
0.0125	1117 ± 25.5	1394 ± 30.5	1418 ± 36.4
0.015	1006 ± 22.1	1297 ± 24.3	1192 ± 26.3
0.0175	869 ± 27.9	1197 ± 31.2	891 ± 14.5
0.02	505 ± 12.2	993 ± 21.1	839 ± 23.3

\*Min. dry transverse strength = 1779 N (ASTM C 1167 – 03; C 1492 – 03)

#### 4.5.1.5 Effect of Coating Layer on Trial Roofing Tiles

Percentage of water absorption is one of the most important criteria for the production of standard roofing tiles as per requirement in ASTM C 67-07a. In a previous study (see sector 4.5.1.1), the hygroscopic behavior of fly ash was shown to lead to the excessive water absorption of the roofing tiles produced. The infiltrations of water molecules into the specimens significantly affect the binding strength, thus weakening the wet transverse strength achieved by the trial roofing tiles. As an effort to overcome the problem of excessive water absorption, the selected trial roofing tiles were coated with

uniform thickness of WEO as a protective layer. WEO is hydrophobic in nature. The coating of WEO layer effectively enhanced the lotus effect exhibited on the surface of the specimen, hence increase the resistance of specimens from the penetration of water. Figure 4.18 shows the percentage of water absorption (bar chart) and wet transverse strength (trend line) achieved by triplicated trial roofing tiles treated in different conditions. It is revealed that specimen I, the optimized WEO-GRT without coated with WEO as protective layer absorbed great amount of water during water absorption test. The water absorption of specimens II and III which was coated with single and multiple layers of WEO were found to be 4.17 % and 3.84 % respectively, fulfilled the standard absorption limit of 6 % as requested in ASTM C 1167-03. Low water absorption resulted in greater wet transverse strength of around 1.1kN, achieving the minimum standard requirement of a medium profile roofing tiles.

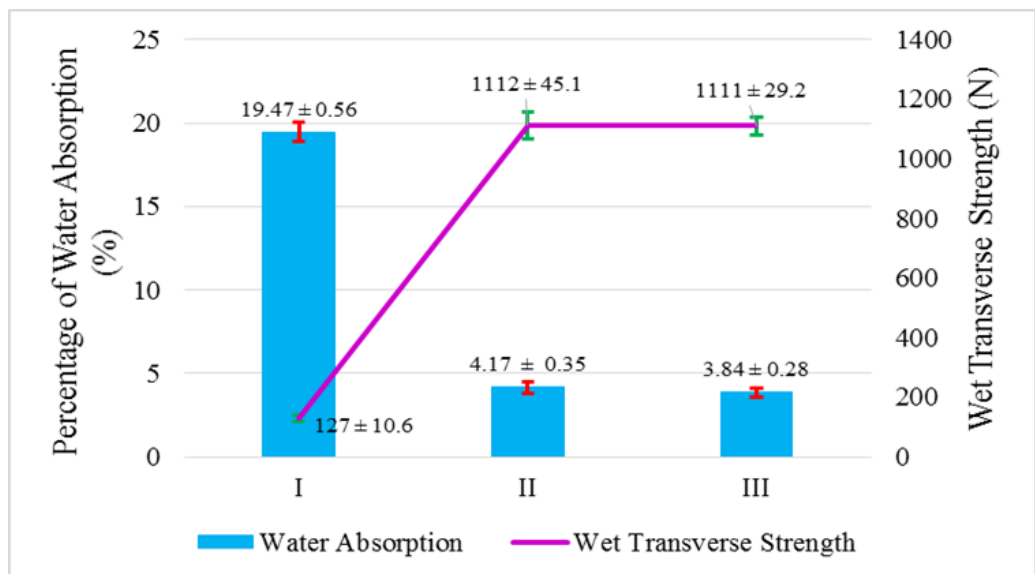


Figure 4.18: Percentage of water absorption and wet transverse strength of WEO-GRT which is (I) Uncoated; (II) Coated with single layer of WEO; and (III) coated with multiple layer of WEO

#### **4.5.1.6 Optimized Waste Engine Oil-made Green Roofing Tiles (WEO-GRT)**

After finishing a series of optimization processes, the optimized WEO-GRT can be produced by using the following parameters:

- (a) 5% of WEO and 95% of fly ash
- (b) 20 times of Marshall Compaction
- (c) 24 hours of curing duration
- (d) 0.0075% of H<sub>2</sub>SO<sub>4</sub> as catalyst

In order to determine the weight category of the innovated roofing tiles produced, the density of optimized WEO-GRT was calculated. Table 4.11 shows the average density of triplicate optimized specimens, which were produced according to the optimized parameters. The results obtained reveal that the average density of WEO-GRT is 1.985 g/cm<sup>3</sup>. According to ACI 213R, American Concrete Institute, the structural lightweight concrete building materials have density in between 1.440 to 1.840 g/cm<sup>3</sup>, while normal-weight concrete has an in-place density from 2.240 to 2.400 g/cm<sup>3</sup>. As the density of WEO-GRT is above the range of lightweight concrete, it can be classified as normal-weight roofing tiles.

Table 4.11: Density of optimized WEO-GRT

Samples	Mass (g)	Volume (cm <sup>3</sup> )	Density (g/cm <sup>3</sup> )
1	396.2	199.5	1.986
2	395.9		1.984
3	395.8		1.984
Average			1.985

Thickness of specimens = 2.54 cm

Radius of specimens = 5 cm

During the optimization process, the prototypes were manufactured in the round shape mould with diameter of 100 mm and being analyzed. However, to further investigate the capability of waste engine oil to be used as sole binder of building materials, the standard catalyzed WEO-GRT were manufactured in real size dimension (390 mm × 240 mm × 25 mm) in accordance to the optimized curing temperature which is under 190°C. Similar mechanical tests were performed on the standard roofing tiles to ensure that the physical properties achieved were matched with its corresponding prototypes.

The permeable characteristic of optimized WEO-GRT fulfilled the ASTM requirement, as no penetration of water droplet encountered at the end of the investigation study. As shown in Table 4.12, the percentage of water absorption of standard catalyzed WEO-GRTs were calculated using the standard formula as provided in ASTM 67 – 07a. It was indicated that the percentage of water absorption of triplicate standard specimens were limited in the range of 4.5 – 6.5 %, with average value of 5.35%. Compared to ASTM

standards, the data obtained were under the standard water absorption limitation of 8 % for single analyzed tile and 6 % of average water absorption. The low percentage of water absorption was credited to WEO protecting layer coated at the exterior surface of specimens, which its function is in minimizing the absorption and infiltration of water by decreasing the pores of the tiles (Nasir et al., 2011). The boiling water absorption test showed that the WEO coating layer has proved that it is able to function well under high temperature and humidity condition. With the data obtained, the percentage of boiling water absorption of triplicate standard specimens was controlled in the range between 10 – 11 %. While the saturation coefficient of standard WEO-GRT were determined in the range of 0.44 to 0.60, which are within the maximum requirement of 0.74 as per ASTM C 1167 – 03. The saturation coefficient can be used as an preliminary indicator to determine the practicality of building materials, where the saturation coefficient of greater than 1.0 indicated the specimens are vulnerable, while saturation coefficient of lower than 1.0 represents the high durability and resistance of masonry units against damage (Humayun et al., 2017a).

Table 4.12: Percentage of cold/boiling water absorption and saturation coefficient achieved by optimized catalyzed WEO-GRT

Tiles No.	Weight of Dried Specimen, $W_d$ (g)	Weight of Saturated Specimen (24 hours immersion in cold water), $W_s$ (g)	Percentage of Cold Water Absorption (%)	Weight of Saturated Specimen (5 hours immersion in hot water), $W_b$ (g)	Percentage of Boiling Water Absorption (%)	Saturated Saturation Coefficient
1.	398.6	419.1	5.14	440.3	10.5	0.49
2.	387.4	412.5	6.48	429.4	10.8	0.60
3.	392.4	409.8	4.43	432.3	10.1	0.44
Average			$5.35 \pm 1.04$		$10.5 \pm 0.35$	$0.51 \pm 0.08$

\*Max. Percentage of water absorption = 6% (ASTM C 1167 – 03)

\*Max. Saturated Saturation coefficient = 0.74 (ASTM C 1167 – 03)

The transverse strengths and flexural strength of triplicate catalyzed WEO-GRT manufactured with optimized parameters were shown in Table 4.13. The average wet and dry transverse strengths achieved by the catalyzed roofing tiles are 2037 N and 1191 N respectively. In this case, the dry transverse strength achieved by the specimens fulfilled the ASTM standards as a high profile roofing tiles, while the wet transverse strength achieved fulfilled the minimum requirement as a medium profile roofing tile as per ASTM standards. Hence, it indicates that the standard roofing tiles produced are

capable to withstand high pressure under both the arid and humid weather. Furthermore, the flexural strength achieved by the optimized WEO-GRT was found to be 3.26 MPa, which is comparable with other types of waste replacement masonry units, such as building materials incorporated with cotton and limestone powder that possessed of maximum flexural strength of 3.5 MPa (Halil and Tugut, 2008).

Table 4.13: Dry transverse strength, wet transverse strength and flexural strength achieved by optimized catalyzed WEO-GRT

Tiles No.	Dry Transverse Strength (N)	Wet Transverse Strength (N)	Flexural Strength (MPa)
1.	1998	1215	3.19
2.	1968	1136	3.15
3.	2145	1221	3.43
Average	2037 ± 94.7	1191 ± 47.4	3.26 ± 0.15

\*Min. dry transverse strength = 1779 N (ASTM C 1167 – 03; C 1492 – 03)

\*Min. wet transverse strength = 1334 N (ASTM C 1167 – 03; C 1492 – 03)

#### **4.5.2 Optimization Parameters of UCO-made Green Roofing Tiles (UCO-GRT)**

In the manufacturing process of UCO-GRT, used cooking oil instead of waste engine oil was utilized as sole binder to promote the development of binding matrix in the roofing material. Optimization process of UCO-GRT involved optimizing the waste oils composition, curing duration and amount of catalyst incorporated. Even though both the alternative binders used in the research study are defined as “waste oils”, they possessed of different chemical components, as well as viscosity that is strongly related to the workability of raw materials during the manufacturing process. Hence, it is important to determine the optimized UCO composition, heat curing duration, as well as amount of catalyst incorporated in the production of UCO-GRT. Table 4.14 reveals the selected parameter to be optimized associated with their descriptions.

Table 4.14: Selected parameters to be optimized in the manufacturing process of UCO-GRT

Optimizing parameters	Decision	Reason
Optimization of oil composition	Proceed to optimization process.	<ul style="list-style-type: none"> <li>• WEO and UCO possessed of different chemical properties, which may directly affect the strength developed by roofing tiles.</li> <li>• Optimization process is necessary.</li> </ul>
Optimization of curing duration		
Optimization of no. of Marshall compaction	Not proceed to optimization process.	<ul style="list-style-type: none"> <li>• The compactness is depended on the compaction process and the ratio of the ingredients.</li> <li>• Fixed at 20x compactions as in manufacturing process of WEO-GRT.</li> </ul>
Optimization of types and amount of acids incorporated	Proceed to optimization process.	<ul style="list-style-type: none"> <li>• Only H<sub>2</sub>SO<sub>4</sub> was used as catalyst in the manufacturing process.</li> </ul>
Coating as protective layer	Not proceed to optimization process.	<ul style="list-style-type: none"> <li>• UCO-GRT showed acceptable water resistance without the waste oil as protective layer.</li> </ul>

#### 4.5.2.1 Optimization of Curing Duration

Initially, the optimized parameters for the manufacturing of WEO-GRT were applied as the estimated appropriate approach in the production of UCO-GRT. In the manufacturing process, 5% of UCO and 95% of fly ash were blended thoroughly in a bench-mounting mixer for around 15 minutes. The resultant mixture was then compacted with 20 bowls of Marshall Compaction, followed by heat curing process in a ventilated oven under 190°C for 24 hours duration. As a result, the average dry transverse strength achieved by the roofing tiles produced is 1913.2 N, which is higher than the greatest strength achieved by the optimized WEO-GRT. However, it was believed the curing duration required for different type of waste oils to polymerize completely is differ from each other. In order to prove the assumption made, the heat curing duration for the manufacturing of UCO-GRT was varied from 12 to 30 hours. Table 4.15 shows the results obtained from the optimization process of curing duration. It was revealed that the strength of trial roofing tiles produced were gradually increased along with the curing duration, and reached the highest site after being heat cured for 18 hours. Hence, it was concluded that the optimized curing duration for the production of UCO-GRT is relatively shorter with respect to production of WEO-GRT. The strength achieved by the roofing tiles declined after the optimized curing duration. This condition was due to the excessive heat energy applied on the prototypes beyond the optimized value may lead to the deterioration of the chemical structure of UCO, consequently weakening the strength of the products.

Table 4.15: Average dry transverse strength and flexural strength of UCO-GRT heat cured for different durations

No.	Heat curing duration (hours)	Average dry transverse strength (N)	Average flexural strength (MPa)
1	12	1528.4 ± 58.0	2.45 ± 0.09
2	16	2064.1 ± 121.6	3.30 ± 0.19
3	18	2318.8 ± 108.7	3.71 ± 0.17
4	20	2273.2 ± 127.4	3.64 ± 0.20
5	22	2039.6 ± 108.7	3.26 ± 0.17
6	24	1913.2 ± 128.6	3.06 ± 0.21
7	30	1573.0 ± 71.4	2.52 ± 0.11

\*Min. dry transverse strength = 1779 N (ASTM C 1167 – 03; C 1492 – 03)

#### 4.5.2.2 Optimization of UCO and Filler Content

In the manufacturing process of UCO-GRT, used cooking oil that served as alternative binder is an important factor which directly affecting the mechanical properties of roofing tiles produced. The chemical compositions of UCO, including glycerol, free fatty acid and secondary oxidation products were took part in the complex oxy-polymerization reaction and further contributed in developing the strength of roofing tiles. Hence, it was noted that the amount of UCO incorporated in the manufacturing process is strongly related to the strength that can be achieved by roofing tiles. In order to maximize the strength of proposed roofing tiles, a series of triplicate prototypes were manufactured with different proportions of UCO to fly ash.

The composition of UCO used in the production of prototypes associated with their strength achieved is shown in Table 4.16. From the results, the prototypes possessed of lowest transverse strength when only 4.0% of UCO was used as binder. Along with the increasing of UCO composition, it was found that the dry transverse strength achieved by triplicate roofing tiles was gradually increased. However, when more or equal to 7.0% of UCO was incorporated, some cracks were encountered at the side of prototypes, which will severely affect the strength of the roofing tiles. As used cooking oil contains several types of volatile components, those species will evaporate under the elevated temperature. Hence, it was assumed that when too much of UCO was incorporated, great amount of volatile components would be converted into gaseous compounds during the thermal treatment. When the amount of gas is too much to escape from the existing pores, they will break through the compacted mixture, resulted in the cracks at the end of the heat curing process. Conclusively, the greatest strength was achieved when 6.5% of UCO and 93.5% of fly ash were utilized in the production of trial roofing tiles. This is due to the UCO components is sufficient in developing the strength of roofing tiles, whilst below the extent which would lead to the cracks at the end of the thermal treatment.

Table 4.16: Average dry transverse strength and flexural strength achieved by WEO-GRT produced with different composition of binder and filler content

No.	Composition of used cooking oil (%)	Average dry transverse strength (N)	Average flexural strength (MPa)
1	4.0	1594.5±55.2	2.55±0.09
2	4.5	1759.4±76.5	2.82±0.12
3	5.0	2318.8±108.7	3.71±0.17
4	5.5	2522.7±140.9	4.04±0.23
5	6.0	2852.6±94.9	4.57±0.15
6	6.5	3447.0±148.1	5.52±0.24
7	7.0	2889.7±54.5	4.63±0.09
8	8.0	2815.3±58.0	4.51±0.10

\*Min. dry transverse strength = 1779 N (ASTM C 1167 – 03; C 1492 – 03)

#### 4.5.2.3 Optimization of Amount of Catalyze Incorporated

In the previous optimization study, three different catalysts (nitric acid, HNO<sub>3</sub>; sulfuric acid, H<sub>2</sub>SO<sub>4</sub>; and hydrochloric acid, HCl) were utilized in enhancing the rate of polymerization reaction (see sector 4.5.1.4). The study reveals that H<sub>2</sub>SO<sub>4</sub> shows greatest performance in further enhancing the strength achieved by building materials. Compared to HCl and HNO<sub>3</sub>, H<sub>2</sub>SO<sub>4</sub> can release two hydrogen ions (H<sup>+</sup>) to promote the polymerization reaction in the waste oil. Hence, it can effectively enhance the rate of polymerization reaction during the thermal treatment. Hence, H<sub>2</sub>SO<sub>4</sub> was selected as the only catalyst to be studied in the manufacturing process of UCO-GRT.

In this investigation study,  $H_2SO_4$  was added as catalyst during the mixing process of raw materials. Since catalyst will not be consumed at the end of the chemical reaction, excessive addition of  $H_2SO_4$  would adversely affect the strength achieved. Hence, minor amount of  $H_2SO_4$  was incorporated to avoid the side effects besides enhancing the rate of polymerization reaction. As shown in Table 4.17, the composition of catalyst added is ranging from 0.0025 to 0.02 with respect to the total weight of prototypes. As a result, the strength of roofing tiles showed significant enhancement after the addition of  $H_2SO_4$ , and achieved the highest strength when 0.0125% of  $H_2SO_4$  was added. The optimized composition of catalyst is considered reasonable. If more UCO was used in the production of UCO-GRT, more catalyst is needed to trigger the oxy-polymerization reaction.

However, the excessive catalyst added beyond the optimum value will lead to the declination of strength of the roofing tiles. This is because catalyst was not be consumed at the end of the chemical reactions. As catalyst does not contribute in developing the strength of roofing tiles, it would obstruct the well binding of raw materials, subsequently decreased the strength of roofing tiles.

Table 4.17: The dry transverse strength and flexural strength of UCO-GRT incorporated with different composition of H<sub>2</sub>SO<sub>4</sub>

Percentage of catalyst added (%)	Dry transverse strength achieved by catalysed UCO-GRT (N)	Flexural strength achieved by catalysed UCO-GRT (MPa)
0.0025	3300.5±59.6	5.28±0.10
0.0050	3407.1±140.1	5.45±0.22
0.0075	3660.9±122.3	5.85±0.20
0.0100	3711.4±120.3	5.93±0.19
0.0125	4256.7±98.6	6.80±0.16
0.0150	3452.6±110.2	5.52±0.18
0.0175	3212.2±122.1	5.13±0.20
0.0200	3100.5±87.6	4.96±0.14

\*Min. dry transverse strength = 1779 N (ASTM C 1167 – 03; C 1492 – 03)

#### 4.5.2.4 Optimized Used Cooking Oil-made Green Roofing Tile (UCO-GRT)

In the optimization process of UCO-GRT, the prototypes with greatest properties can be produced by using following parameters:

- (a) 6.5% of UCO and 93.5% of fly ash
- (b) 20 times of Marshall Compaction
- (c) 18 hours of curing duration
- (d) 0.0125% of H<sub>2</sub>SO<sub>4</sub> as catalyst

According to the standard of American Concrete Institute, ACI 213R, the lightweight concrete building materials possessed of density between 1.440 to 1.840 g/cm<sup>3</sup>, while in-place density of normal-weight concrete is between 2.240 to 2.400 g/cm<sup>3</sup>. In Table 4.18, the average density of optimized UCO-GRT was calculated by using triplicate specimens. As a result, the average density of optimized UCO-GRT is 1.982 g/cm<sup>3</sup>. Hence, it was suggested to be categorized as normal-weight roofing tiles according to the standard of American Concrete Institute.

Table 4.18: Density of optimized UCO-GRT

Samples	Mass (g)	Volume (cm <sup>3</sup> )	Density (g/cm <sup>3</sup> )
1	395.6	199.5	1.983
2	395.3		1.981
3	395.7		1.983
Average			1.982

Thickness of specimens = 2.54 cm

Radius of specimens = 5 cm

In the verification process, the specimens were produced in the standard size with the dimension of 390 mm × 240 mm × 25 mm. The roofing tiles were manufactured by using the optimized parameters obtained from sectors 4.5.2.1 to 4.5.2.3. The mechanical properties in terms of transverse strength, flexural strength, percentage of water absorption and permeability of the manufactured standard catalyzed UCO-GRT were determined. This process allow the confirmation on the durability of the UCO to be used as sole binder in the manufacturing of masonry units, and ensure that the properties

achieved by the standard roofing tiles are similar or in-line with the results obtained from the round prototypes.

Table 4.19 shows the physical properties of the triplicate UCO–GRT produced. The results obtained reveal that the average dry transverse strength and flexural strength achieved by the optimized tiles are 4314.7 N and 6.91 MPa respectively. According to the ASTM standards, the minimum requirement of dry transverse strength is 1779 N for high profile tiles, and 1334 N for medium or low profile tiles. The results show that the standard UCO-GRT can be categorized as high profile roofing tile. In addition, the average percentage of water absorption achieved by the standard roofing tiles is 5.24%, which is limited below 6% as per requirement of ASTM standards. Hence, no additional treatment is required such as coating with waste oil as protective layer to lower the percentage of water absorption. This phenomenon was probably related to the amount of UCO incorporated in the manufacturing process. High amount of UCO utilized in the production of roofing tiles enable the well binding of the polymerized UCO components. The well binding matrix minimizes the surface pores of the roofing tiles. In addition, the hydrophobic nature of UCO provided lotus effect on the hydrophobic porous surface of UCO-GRT. This effect led to high surface tension of water molecules, hence minimized the solid-liquid surface energy between UCO-GRT and water. Those factors significantly decrease the penetration of water molecules into roofing tiles, hence resulted in UCO-GRT with acceptable water absorption. In addition, the average wet transverse strength achieved by UCO-GRT is 3288.1 N. Lastly, the well compacted roofing tiles restrict the

penetration of water molecules through the interior of roofing tiles to enable UCO to be used as the good binder for the production of roofing tiles.

Table 4.19: Physical properties of standard catalyzed UCO-GRT produced with optimized parameters

Mechanical properties	Achieved value	Requirements (ASTM standards)
Optimized dry transverse strength	$4314.7 \pm 01.6$ N	$\geq 1779$ N
Optimized flexural strength	$6.91 \pm 0.16$ MPa	-
Percentage of water absorption	$5.24 \pm 0.68$ %	$\leq 6.0$ %
Wet transverse strength	$3288.1 \pm 107.1$ N	$\geq 1334$ N
Permeability	Pass	No penetration of water after 24 hours

### **4.5.3 Comparison Study of UCO-RT and WEO-RT**

In this section, a comparison study among the roofing tiles produced from WEO and UCO was conducted. Different from previous sections, the manufacturing process of corresponding roofing tiles incorporated the fine sand as aggregate, which are the commonly used aggregate in the conventional building materials. In addition, both type of roofing tiles proposed (WEO-RT and UCO-RT) were manufactured under similar manufacturing parameters (number of compaction applied; curing temperature; curing duration; fine sand to fly ash ratio). A fair comparison was conducted on the strength based on different types of waste oils which acted as sole binder of building materials.

#### **4.5.3.1 Optimization of Fine Sand to Fly Ash Ratio**

Fine sand is one of the most commonly used materials incorporated in the traditional building materials. It serves as natural aggregate and being used to enhance the physical strength of the building materials produced. However, excessive addition of sand aggregate would adversely affect the developed strength. Fine sand is irregular in shape, hence the space left between the sand will lead to the loss of strength of the building materials. In addition, 1% of pores in the building materials will lead to the decrease of 6% of the total strength of building materials produced (Humayun et al., 2017b). Hence, fly ash which is serving as an important roles as filler, tasked to fill the spaces between the sand aggregate, hence to minimize the pores in the roofing tile. In order to determine the optimized ratio between fly ash and fine sand, a series

of prototypes were produced with different fine sand to fly ash ratio as shown in Table 4.20. The other parameters involved in the optimization process are as follows:

- 1) Type of waste oil incorporated: waste engine oil.
- 2) Composition of waste oil incorporated: 4% with respect to total weight of fly ash and fine sand.
- 3) Number of Marshall Compaction applied: 20 times.
- 4) Curing temperature: 190°C.
- 5) Curing duration: 24 hours.

Table 4.20: Dry transverse strength and flexural strength of roofing tiles produced from different fly ash to fine sand ratio

No.	Fine sand : Fly ash	Thickness (mm)	Average dry transverse strength (N)	Average flexural strength (MPa)
1	90:10	24.5	731.9	1.22
2	80:20	23.8	826.6	1.46
3	70:30	22.8	1304.1	2.51
4	65:35	22.0	1359.3	2.81
5	60:40	21.6	1291.7	2.77
6	50:50	21.4	1043.6	2.28
7	40:60	20.8	237.8	0.55
8	30:70	20.5	138.6	0.33

As the density of fine sand and fly ash are different, the prototypes produced from different fly ash to fine sand ratios possessed of different thickness. Prototypes that produced from 90 % of fly ash are thickest. The thickness of prototypes was gradually decrease when the percentage of fine sand incorporated in the manufacturing process was gradually increased. In addition, the greatest flexural strength was achieved when 65 % of fine sand and 35 % of fly ash were utilized, with average strength of 2.81 MPa. At the optimized point, it was assumed that the maximum fine sand would contribute in developing the strength of prototypes produced. The function of fly ash is to occupy all the spaces in between the fine sand. The optimized ratio of fly ash and fine sand was found as 35:65.

#### **4.5.3.2 Optimization of Waste Oils Compositions**

In the comparison study, two different types of waste oils, which are waste engine oil and used cooking oil were utilized as sole binder in the production of roofing tiles. In the optimization process of waste oils compositions, different percentages of waste oil varied from 3.0 % to 5.0 % were mixed with fixed ratio of aggregate to filler content to produce the waste oil-made roofing tiles. Table 4.21 shows the preliminary result obtained from the triplicate samples of UCO-RT and WEO-RT based on the flexural strength achieved and their physical observation. It was revealed that UCO3.5, UCO4.0 and UCO4.5 which were produced from 3.5, 4.0 and 4.5% of used cooking oil showed applicable results, similar to WEO<sub>3.5</sub> and WEO<sub>4.0</sub> which manufactured by using 3.5 and 4.0 % of waste engine oil. The remaining samples were

concluded as not suitable for further investigation as described in Table 4.21. Generally, UCO-RT possessed greater strength with respect to WEO-RT. As explained previously, the strength of roofing tiles are strongly related to the quantity of C=O group presented in the corresponding binder. Hence UCO which consists of more C=O containing species would be able to produce harder, stronger roofing tiles compared to WEO. In addition, the present of soot in WEO may adversely affect the binding matrix of the samples, consequently weakening the samples' strength.

Conclusively, it was found that the greatest strength was achieved when 4.0 % of UCO was incorporated. The breaking strength and flexural strength of UCO<sub>4.0</sub> are 4.971 kN and 10.498 MPa respectively, hence categorized as high profile roofing tiles in accordance to ASTM standards (ASTM C 1167-03; ASTM C 1492-03). Even though prototypes of WEO-RT possessed lower strength compared to UCO-RT, they fulfil the minimum requirement of 1.334 kN as per ASTM standards, and were classified as medium profile roofing tiles (ASTM C 1167-03; ASTM C 1492-03).

Table 4.21: Breaking strength, flexural strength achieved and observation on the samples made from different composition of waste oil

Sample Name	Binders	Composition (%)	Thickness (mm)	Transverse Strength (kN)	Flexural Strength (MPa)	Observation
UCO <sub>3.0</sub>	UCO	3.0	-	-	-	-Can support self-weight but too weak to handle
UCO <sub>3.5</sub>		3.5	21.55	3.969 ± 0.084	8.538 ± 0.18	-Stable and able to maintain self-weight
UCO <sub>4.0</sub>		4.0	21.75	4.971 ± 0.093	10.498 ± 0.20	-Show significant strength
UCO <sub>4.5</sub>		4.5	21.80	2.573 ± 0.064	5.409 ± 0.13	-Proceed for further tests
UCO <sub>5.0</sub>		5.0	-	-	-	-Unable to maintain self-weight
WEO <sub>3.0</sub>	WEO	3.0	-	-	-	-Can support self-weight but too weak to handle
WEO <sub>3.5</sub>		3.5	22.00	1.573 ± 0.048	3.247 ± 0.10	-Stable and able to maintain self-weight
WEO <sub>4.0</sub>		4.0	21.80	1.360 ± 0.039	2.859 ± 0.08	-Proceed to further tests
WEO <sub>4.5</sub>		4.5	-	-	-	-Unable to maintain self-weight
WEO <sub>5.0</sub>		5.0	-	-	-	

#### 4.5.3.3 Water Absorption and Permeability

Water absorption of the construction materials is one of the most important criteria to preserve the durability of a building. By determining the percentage of water absorbed by waste oil-made roofing tiles, the information of structural pores, durability and permeation characteristic of roofing tiles produced can be obtained (Zhang and Zong, 2014). In addition, good building materials should have great resistance towards the penetration of water or other aggressive agents such as sodium chloride (NaCl) and acid solution. Table 4.22 reveals the percentage of water absorption and the permeation characteristic of triplicate samples. Due to the “like dissolves like” concept, the waste oil that is non-polar in nature will push away the water molecules that are polar in nature when interacted (Deborah, 2017). This phenomenon resists and retard the infiltration of water into the interior part of the samples, and successfully controlled the rate of water absorption within the standard limit of 6% as per ASTM standards (ASTM C 1167–03; ASTM C 1492–03). In addition, all of the samples were found impermeable to water, sodium chloride solution and diluted acid, as no corresponding liquid droplets were encountered after the duration of permeability test. Even though the specimens fulfilled the water absorption limitation according to ASTM standards, the penetration of water molecules into the specimens adversely affected the strength of roofing tiles produced. As a result, the average flexural strength achieved by specimens after the water absorption test are relatively lower compared to their flexural strength achieved under dried condition (see section 4.5.3.2). This phenomenon indicated that the present of water molecules

between the binding matrixes weakening the bonding strength, consequently decreasing the strength developed by the roofing tiles.

Table 4.22: Percentage of water absorption, flexural strength (wet condition) and permeation characteristic of samples produced from different composition of waste oil

Sample Name	Water Absorption (%)	Flexural Strength under Wet Condition (MPa)	Permeability		
			H <sub>2</sub> O	NaCl (0.1M)	Diluted Acid (0.1M)
UCO <sub>3.5</sub>	3.927	5.089 ± 0.16	Pass	Pass	Pass
UCO <sub>4.0</sub>	3.785	6.330 ± 0.27	Pass	Pass	Pass
UCO <sub>4.5</sub>	3.676	3.838 ± 0.18	Pass	Pass	Pass
WEO <sub>3.5</sub>	4.879	1.878 ± 0.09	Pass	Pass	Pass
WEO <sub>4.0</sub>	4.511	2.14 ± 0.11	Pass	Pass	Pass

#### 4.5.3.4 Specific Heat Capacity

Based on all of the results in Section 4.5.3.2 and 4.5.3.3, it can be concluded that UCO<sub>4.0</sub> and WEO<sub>3.5</sub> are the optimized combinations for manufacturing of UCO-RT and WEO-RT respectively. Both of the samples achieved the greatest strength in each category, whilst fulfilling the minimum requirement for water absorption and permeability test. As excellent thermal resistance is one of the desire qualifications for roofing tiles, the specific heat capacity of UCO<sub>4.0</sub> and WEO<sub>3.5</sub> were determined. Table 4.23 demonstrates the

specific heat capacity achieved by samples and a comparison was made with the commercial building materials. The specific heat capacity of UCO<sub>4.0</sub> and WEO<sub>3.5</sub> were calculated to be 1039 and 874 J/kg.°C. From Figure 4.19, it was revealed that the specific heat capacity of WEO<sub>3.5</sub> is similar to brick or concrete building materials. Hence, it was assumed that the thermal resistance of WEO<sub>3.5</sub> is comparable with those building materials. In addition, it was revealed that the specific heat capacity of UCO<sub>4.0</sub> is 18.9 %, 23.7 % and 18.1 % higher than WEO<sub>3.5</sub>, brick and concrete, indicated more heat energy is required to raise the temperature of UCO-made roofing tiles. However, the thermal conductivity of UCO<sub>4.0</sub> is higher than WEO<sub>3.5</sub>. Hence, it can be concluded that UCO<sub>4.0</sub> has weaker thermal insulation with respect to the WEO<sub>3.5</sub>. Table 4.23 shows the thermal properties of both of the optimized tiles produced.

Table 4.23: Thermal properties of optimized roofing tiles

Sample name	Heat capacity (J/kg. °C)	Heat transfer rate (kJ/s)	Thermal conductivity (J/mm. °C)
WEO <sub>3.5</sub>	874	33.005 ± 0.35	0.350 ± 0.003
UCO <sub>4.0</sub>	1039	39.241 ± 0.35	0.416 ± 0.003

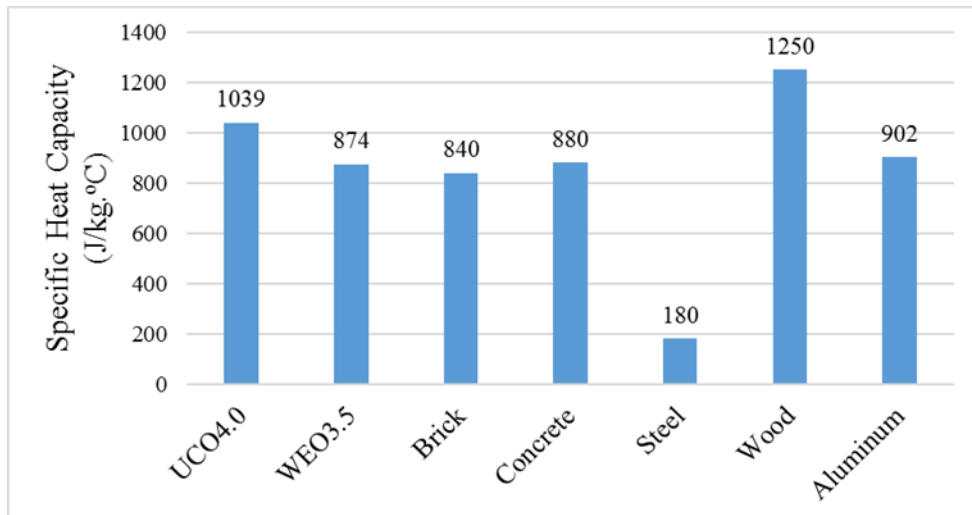


Figure 4.19: Specific heat capacity of UCO<sub>4.0</sub>, WEO<sub>3.5</sub> and other commercial building materials (Designing Buildings, 2016).

#### 4.5.3.5 Ultra-violet (UV) Acceleration Test

As the topping of a building, roofing tiles play important roles as protector to resist the direct exposure of sunlight. Ultra-violet (UV) is electromagnetic radiation with wavelength between 10 nm to 400 nm. In sunlight, UV constituted of around 10% of the total light output of the Sun. UV with shorter wavelength are considered as ionizing radiation. It consists of photons with greater energy, which are able to ionize atoms. Over-exposure of organic molecules to UV radiation consequently lead to the chemical and biological effects. Sunburn are the most common effect after long-term exposure of the skin to UV, whilst consists of higher risk of skin cancer. In addition, the ionizing UV radiation would lead to re-polymerization of the polymer materials, hence causing the restructuration of the polymer chains. The properties of the restructured will be affected and its original properties will be lost.

The roofing tiles were exposed to sunlight continuously for long duration, the UV resistance of them was investigated by performing UV acceleration test. Two UV light bulbs with intensity five folds greater than the UV from sunlight were utilized in the investigation study. It was assumed that the daily exposure of roofing tiles toward sunlight is around 8 hours (from 10 a.m. to 6 p.m.), while the UV acceleration test was carried out with 24 hours basis. Hence, it was estimated that the exposure of the novel roofing tiles towards UV radiation in the UV chamber for 1 day resemble 30 day as in the normal atmosphere condition. Figure 4.20 shows the change in the strength of oil-made roofing tiles along with the exposure duration toward the UV radiation. Initially, the strength of UCO-RT and WEO-RT was determined to be 4.971 and 1.573 kN respectively. Along with the increase of UV exposure duration, the strength of roofing tiles was gradually increased. According to Humayun et al. (2017a), exposure to the UV light would increase the hardness of oil-made building materials. However, the fragility of the corresponding construction materials would also being affected. After being exposed for around 360 days (equivalent to 30 years) of UV light, the strength of UCO-RT increased by 6.26%, while the strength of WEO-RT increased by 58.23%.

Since the UV radiation only emitted on the exposure surface of roofing tiles, the re-polymerization will only occur within the corresponding area. The interior part of innovated roofing tiles was not affected. Hence, the strength of UCO-RT was only slightly increased after being exposed to the UV radiation over the time. In addition, it was noticed that the strength of WEO-RT was increased by 58.23 % after the UV treatment. However, the re-polymerization

reaction occurred during the UV treatment is only certainly contributed to the huge enhancement. It is believed that other chemical reaction was occurred during the experimental period, but does not involved the UV radiation. An assumption was made, in which the oxy-polymerization that supposedly occurred at 190°C, was occurred continuously within the WEO-RT under the ambient temperature, but with relatively slower rate. It was suspected that this condition only happen for the tiles with incomplete polymerization reaction during the manufacturing process. The occurrence of oxy-polymerization consequently strengthen the binding matrix of WEO-RT, resulted in the significant enhancement in its strength. However, more experiment should be carry out to prove the rationality of the mentioned assumption.

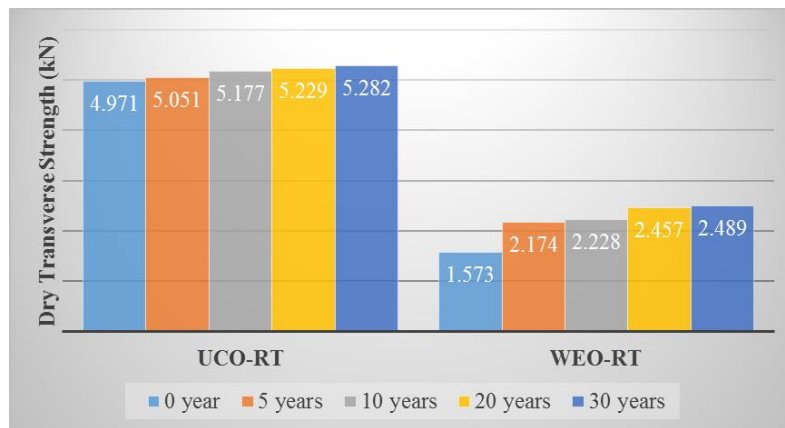


Figure 4.20: Flexural strength of innovated roofing tiles along with the exposure duration towards UV light

#### 4.5.3.6 Freeze-thaw Analysis

The stability of roofing tiles put under repeatedly extreme weather was investigated using freeze-thaw stability test. Two types of innovated roofing tiles, which were produced from 4% of UCO and 3.5% of WEO were subjected to 50 cycles of freeze-thaw analysis. Initially, the weight of UCO-RT and WEO-RT were recorded at 405g and 404g respectively. At 10th, 30th and 50th cycle, the changes in the weight of these roofing tiles were determined as shown in Table 4.24. At the end of the test, no new cracks was observed on the samples' surface. The total weight loss of UCO-RT and WEO-RT are determined as 2.47% and 2.97% with respect to their original weight. In addition, the dry transverse strength of the innovated roofing tiles which experienced 50 cycles of freeze-thaw analysis were determined to be 3.929 and 1.211 kN. Compared to the initial flexural strength of UCO<sub>4.0</sub> and WEO<sub>3.5</sub>, which are 4.971 and 1.573 kN, the strength of the roofing tiles were decreased for 20.96 and 23.01 %. However, the strength achieved by UCO<sub>4.0</sub> and WEO<sub>3.5</sub> after experienced 50 cycles of freeze-thaw test are still within the minimum requirement of dry transverse strength in accordance to ASTM standards.

Table 4.24: Weight loss of roofing tiles over freeze-thaw cycles

Types of tiles	Initial mass (g)	10 <sup>th</sup> cycle (g)	30 <sup>th</sup> cycle (g)	50 <sup>th</sup> cycle (g)	Total weight lost (%)
UCO <sub>4.0</sub>	405	399	396	395	2.47
WEO <sub>3.5</sub>	404	397	395	392	2.97

## **4.6 Life Cycle Assessment**

Life Cycle Assessment (LCA) is a holistic approach that has been widely used in estimating the environmental impact, as well as quantifying the rate of carbon emissions and energy usage of different building materials and components (Dixit et al., 2012). By determining the embodied carbon (EC) and embodied energy (EE) of the invented products, the environmental suitability of the innovated roofing tiles can be determined.

### **4.6.1 LCA of Catalyzed WEO-GRT**

The total carbon emissions of innovated roofing tiles was quantified, including “cradle to gate”, “cradle to site” and “cradle to grave” embodied carbon. Cradle to gate carbon emissions account for the CO<sub>2</sub> released during manufacturing of materials and operation progress (Dixit et al., 2010), or release of carbon compounds from the materials incorporated (Gartner, 2004). Waste materials composed of relatively lower EC than virgin components. Recycle or reuse of materials that has lost the invented carbon in their service life able to reduce the carbon emissions while being utilized in manufacturing a new product (Ali and Xiao, 2017). For example, fly ash has extremely low embodied carbon (0.004 kg CO<sub>2</sub> per equivalent) as it is the by-product generated after ignition of coal under high temperature in electricity generator (Humayun et al., 2017a). Cradle to site emission accounts for the CO<sub>2</sub> released during transporting the materials or facilities from the suppliers and to the

construction site. While cradle to grave included the carbon emissions incurred in the end-of-life (EOL) of the building materials.

Table 4.25 shows the embodied carbon of catalyzed WEO-GRT from different emission sectors, including carbon dioxide released during materials extraction process, distribution of products and disposal of waste materials (Humayun et al., 2017a). From Table 4.25, it is revealed that 0.4628 kg CO<sub>2</sub> was released while producing a 3 kg catalyzed WEO-GRT, and its embodied carbon is calculated as 0.1542 kg CO<sub>2</sub>/kg. A comparison analysis is as shown in Figure 4.21. It indicates that embodied carbon of catalyzed WEO-GRT is relatively low compared to the traditional roofing tiles. The embodied carbon for catalyzed WEO-GRT is 36%, 198% and 282% lower with respect to cementitious, kiln-fired and ceramic roofing tiles as determined by ICE Ver. 1.6 a (Hammond and Jones, 2008). It indicates that the catalyzed WEO-GRT produced are more environmental friendly. Implementation of recycling or reusing waste materials could effectively reduce the total carbon emissions during the manufacturing process.

In addition, the embodied energy of catalyzed WEO-GRT was taken as the total primary energy consumed over its manufacturing process. It was found that the embodied energy of the novel tiles is in the lower site with respect to the traditional roofing tiles. Table 4.26 indicates that 1.27 MJ of energy was consumed while producing a catalyzed WEO-GRT, and its embodied energy was calculated to be 0.42 MJ/kg. As the data provided in ICE Ver. 1.6 a, the emission of energy for catalyzed WEO-GRT is 231%,

1448% and 2043% lesser than concrete, clay and ceramic roofing tiles respectively. The replacement of traditional high energy consuming binders, such as kiln firing in clay and cement production in concrete roofing tiles successfully reduces the energy consumption to a significant extent. Hence, the binder from waste, i.e. waste engine oil with lower embodied energy could be classified as environmental friendly binder

Table 4.25 Embodied carbon of catalyzed WEO-GRT

Cradle to Gate Embodied Carbon of Materials				
Materials / Operation	Emission factor (kg CO <sub>2</sub> /equiv.)	Quantity incorporated (kg)	Electricity usage (kWh)	Total Emission (kg CO <sub>2</sub> )
Waste Engine Oil	1.00	0.15	-	0.15
Coal-fired ash	0.004	2.85	-	0.0114
Sulfuric Acid (1M)	0.17	0.00225 (diluted to 0.1M)	-	0.0004
Mixing Process	0.63	-	0.006 (20min)	0.004
Heat curing process	0.63	-	0.4 (24hours)	0.252
Total Phase Emission				0.4178
Cradle to Site Embodied Carbon – Impact of Transportation				
Materials	Estimated Transport Distance (km)	Transport Emission (kg CO <sub>2</sub> /km)		Total Emission
Materials Extraction				
Waste Engine Oil	100	0.0001		0.01
Sulfuric Acid	40	0.0001		0.004
Fly Ash	60	0.0001		0.006

Distribution of Product				
Roofing Tiles	200		0.0001	0.02
Total	Phase			0.04
Emission				
Cradle to Grave Embodied Energy				
Materials	Estimated	Transport	Emission	Total
	Transport Distance	(kg CO <sub>2</sub> /km)		Emission
	(km)			
Broken Roofing Tiles	50		0.0001	0.005
Total Phase				0.005
Emission				
Total Emission				0.4628
Embodied Carbon of Roofing Tiles				0.1542

\* Emission factor were obtained from Ecoinvent 3.3 and ICE Ver. 1.6a (Hammond and Jones, 2008)

Table 4.26: Embodied Energy of catalyzed WEO-GRT

Materials	Embodied Energy (MJ/kg)	Quantity (kg)	Total embodied energy per tiles (MJ)
Waste Engine Oil	8.00 <sup>[a]</sup>	0.15	1.20
Coal-fired ash	0.00 <sup>[b]</sup>	2.850	0.00
Sulfuric acid	5.00 <sup>[c]</sup>	0.00225	0.01125
Processing	0.06 <sup>[a]</sup>	-	0.06
Total Emission			1.27
Embodied Energy of Roofing Tiles			0.42

\* a, (Humayun et al., 2017b); b, (Chani et al., 2003); c, (Eric et al, 2002)

#### 4.6.2 LCA of Catalyzed UCO-GRT

Figure 4.21 reveals the comparison study of UCO-GRT along with the innovated roofing tiles produced in this research study, and the conventional roofing tiles available in the market. Generally, the embodied carbon and embodied energy of UCO-GRT are determined to be 0.105 kg CO<sub>2</sub>/kg and 0.156 MJ/kg, which is relatively lower compared to WEO-GRT. The main factor which is affecting the EE and EC of both types of GRT is the alternative binder utilized. Used cooking oil possessed of relatively lower EE and EC. According to Ecoinvent 3.3, no carbon dioxide will be released from UCO during the manufacturing process (0.00 kg CO<sub>2</sub>/kg), while carbon emission factor of WEO was determined to be 1.00 kg CO<sub>2</sub>/equivalent. In addition, the

embodied energy of UCO and WEO were 2.00 MJ/kg and 8.00 MJ/kg respectively. Hence, it indicates that UCO are more environmental friendly when being utilized as the alternative binder.

In comparison to roofing tiles produced from cement, clay and ceramic, it was found that the carbon dioxide emitted during the production of UCO-GRT is 99.0%, 338.1% and 461.9% lesser respectively. In addition, the energy consumption during the manufacturing process UCO-GRT is 802.6%, 4120.8% and 5744.2% lower compared to the mentioned conventional roofing tiles. Hence, it was suggested that the UCO-GRT can be categorized as environmental-friendly building materials. Tables 4.27 and 4.28 show the calculation of the embodied carbon and embodied energy of UCO-GRT.

Table 4.27: Embodied carbon of UCO-GRT

<b>Cradle to Gate – Materials Extraction and Manufacturing</b>					
Material	Quantity	Emission	Estimated	Transport	Total
	(kg)	factor	transportation	emission (kg	Emission
		(kgCO <sub>2</sub> /eq)	distance (km)	CO <sub>2</sub> /km)	
UCO	0.195	0.00	100	0.0001	0.01
Fly ash	2.805	0.004	60	0.0001	0.017
Sulfuric Acid	0.00375	0.17	60	0.0001	0.007
<b>Manufacturing Process</b>					
Operation	Curing time	Electricity Usage (kWh)	Emission factor	Total	
	(hours)		(kgCO <sub>2</sub> /eq)	emission	
Heat Curing	18	0.4	0.63	0.252	
Mixing	0.5	0.008	0.63	0.005	
<b>Cradle to Site – Distribution of Products</b>					
Material	Estimated transportation distance (km)	Transport emission	Total		
		(kg CO <sub>2</sub> /km)	emission		
Tiles	200	0.0001	0.02		
<b>Cradle to Grave – End of Life Management</b>					
Material	Estimated transportation distance (km)	Transport emission	Total		
		(kg CO <sub>2</sub> /km)	emission		
Tiles	40	0.0001	0.004		
Total Carbon Emission Per Tiles (kgCO <sub>2</sub> )					0.315
Embodied Carbon (kgCO <sub>2</sub> /kg)					0.105

\* Emission factor were obtained from Ecoinvent 3.3 and ICE Ver. 1.6a

(Hammond and Jones, 2008)

Table 4.28: Embodied energy of UCO-GRT

Materials	Embodied Energy (MJ/kg)	Quantity (kg)	UCO-GRT
Used Cooking Oil	2.00 <sup>[a]</sup>	0.195	0.39
Fly Ash	0.00 <sup>[b]</sup>	2.805	0.00
Sulfuric Acid	5.00 <sup>[c]</sup>	0.00375	0.01875
Processing	0.06 <sup>[d]</sup>	-	0.06
Total Emission		3.00375	0.469
per Tiles (MJ)			
Embodied Energy			0.156
(MJ/kg)			

\*a (Reijnders and Huijbregts, 2008); \*b (Chani et al, 2003); \*c (Eric et al, 2002); \*d (Humayun et al, 2017b).

#### 4.6.3 LCA of UCO-RT & WEO-RT

The environmental aspects of UCO<sub>4.0</sub> and WEO<sub>3.5</sub> were investigated in terms of their embodied carbon and embodied energy respectively. Tables 4.29 and 4.30 reveal the total carbon dioxide emitted and total energy consumed while manufacturing single tile of UCO<sub>4.0</sub> and WEO<sub>3.5</sub>. A comparison study was made among the innovated roofing tiles produced in this research study with the conventional roofing tiles (cement, clay and ceramic) as demonstrated in Figure 4.21.

From Tables 4.29 and 4.30, the embodied carbon and embodied energy of UCO<sub>4.0</sub> were determined as 0.077 kg CO<sub>2</sub>/kg and 0.154 MJ respectively. It

is revealed that the embodied carbon and embodied energy of WEO<sub>3.5</sub> are 125.9% and 45.4% higher with respected to UCO<sub>4.0</sub>. This indicates that more energy will be consumed and greater carbon dioxide will be released during the production of WEO-RT. The EE and EC of UCO<sub>4.0</sub> and WEO<sub>3.5</sub> are much lower compared to conventional roofing tiles. Hence, both of them were suggested to be categorized as environmental friendly building materials, where UCO is greener and cleaner than WEO as an alternative binder in terms of the environmental aspects.

Table 4.29: Embodied energy of UCO-RT and WEO-RT

Materials	Embodied Energy (MJ/kg)	Quantity (kg)	UCO <sub>4.0</sub>	WEO <sub>3.5</sub>
Used Cooking Oil	2.00 <sup>[a]</sup>	0.16	0.32	-
Waste Engine Oil	8.00 <sup>[b]</sup>	0.14	-	1.12
Fly Ash	0.00 <sup>[c]</sup>	1.40	0.00	0.00
Sand Aggregate	0.10 <sup>[d]</sup>	2.60	0.26	0.26
Processing	0.06 <sup>[b]</sup>	-	0.06	0.06
Total Emission per Tiles (MJ)			0.64	1.44
Embodied Energy (MJ/kg)			0.154	0.348

\*a (Reijnders and Huijbregts, 2008); \*b (Humayun et al., 2017b); \*c (Chani et al, 2003); \*d (Hammond and Jones, 2008)

Table 4.30: Embodied carbon of UCO-RT and WEO-RT

Cradle to Gate – Materials Extraction and Manufacturing						
Material	Quantity (kg)	Emission factor (kgCO <sub>2</sub> /eq)	Estimated transportation distance (km)	Transport emission (kg CO <sub>2</sub> /km)	UCO <sub>4.0</sub>	WEO <sub>3.5</sub>
					Total Emission	
Used Cooking Oil	0.16	0.00	100	0.0001	0.01	-
Waste Engine Oil	0.14	1.00	100	0.0001	-	0.15
Sand	2.60	0.005	60	0.0001	0.019	0.019
Fly ash	1.40	0.004	60	0.0001	0.012	0.012
Manufacturing Process						
Operation	Curing time (hours)	Electricity Usage (kWh)	Emission factor (kgCO <sub>2</sub> /eq)		Total emission	
Heat Curing	24	0.4	0.63		0.252	0.252
Mixing	0.5	0.008	0.63		0.005	0.005

Table 4.30 Embodied carbon of UCO-RT and WEO-RT (continue)

Cradle to Site – Distribution of Products				
Material	Estimated transportation distance (km)	Transport emission (kg CO <sub>2</sub> /km)	Total emission	
Tiles	200	0.0001	0.02	0.02
Cradle to Grave – End of Life Management				
Material	Estimated transportation distance (km)	Transport emission (kg CO <sub>2</sub> /km)	Total emission	
Tiles	40	0.0001	0.004	0.004
Total Carbon			0.322	0.462
Emission Per Tiles				
(kgCO <sub>2</sub> )				
Embodied Carbon			0.077	0.112
(kgCO <sub>2</sub> /kg)				

\* Emission factors were obtained from Ecoinvent 3.3 and ICE Ver. 1.6a (Hammond and Jones, 2008).

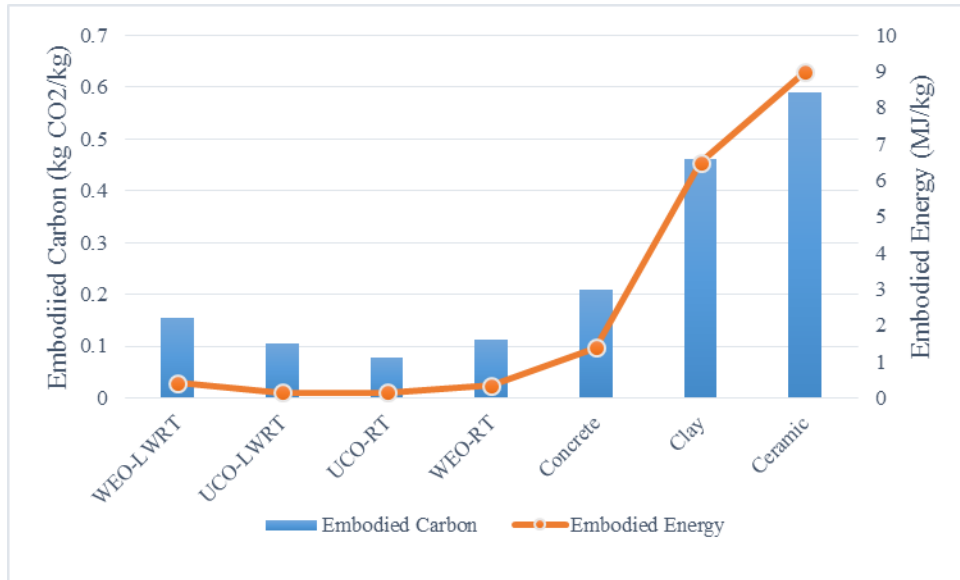


Figure 4.21: Comparison study of EE and EC of innovated and conventional roofing tile

## CHAPTER 5

### CONCLUSIONS AND RECOMMENDATIONS

#### 5.1 Conclusion

##### 5.1.1 General Conclusion

Conclusively, this research study discovers a novel approach for the manufacturing of roofing tiles. Four different types of roofing tiles namely (i) UCO-GRT; (ii) WEO-GRT; (iii) UCO-RT and (iv) WEO-RT were produced and investigated. These roofing tiles were produced from two alternative binders, including used cooking oil and waste engine oil. The chemical properties of the alternative binders, the physical and mechanical properties of innovated roofing tiles and their environmental impacts were studied and discussed. Several conclusions were deduced based on the experimental results, which are as follows:

1. The novel manufacturing approach of roofing tiles involved mixing, compacting and heat curing process. The raw materials utilized in the manufacturing process involved waste oil, fly ash, fine sand, and catalyst. Both types of waste oil (waste engine oil and used cooking oil) can be used as alternative binder in the production of roofing tiles.

2. During the heat curing process, the oxy-polymerization reaction occurred, which led to the hardening of innovated roofing tiles. Chemical investigation of waste oils indicated that as compared to waste engine oil, used cooking oil consisted of greater amount of corresponding components involved in the chemical reaction. The preliminary analysis can be used to predict the strength that can be developed when waste oils are used as the binder in the manufacturing process.
  
3. The physical strength and mechanical properties of used cooking oil-made roofing tiles (UCO-GRT and UCO-RT) is greater and better compared to waste engine oil-made roofing tiles (WEO-GRT and WEO-RT). The flexural strength of all of the optimized roofing tiles produced could achieved the minimum requirements for the standard roofing tiles as per ASTM standards, whilst showed impermeability and acceptable water absorption.
  
4. In terms of environmental issues (embodied carbon and embodied energy), the innovated roofing tiles produced possessed of relatively lower embodied carbon and embodied energy with respect to those conventional roofing tiles, including cementitious, clay and ceramic products. Since the mechanical properties of innovated roofing tiles fulfilled the criteria, they are potentially to be used in replacement of the conventional roofing tiles in the future.

5. The concept of producing 100% waste-made building materials is proved in this research study. The Green roofing tiles (GRT) was produced from waste oil (UCO and WEO), fly ash and minutes amount of catalyst (negligible), showed great enhancement in the waste replacement level in the masonry units.

### **5.1.2 Conclusion for Objective 1**

Oxy-polymerization reaction is the proposed chemical reaction involved in the solidification of waste oil during the thermal treatment (Humayun et al., 2017). Under the elevated temperature, the occurrence of condensation polymerization reactions within the waste oils resulted in the rigidification of roofing tiles. In this study, ATR-FTIR was utilized to determine the chemical changes of waste oils under different temperatures. Two main functional groups involved in the chemical reactions, which are C=O and C-O groups were observed and studied. From the FTIR spectra of used cooking oil, the intensity of C=O bond located at  $1740\text{ cm}^{-1}$  and two C-O bands  $1161$  and  $1116\text{ cm}^{-1}$  respectively were increased gradually along with the elevated temperature. This phenomenon indicated that the concentration of C=O and C-O groups are increased during the heat curing process, which are the products generated from condensation polymerization reactions. Similar phenomena were observed in the FTIR spectra of waste engine oil. In addition, the oxidation extent of UCO and WEO is 1.74 and 0.26 respectively. Carbonyl group is an important component involved in the condensation polymerization reactions. Hence, it was predicted that UCO can contribute more carbonyl

containing species in the polymerization reaction, and produced a roofing tiles with greater strength compared to WEO.

### 5.1.2 Conclusion for Objective 2

Waste engine oil, used cooking oil, fly ash, fine sand and strong acid are the raw materials utilized in the production of innovated roofing tiles. The waste oils served as alternative binder to develop the strength of roofing tiles; fly ash served as filler to occupy the pores within the tiles, fine sand served as aggregate to enhance the strength, and strong acid served as catalyst to increase the rate of polymerization reaction. A series of optimization processes were carried out to determine the optimized compositions and manufacturing parameters of different types of innovated roofing tile. Table 5.1 summarizes the optimized material compositions and the manufacturing parameters of different types of optimized products produced in this study.

Table 5.1: Optimized composition and manufacturing parameters for different types of tile

Name	Compositions	Manufacturing parameters
WEO-GRT	<ul style="list-style-type: none"> <li>• 5.0% of WEO</li> <li>• 95.0% fly ash</li> <li>• 0.0075% H<sub>2</sub>SO<sub>4</sub></li> </ul>	<ul style="list-style-type: none"> <li>• 20 times of Marshall Compaction</li> <li>• 24 hours of curing duration</li> </ul>
UCO-GRT	<ul style="list-style-type: none"> <li>• 6.5% of UCO</li> <li>• 93.5% of fly ash</li> <li>• 0.0125% of H<sub>2</sub>SO<sub>4</sub></li> </ul>	<ul style="list-style-type: none"> <li>• 20 times of Marshall Compaction</li> <li>• 18 hours of curing duration</li> </ul>

WEO-RT	<ul style="list-style-type: none"> <li>• 3.5% of WEO</li> <li>• 96.5% of fine sand: fly ash (65:35)</li> </ul>	<ul style="list-style-type: none"> <li>• 20 times of Marshall Compaction</li> <li>• 24 hours of curing duration</li> </ul>
UCO-RT	<ul style="list-style-type: none"> <li>• 4.0% of WEO</li> <li>• 96.0% of fine sand: fly ash (65:35)</li> </ul>	<ul style="list-style-type: none"> <li>• 20 times of Marshall Compaction</li> <li>• 24 hours of curing duration</li> </ul>

### 5.1.3 Conclusion for Objective 3

In this study, American Society for Testing and Materials (ASTM) standard was used as a guideline to determine the mechanical properties of innovated roofing tiles produced. Based on the results obtained, all of the roofing tiles produced fulfil the minimum requirement of transverse strength ( $\geq 1.779$  kN), having acceptable water absorption ( $\leq 6.0$  %) and impermeable to water. Among the optimized tiles produced, UCO-RT has the greatest flexural strength, which is 10.5 MPa, followed by UCO-RT (6.91 MPa), WEO-GRT (3.26 MPa) and WEO-RT (3.25 MPa). The roofing tiles produced by utilizing UCO as binder showed higher strength compared to WEO-made roofing tiles, indicated the binding effect of UCO is much greater than WEO. In addition, UCO shows lotus effect on the surface of UCO-made roofing tiles (UCO-GRT and UCO-RT) produced, which successfully controlled their percentage of water absorption below the limitation. However, the percentage of water absorption of WEO-GRT is excess the limitation, which is due to the weak lotus effect of WEO and hygroscopic behavior of fly. Hence, post coating of extra WEO layer on the surface of WEO-GRT was carried out to

enhance its lotus effect, hence controlled the percentage of water absorption of the coated tile at 5.35%.

#### **5.1.4 Conclusion for Objective 4**

The environmental impacts in terms of embodied carbon and embodied energy are the important issues to be concerned during the production of building materials. The EE and EC of innovated roofing tiles were calculated and compared. Among the innovated roofing tiles, UCO-RT possesses the lowest EE and EC, which are 0.077 kgCO<sub>2</sub>/kg and 0.154 MJ/kg respectively; while WEO-GRT is consisted of highest EE and EC, which are 0.154 kgCO<sub>2</sub>/kg and 0.42 MJ/kg respectively. In comparison with conventional roofing tiles, all types of innovated roofing tiles possess of lower EE and EC. Since all of the innovated roofing tiles fulfil the minimum requirement of mechanical properties as listed in ASTM standards, they are considered as more environmental-friendly products. Hence, it can be concluded that the innovated roofing tiles can replace the conventional roofing tiles.

## 5.2 Limitations

In this study, several limitations were encountered during the manufacturing process of roofing tiles. The limitations are as follows:

(1) Waste oils especially waste engine oil are chemically complicated. They may contain high concentrations of toxic species. In addition, waste engine oil and fly ash consist of significant amount of heavy metals and metal related components. Since waste oils and fly ash were utilized as the raw materials for the production of innovated roofing tiles, the toxic and metal components were indirectly incorporated into the building materials. During the service lifetime of innovated roofing tiles, the rainwater may cause leakage of those harmful components, consequently may result water and soil contaminations. Hence, it is an important issue to be addressed in order to minimize the environmental problems caused by the innovated roofing tiles.

(2) Heat curing process is one of the most important manufacturing steps which promote the rigidification of waste oil-made roofing tiles. However, the treatment of waste oil under an elevated temperature gives rise to toxic compounds. Furthermore, several volatile oil components will be released into the atmosphere during the heat curing process. If the harmful gaseous components were accidentally inhaled, it may affect human's health. Hence, some precaution action should be taken during the manufacturing process in order to avoid the inhalation of those toxic gases.

### 5.3 Future Recommendations

Future recommendations to further the research study are suggested as follows:

- (1) The novel approach of manufacturing roofing tiles can also be applied on other construction application, such as production of building bricks, wall tiles floor tiles etc. However, additional work is required to investigate and reach the standards requirements related to the corresponding applications.
- (2) Implementation of self-healing mechanism in the innovated roofing tiles is suggested to enhance the service lifetime. The recommended mechanisms including (I) autogenous self-healing; (II) self-healing based on adhesive agent and (III) self-healing based on mineral admixture. Different mechanisms are effective only under particular condition. Hence, plenty of research studies are required to determine the optimum mechanisms for the proposed roofing tiles.
- (3) Incorporation of hydrophobic-type fibre in the manufacturing process of waste oil-made roofing tiles is recommended. Since waste oil served as the binder, it was believed that hydrophobic fibre is able to form a stronger binding matrix, consequently enhance the mechanical properties, as well as production of bendable waste oil-made building materials.

(4) In this study, several limitations were encountered. Extra investigation study is necessary in order to determine the uncertainty of the innovated roofing tiles produced. In addition, enhancing the properties of roofing tiles to reduce its environmental impacts. The limitations which require further study are as follows:

- a. Elimination of the heavy metals in the WEO and the toxic compounds released during the manufacturing process in order to decrease the environmental impacts which may be caused by the innovated roofing tiles.
- b. Study of the relationship between flexural strength and the pore-pore connectivity of innovated roofing tiles produced.
- c. Study the effect of HCl to find out the factors causing it reduces the strength of the innovated roofing tiles.
- d. Calculation of the EE and EC of innovated roofing tiles during pre-treatment process of raw materials.

## REFERENCES

- Ablerroof, 2017. Different roof types: Pros and cons. Available from <https://www.able-roof.com/different-roof-types-pros-and-cons>". Retrieved at 7/4/2018.
- Adams T.H., 2015. About Coal Ash. Available from: <https://www.aaaa-usa.org/About-Coal-Ash/What-are-CCPs/Fly-Ash>. Or <http://www.aaaa-usa.org/About-Coal-Ash/A-Sustainable-Future>. Retrieved at 19/7/2017.
- Ahmari S and Zhang L., 2012. Production of eco-friendly bricks from copper mine tailings through geopolymerization. *Construction and Building Materials*, 29, pp.323–331.
- Ahmari S, and Zhang L., 2013. Utilization of cement kiln dust (CKD) to enhance mine tailings-based geopolymer bricks. *Construction and Building Materials*, 40, pp.1002–1011.
- Al-Ghouti, M. a, & Al-Atoum, L., 2009. Virgin and recycled engine oil differentiation: a spectroscopic study. *Journal of environmental management*, 90(1), 187–95. doi:10.1016/j.jenvman.2007.08.018.
- Ali A. and Xiao J., 2017. Estimation and Minimization of Embodied Carbon of Buildings: A Review. *Buildings*, 7 (1), pp. 5–28.
- Alongi P., 2012. Greenville County Hopes to Accelerate Oil Recycling. Available from: <http://www.Greenvilleonline.com>. Retrieved at 26/6/2017.
- Aslam A. Al-Omari, Taisir S. Khedaywi and Mohammad A. Khasawneh, 2018. Laboratory characterization of asphalt binders modified with waste vegetable oil using SuperPave specifications. *International Journal of Pavement Research and Technology*, 11, pp. 68–76.
- Baoguo Han, Yunyang Wang, Sufen Dong, Liqing Zhang, Siqi Ding, Xun Yu and Jinping Ou, 2015. Smart concrete and structure: A review. *Journal of Intelligent Material System and Structures*, 26 (11), pp. 1303–1345.
- Beddu S., Shafiq N., Nuruddin M.F., Kamal N.L.M., and Sadon S.N., 2016. Effect of used engine oil as an admixture in concrete durability. *British Journal of Applied Sciences and Technology*, 15(6), pp. 1–10.
- Beth Peterson, 2017. How Temperature Changes Clay: The 6 Stages Clay Goes Through during Temperature Change, *The Spruce*. Available from "<https://www.thespruce.com/how-temperature-changes-clay>". Retrieved at 9/4/2018.

Bilal S. Hamad, Ahmad A. Rteil and Mutassem El-Fadel, 2003. Effect of used engine oil on properties of fresh and hardened concrete. *Construction and Building Materials*, 17, pp. 311–318.

Capuano D., Costa M., Fraia S. Di, Massarotti N. and Vanoli L., 2017. Direct use of waste vegetable oil in internal combustion engine. *Renewable and Sustainable Energy Reviews*, 69, pp. 759–770. doi: <http://dx.doi.org/10.1016/j.rser.2016.11.016>

Chani, P.S., Najamuddin., Kaushik, S.K., 2003. Comparative analysis of embodied energy rates for walling elements in India. *Journal of The Institution of Engineering (India)*, 84, pp. 47–50.

ChartsBin statistics collector team, 2011. Fat Composition in different Cooking Oils. Available from: “<http://chartsbin.com/view/1961>”. Retrieved at 13/3/2018.

Choe E and Min DB, 2007. Chemistry of Deep-Fat Frying Oil. *Journal of Food Science*, 72, pp. 78 – 86.

Chris Collins, 2007. Implementing Phytoremediation of Petroleum Hydrocarbons. *Methods in Biotechnology*, 23, pp. 99–108.

Clara Jeyageetha .J and Sugirtha P. Kumar, 2016. Study of SEM/EDXS and FTIR for Fly Ash to Determine the Chemical Changes of Ash in Marine Environment. *International Journal of Science and Research*, 5(7), pp. 1688–1693.

Cvengros, J., & Cvengrosova, Z. (2004). Used Frying Oils and Fats and their Utilization in the Production of Methyl Esters of Higher Fatty Acids, *Biomass and Bioenergy*, 27, 173-181.

Deborah Walden, 2017. Why oil won't mix in water? Available from: “<http://sciencing.com/oil-wont-mix-water-7996109.html>”. Retrieved at 25/8/2017.

Dlugokencky Ed and Pieter Tans, 2018. Global Greenhouse Gases Reference Network. National Oceanic & Atmospheric Administration / Earth System Research Laboratory. Available from: “[www.esrl.noaa.gov/gmd/ccgg/trends/](http://www.esrl.noaa.gov/gmd/ccgg/trends/)”. Retrieved at 26/3/2018.

Dixit M.K., Fernandez-Solis J.L., Lavy S., and Culp C.H., 2010. Identification of parameters for embodied energy measurement: A literature review. *Energy and Buildings*, 42, pp. 1238–1247.

Dixit, M.K.; Fernandez-Solis, J.L.; Lavy, S; Culp, C.H., 2012. Need for an embodied energy measurement protocol for buildings: A review paper. *Renewable & Sustainable Energy Reviews*. 16, pp. 3730–3743

Edvardsen C., 1999. Water permeability and autogenous healing of cracks in concrete, *ACI Materials Journal*, 96(4), pp. 448–454.

Efsun DİNDAR, Fatma Olcay TOPAÇ ŞAĞBAN and Hüseyin Savaş BAŞKAYA, 2015. Biodegradation of used engine oil in a wastewater sludge-amended agricultural soil. *Turkish Journal of Agriculture and Forestry*, 40, pp. 631 – 641.

Elena D.R., and John P., 2003. Chemical characterization of fresh, used and weathered motor oil via GC/MS, NMR and FTIR techniques. *Proceedings of the Indiana Academy of Science*, 112 (2), pp. 109–116.

Eliche-Quesada D, Corpas-Iglesias FA, Pérez-Villarejo L and Iglesias-Godino FJ, 2012. Recycling of sawdust, spent earth from oil filtration, compost and marble residues for brick manufacturing. *Construction and Building Materials*, 34, pp. 275–284.

El-Fadel, M., & Khoury, R., 2001. Strategies for vehicle waste-oil management: a case study. *Resources, Conservation and Recycling*, 33, 75–91.

Enweremadu CC and Mbarawa M, 2009. Technical aspects of production and analysis of biodiesel from used cooking oil—a review. *Renewable and Sustainable Energy Reviews*, 13(9), pp. 2205–2224.

Eric M. Fujita, David E. Campbell and Barbara Zielinska, 2006. *Chemical Analysis of Lubrication Oil Samples from a Study to Characterize Exhaust Emission from Light-Duty Gasoline Vehicles in the Kansas City Metropolitan Area*. Desert Research Institution. Prepared for National Renewable Energy Laboratory and Coordinating Research Council.

Forth J.P. and Zoorob S.E., 2006. Non-traditional binders for construction materials. Paper presented at the IABSE Henderson Colloquium, Cambridge.

Garbacz, A. and Sokolowska, J.J., 2013. Concrete-like polymer composites with fly ashes – Comparative study. *Construction and Building Materials*, 38, pp. 689–99.

Gartner, E., 2004. Industrially interesting approaches to “low-CO<sub>2</sub>” cements. *Cement and Concrete Research*, 34, pp. 1489–1498.

Gertz C., 2000. Chemical and Physical Parameters as Quality Indicators of Used Frying Fats. *Euro Lipid Science Technology*, 102, pp. 566 – 572.

Gonzalez, M.J. and Navarro, J.G., 2006. Assessment of the decrease of CO<sub>2</sub> emissions in the construction field through the selection of materials: Practical case study of three houses of low environmental impact. *Building and Environment*, 41, pp. 902–909.

Grzegorz Zajac, Joanna Szyszlak-Barglowicz, Tomasz Slowik, Andrzej Kuranc and Agnieszka Kaminska, 2015. Designation of Chosen Heavy Metals in Used Engine Oils Using XRF Method. *Polish Journal of Environmental Studies*, 24 (5), pp. 2277 – 2283.

Guggenheim S. and Martin R. T., 1995. Definition of clay and clay mineral: Journal report of the AIPEA nomenclature and CMS nomenclature committees. *Clays and Clay Minerals*, 43(2), pp. 255–256, doi:10.1346/CCMN.1995.0430213.

Halil M.A. and Tugut p., 2008. Cotton and limestone powder wastes as brick material. *Construction and Building Materials*, 22, pp. 1074–1080.

Hammond G. and Jones C. (2008). Inventory of carbon & energy – ICE version 1.6a. University of Bath, UK. [www.bath.ac.uk/mech-eng/sert/embodied/](http://www.bath.ac.uk/mech-eng/sert/embodied/)

Hammond G. and Jones C. (2011). Inventory of carbon & energy – ICE version 2.0. University of Bath, UK. [www.bath.ac.uk/mech-eng/sert/embodied/](http://www.bath.ac.uk/mech-eng/sert/embodied/)

Haoliang Huang, Guang Ye, Chunxiang Qian and Erik Schlangen, 2016. Self-healing in cementitious materials: Materials, method and service condition. *Materials and Design*, 92, pp. 499–511. <http://dx.doi.org/10.1016/j.matdes.2015.12.091>.

Haiying Z, Youcai Z, Jingyu Q, 2011. Utilization of municipal solid waste incineration (MSWI) fly ash in ceramic brick: product characterization and environmental toxicity. *Waste Manage (Oxford)*, 31, pp.331–341.

He J, Jie Y, Zhang J, Yu Y and Zhang G, 2013. Synthesis and characterization of red mud and rice husk ash-based geopolymer composites. *Cement and Concrete Composition*, 37, pp. 108–118.

Heaton T., Sammom C., Ault J., Black L. and Forth J.P., 2014. Masonry units bound with waste vegetable oil – Chemical analysis and evaluation of engineering properties. *Construction and Building Materials*, 64, pp. 460–472.

Hegerl GC, et al., 2007. IPCC Climate Change 2007: The Physical Science Basis, eds S Solomon et al. (Cambridge Univ Press, Cambridge, UK), pp 663–746.

Hewlett, P. C., and Young, J. F., 1987. Physico-Chemical Interactions Between Chemical Admixtures and Portland Cement. *Journal of Materials Education*, 9(4).

Hu S, Wang H, Zhang G and Ding Q, 2008. Bonding and abrasion resistance of geopolymeric repair material made with steel slag. *Cement and Concrete Composition*, 30, pp. 239–244.

Humayun Nadeem, Noor Zainab Habib, Ng Choon Aun, Salah Elias Zoorob, Zahiraniza Mustaffa, Swee Yong Chee and Muhammad Younas, 2017a. Utilization of Catalyzed Waste Vegetable Oil as a Binder for the Production of Environmental friendly Roofing Tiles. *Journal of Cleaner Production*, doi: 10.1016/j.jclepro.2017.01.028.

Humayun Nadeem, Noor Zainab Habib, Ng Choon Aun, Salah Elias Zoorob, Zahiraniza Mustaffa, Ricardo Mesney and Spencer Suubita, 2017b. Used engine oil as alternative binder for buildings – a comparative study. *Waste and Resource Management*. doi: 10.1680/jwarm.17.00005.

Huseyin Sanli, Mustafa Canakci and Ertan Alptekin, 2011. Characterization of Waste Frying Oils Obtained from Different Facilities. *World Renewable Energy Congress*, pp. 479 – 485.

IPCC, 2013. Summary for Policymakers. In: *Climate Change 2013: The Physical Science Basis. Contribution of Working Group I to the Fifth Assessment Report of the Intergovernmental Panel on Climate Change*.

J. Paya, J. Monzo, M.V. Borrachero, E. Peris, F. Amahjour, Mechanical treatments of fly ashes: Part IV. Strength development of ground fly ash-cement mortars cured at different temperatures, *Cement and Concrete Research*, 30 (4), pp. 543–551.

Jatuphon Tangpagasit, Raungrut Cheerarot, Chai Jaturapitakkul and Kraiwood Kiattikomol, 2005. Packing effect and pozzolanic reaction of fly ash in mortar. *Cement and Concrete Research*, 35, pp. 1145–1151.

Jia Xiaoyang, Baoshan Huang, Sheng Zhao, 2014. Infrared spectra and rheological properties of asphalt cement containing waste engine oil residues. *Construction and Building Materials*, 50, pp. 683–691.

Johnny, B., Taher, A., and Ellie, F., 2013. Utilization of Recycled and Waste materials in various construction applications. *American Journal of Environmental Science*, 9, pp. 15-22.

Johnson O.A., Madzlan N. and Kamaruddin I., 2015. Encapsulation of petroleum sludge in building blocks. *Construction and Building Materials*, 78, pp. 281 – 288.

Kamal M, Liyana N, Beddu S, Nurudinn MF, Shafiq N, Muda ZC, 2014. Microwave Incinerated Rice Husk Ash (MIRHA) and Used Engine Oil (UEO): Towards sustainable concrete production. *Applied Mechanics and Materials*, 567, pp. 434–439.

Karak, N. (2012). *Vegetable oil-based polymers*. Woodhead Publishing Limited.

Kim SS, Kim J, Jeon JK, Park YK and Park CJ, 2013. Non-isothermal pyrolysis of the mixtures of waste automobile lubricating oil and polystyrene in a stirred batch reactor. *Renewable Energy*, 54, pp.241–247.

Kosmatka, Steven H., and Panarese, William C, 1988. *Design and Control of Concrete Mixtures*, Thirteenth edition, Portland Cement Association.

Kumar S., 2001. A perspective study of fly ash-lime-gypsum bricks and hollow blocks for low cost housing development. *Construction and Building Materials*, 16, pp. 519–525.

Li, Lijuan and Chen, Kanghai, 2016. Quantitative assessment of carbon dioxide emissions in construction projects: A case study in Shenzhen. *Journal of Cleaner Production*, 141, pp. 394–408.

Li Yanmei, Ruo Zhao, Tianshu Liu and Jianfeng Zhao, 2015. Does urbanization lead to more direct and indirect household carbon dioxide emissions? Evidence from China during 1996–2012. *Journal of Cleaner Production*, 102, pp. 103–114.

Lorecentral, 2017. Types of roof, advantages and disadvantages of each. Available from: “<https://www.lorecentral.org/2017/11/types-roofs-advantages-disadvantages.html>”. Retrieved at 7/4/2018.

Luo M., C.-X. Qian, R.-Y. Li, 2015. Factors affecting crack-repairing capacity of bacteria based self-healing concrete, *Construction and Building Materials*, 87, pp. 1–7.

Maceiras R., Alfonsin V. and Morales F.J., 2016. Recycling of waste engine oil for diesel production. *Waste Management*, doi: <http://dx.doi.org/10.1016/j.wasman.2016.08.009>

Mangesh G. Kulkarni and Ajay K. Dalai, 2006. Waste Cooking Oil – An Economical Source for Biodiesel: A Review. *Industrial & Engineering Chemistry Research*, 45, pp. 2901–2913.

Mariana A.P., George M., Ersilia A., Diana M., Monica N., and Mateescu C., 2012. Application of FT-IR spectroscopy to assess the olive oil adulteration. *Journal of Agroalimentary Processes and Technologies*, 18 (4), pp. 277–282.

Marvin Charton, 1974. Steric effect. I. Esterification and acid catalyzed hydrolysis of esters. *Journal of American Chemical Society*, 97 (6), pp. 1152–1156.

Mei-In. M. Chou, Vinod Patel, Charles J. Laird, Ken K. Ho, 2001. Chemical and engineering properties of fired bricks containing 50 weight percent of class F fly ash. *Energy Sources*, 23, pp. 665–673.

Meizhu Chen, Binbin Leng, Shaopeng Wu and Yang Sang, 2014. Physical, chemical and rheological properties of waste edible vegetable oil rejuvenated asphalt binders. *Construction and Building Materials*, 66, pp. 286–298. doi: <https://doi.org/10.1016/j.conbuildmat.2014.05.033>.

Michael C.G. and John B., 2007. FT-IR analysis of used lubricating oils – General considerations. Thermo Fisher Scientific. Available from: <http://analyteguru.com/resources/ft-ir-analysis-of-used-lubricating-oilsgeneral-considerations/>. Retrieved at 7/5/2017.

Mindess S. and Young, J.F., 1981. *Concrete*, Prentice-Hall, Englewood Cliffs, N.J

Mohammed Abdul Raqeed and Bhargavi R., 2015. Biodiesel production from waste cooking oil. *Journal of Chemical and Pharmaceutical Research*, 7(12), pp. 670 – 681.

Mohammad A. Al-Ghouti, & Lina Al-Atoum, 2009. Virgin and recycled engine oil differentiation: a spectroscopic study. *Journal of Environmental Management*, 90(1), pp. 187–195. doi:10.1016/j.jenvman.2007.08.018.

Mora C. et al., 2013. The projected timing of climate departure from recent variability. *Nature*, 502, pp. 183–187. doi:10.1038/nature12540.

Nasir Shafiq, Muhd Fadhil Nuruddin and Salmia Beddu, 2011. Properties of concrete containing used engine oil. *International Journal of Sustainable Construction Engineering & Technology*, 2, pp. 72–82.

National Aeronautics and Space Administration, Goddard Institute for Space Study (NASA GISS), 1998. Greenhouse Gases: Refining the Role of Carbon Dioxide. Available from: “[https://www.giss.nasa.gov/research/briefs/ma\\_01/](https://www.giss.nasa.gov/research/briefs/ma_01/)”. Retrieved at 26/3/2018.

Negishia H., Nishida M., Endo Y., & Fujimoto K. (2003). Effect of a Modified Deep-Fat Fryer on Chemical and Physical Characteristics of Frying Oil, *Journal of American Oil Chemists*, 80, 163-66.

Negulescu I, Mohammad L, Daly W, Abadie C, Cueto R, Daranga C, et al., 2006. Chemical and rheological characterization of wet and dry aging of SBS copolymer modified asphalt cements: laboratory and field evaluation. *Journal of Association of Asphalt Paving Technologists*, 75, pp. 267–318.

Nerin C., Domeño C., Moliner R., Lázaro M.J., Suelves, I. and Valderrama, J., 2000. Behaviour of different industrial waste oils in a pyrolysis process: metals distribution and valuable products. *Journal of Analytical and Applied Pyrolysis*, 2, pp. 171–183.

Ning Zheng and Jinho Yoon, 2009. Expansion of the world’s deserts due to vegetation-albedo feedback under global warming. *Geophysical Research Letter*, 36, L17401. doi: 10.1029/2009GL039699.

Noor et.al. 2015. Environmentally friendly vege-roofing tile: an investigation study. Proceedings of the First International Conference on Bio-based Building Materials. PRO 99, RILEM Publications.

Nurcan Tugrul, Nil Baran Acarali, Seyma Kolemen, Emek Moroydor Derun, and Sabriye Piskin, 2012. Characterization of Catalagzi Fly Ash for Heavy Metal Adsorption. International Journal of Chemical, Molecular, Nuclear, Materials and Metallurgical Engineering, 6 (11), pp. 1063 – 1067.

Nurul Hidayah, Mohd Rosli, Norhidayah and Mohd Ezree, 2013. A short review of waste oil application in pavement materials. In: 9th International Conference of Geotechnical and Transportation Engineering (GEOTROPIKA) and 1st International Conference on Construction and Building Engineering (ICONBUILD).

Pardon K.K., Cledwyn T.M., Olga K. and Admire C., 2015. Use of Pulverized Fuel Ash in the Manufacture of Concrete Roofing Tiles. International Journal of ChemTech Research, 8(3), pp. 1019–1025.

Petersen J.C., 1984. Chemical composition of asphalt as related to asphalt durability: state of the art. Transportation Research Record, 999, pp. 13–30.

Ramasamy V., Rajkumar P. and Ponnusamy V., 2006. FT-IR Spectroscopic analysis and mineralogical characterization of Velar river sediments. Bull. Pure Appl. Sci., 25, pp. 49–55.

Rawaid Khan, Abdul Jabbar, Irshad Ahmad, Wajid Khan, Akhtar Naeem Khan and Jahangir Mirza, 2011. Reduction in environmental problems using rice husk ash in concrete. Construction and Building Materials, 30, pp. 360–365.

Reijnders, L., Huijbregts, M.A.J., 2008. Palm oil and the emission of carbon-based greenhouse gases. Journal of Cleaner Production, 16, pp. 477–482.

Roddy S. and Doug M., 2013. Sun Roof: Solar Panel Shingles come Down in Price, Gain in Popularity. Scientific American. Available at: “<https://www.scientific-american.com/article/im-getting-my-roof-redone-and-heard-about-solar-shingles/>” Retrieved at 7/4/2018.

Roig-Flores M., S. Moscato, P. Serna, L. Ferrara, 2015. Self-healing capability of concrete with crystalline admixtures in different environments, Construction and Building Materials, 86, pp. 1–11. <https://doi.org/10.1016/j.conbuildmat.2015.03.091>

Salem S, Salem A and Babaei AA, 2015 Application of Iranian nano-porous Ca-bentonite for recovery of waste lubricant oil by distillation and adsorption techniques. Journal of Industrial and Engineering Chemistry, 23, pp. 154–62.

Samara M, Lafhaj Z, and Chapiseau C., 2009. Valorization of stabilized river sediments in fired clay bricks: factory scale experiment. Journal of Hazardous Materials, 163 (2–3), pp.701–710.

Schlosberg R.H., Chu J.W., Knudsen G.A., Suci E.N. and Aldrich H.S., 2001. High stability esters for synthetic lubricant applications. *Lubrication Engineering*, pp. 21–26.

Shiva Salem, Amin Salem and Aylin Agha Babaei, 2015. Preparation and characterization of nano porous bentonite for regeneration of semi-treated waste engine oil: Applied aspects for enhanced recovery. *Chemical Engineering Journal*, 260, pp. 368–376.

Sivakumar S, Ravisankar R., Raghu Y., Chandrasekaran A., and Chandramohan J., 2012. FTIR Spectroscopic Studies on Coastal Sediment Samples from Cuddalore District, Tamilnadu, India. *Ind. J. of Advances in Chemical Sci.*, 1, pp. 40–46.

Stevenson SG, Vaisey-Genser M, Eskin NAM, 1984. Quality Control in the Use of Deep Frying Oils. *Journal of American Oil Chemists' Society*, 61, pp. 1102 – 1108.

Strine Environments, 2018. Concrete and Embodied Energy – Can using concrete be carbon neutral. Available from: “<http://strineenvironments.com.au/factsheets/concrete-and-embodied-energy-can-using-concrete-be-carbon-neutral/>”. Retrieved at 9/4/2018

Teoh Wei Ping, Noor Zainab Habib, Ng Choon Aun and Chee Swee Yong, 2018. Catalyzed waste engine oil as alternative binder of roofing tiles – Chemical analysis and optimization of parameters. *Journal of Cleaner Production*, 174, pp. 988 – 999.

Thao T.D.P., T.J.S. Johnson, Q.S. Tong, P.S. Dai, 2009. Implementation of self-healing in concrete — proof of concept, *The IES Journal Part A: Civil & Structural Engineering*, 2, pp. 116–125.

The Concrete Centre, Mineral Product Association (MPA), 2017. Embodied Carbon. Available from: “[https://www.concretecentre.com/Performance-Sustainability-\(1\)/low-energy-buildings-\(1\)/Low-Energy-Buildings.aspx](https://www.concretecentre.com/Performance-Sustainability-(1)/low-energy-buildings-(1)/Low-Energy-Buildings.aspx)”. Retrieved 9/4/2018.

Tsui, T.Y., Vlassak, J.J., Taylor, K., McKerrow, A.J. and Kraft, R., 2005. Effects of absorption of water and other reactive species on the fracture properties of organosilicate glass thin films. *month*, 4, p.5.

Turgut P., 2010. Masonry composite material made of limestone powder and fly ash. *Powder Technology*, 204, pp.42–47.

Wang, Xiao-Yong and Park, Ki-Bong, 2016. Analysis of Compressive Strength Development and Carbonation Depth of High Volume Fly Ash Cement Pastes. *ACI Materials Journal*, 113(2), pp. 151–161.

Wu, Lichao, Wu, Limin, Lin, Junmin, 2014. Dynamic relationship between urbanization and carbon emissions - Rethinking based on the panel smooth transition regression model (in Chinese). *Journal of China University of Geosciences*, 14 (1), 31 – 35.

Yazici E.Y. and Deveci H., 2010. Factor Affecting the Decomposition of Hydrogen Peroxide. *Proceeding of the XIIth International Mineral Processing Symposium*.

You, Z., Mills-beale, J., Fini, E., Goh, S. W., & Colbert, B., 2011. Evaluation of Low- Temperature Binder Properties of Warm-Mix Asphalt , Extracted and Recovered RAP and RAS , and Bioasphalt. *Journal of Materials in Civil Engineering*, 23(11), 1569–1574. doi:10.1061/(ASCE)MT.1943-5533.0000295.

Zhang L, Ahmari S and Zhang J, 2011. Synthesis and characterization of fly ash modified mine tailings-based geopolymers. *Construction and Building Materials*, 25(9), pp. 3773–3781.

Zhang S.P. and Zong L., 2014. Evaluation of relationship between water absorption and durability of concrete materials. *Advances in Materials Science and Engineering*, 2014, pp. 1–8. <http://dx.doi.org/10.1155/2014/650373>